PhD Expo 2017

25 maggio – 5 giugno 2017
Campus Rizzi
via delle Scienze 206
Udine

L'evento, organizzato dall'Università di Udine in collaborazione con l'Acceleratore digitale 'Friuli Innovazione', presenta la vetrina delle attività di ricerca condotte dai dottorandi iscritti al terzo anno dei corsi di dottorato.

Gli obiettivi:
- **comunicare** i risultati di ricerche e progetti
- **condividere** le idee e le proposte
- **confrontare** le esperienze e le competenze
- **contaminare** i diversi saperi

HR EXCELLENCE IN RESEARCH

UNIVERSITÀ DEGLI STUDI DI UDINE
hic sunt futura

FRIULI innovazione®
Centro di Ricerca e di Trasferimento Tecnologico

FONDAZIONE FRIULI

PhD Expo 2017

25 maggio – 5 giugno 2017
Campus Rizzi
via delle Scienze 206

Corso di dottorato in Ingegneria industriale e dell'informazione

HR EXCELLENCE IN RESEARCH

31° e 32° ciclo

31° CICLO

BORGHELLO GIULIO
Reliability of nanoscale devices in extreme radiation environments

COSSETTINI ANDREA
Viruses and Particles Detection with Nanoelectrode Array Platforms

DAL BO LORIS
Electromagnetic and piezoelectric seismic vibration energy harvesters

DE ZANET DENISE
Structural and functional blood characterization through electrical impedance sensing and optical signals analysis

MASET ELEONORA
Multi-view matching

OCELLO ELISABETTA
LEAN HEALTHCARE: evaluating functional and technical outcomes from both physicians' and patients' perpective

PINAROLI GIOVANNI
Development and characterization of a Soft X-Rays Imager Detector for FEL

RIZZOLATTI ROBERTO
High voltage distribution system in data-center

ROLLO TOMMASO
Kirchhoff's Laws and Energy Minimization in NCFETs

SCALERA LORENZO
Dynamic modeling and simulation of flexible multibody systems

VAGLIO EMANUELE
Optimization of Selective Laser Melting process parameter

32° CICLO

BATTISTELLA NICOLA
Multivariable modelling of the dynamic response of professional washing machines

LI WAN
The European Monitor of Reshoring & The Drivers of Reshoring Strategy

MOLINARO MARGHERITA
Managing the evolutionary path in Sales and Operations Planning

NASEER MUHAMMAD
Statistical fluctuation Effects on Nano Electronic Bio-Sensors

PASCOLO FILIPPO
FPGAs for real time particle trajectory reconstruction in the ATLAS experiment at the LHC

PASSAROTTO MAURO
Iterative solution of eddy current problems on polyhedral meshes

PIN ALESSANDRO
Positioning using LTE signals

PIRAS ALESSANDRO
Processing of bio-signals for biomedical applications and psyco-physical state analysis

SCALZO FEDERICO
Optimization of components designed for AM, simulation and monitoring of SLM process

STACCHI FRANCESCO
A new model for the simulation of a cable-in-conduit cabling procedure

URSINO MARIO
Parallel resonant high-power-density converters for data center and mobile applications

UNIVERSITÀ DEGLI STUDI DI UDINE
hic sunt futura

FRIULI innovazione
Centro di Ricerca e di Trasferimento Tecnologico

FONDAZIONE FRIULI

RELIABILITY OF NANOSCALE DEVICES IN EXTREME RADIATION ENVIRONMENTS

ABSTRACT

- Radiation can heavily affect nanoscales devices' behaviour.
  - Performance degradation and possible failures.
  - Long-term effects hard to predict.
- Transistors' dimensions play a central role in the current evolution during irradiation as well as bias voltage, temperature, fabrication process and dose rate [1] [2] [3].
- The goal is to elaborate a model of performance degradation to guarantee devices' reliability in extreme conditions.
- Radiation hardness is a key issue for, e.g., space applications, nuclear power plant and high energy physics experiments.

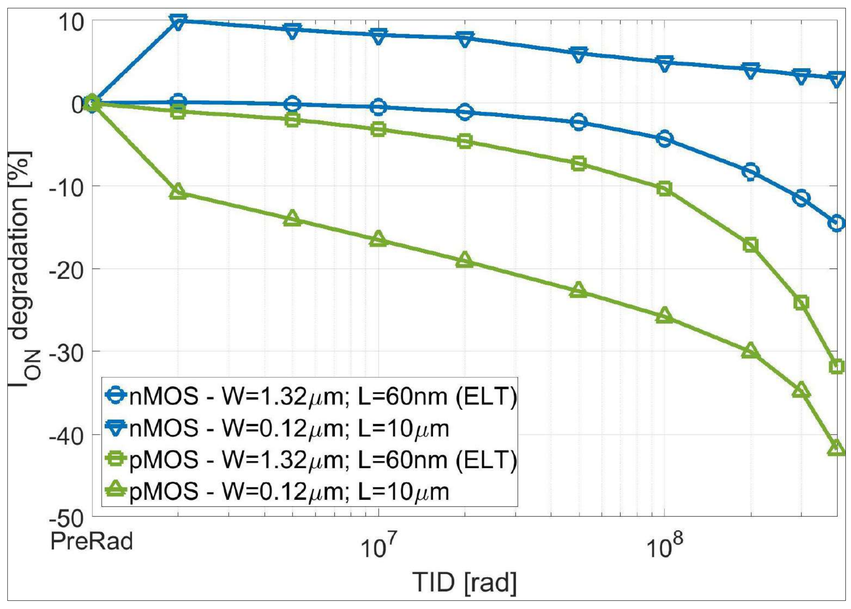

HIGH LUMINOSITY LHC

- The LHC running at CERN will soon be upgraded to increase the luminosity up to $5 \times 10^{34}\mathrm{cm}^{-2}\mathrm{s}^{-1}$ (HL-LHC).
- New detectors with higher pixel density. ➡ MOS technology scaled from 250 to 65 nm.
- Detectors will have to withstand unprecedented radiation. ➡ Total Ionizing Dose (TID) up to 1 Grad.
- Will 65 nm technology be viable for the LHC upgrades ?

High Luminosity LHC

RADIATION EFFECTS ON 65nm CMOS TECHNOLOGY [4]

- The main cause of degradation is the radiation-induced charge trapped in thick oxides like Shallow Trench Isolation (STI) oxides and spacers.

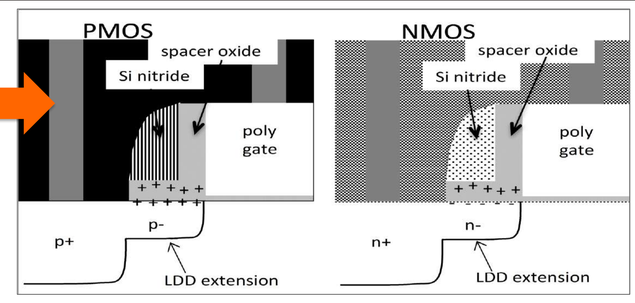

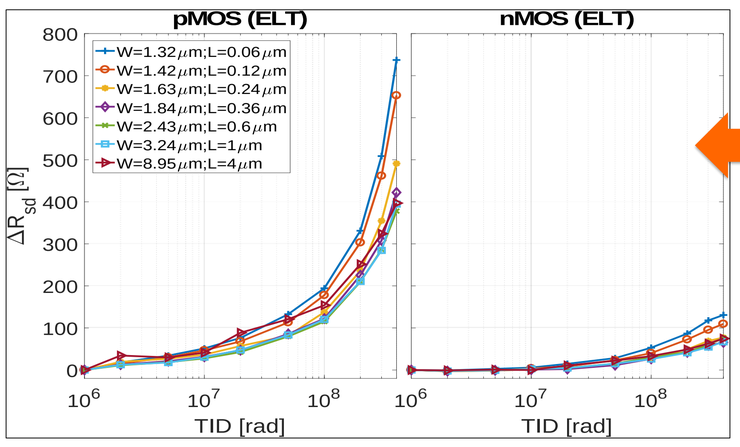

- Irradiation causes a large increment of series resistance in pMOS transistors.

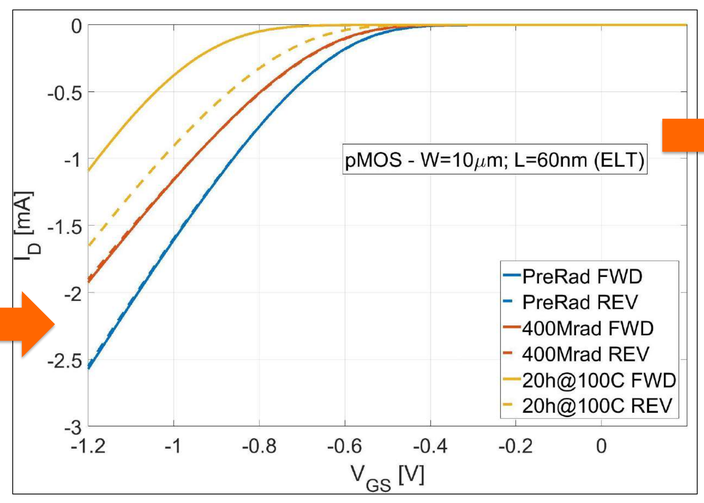

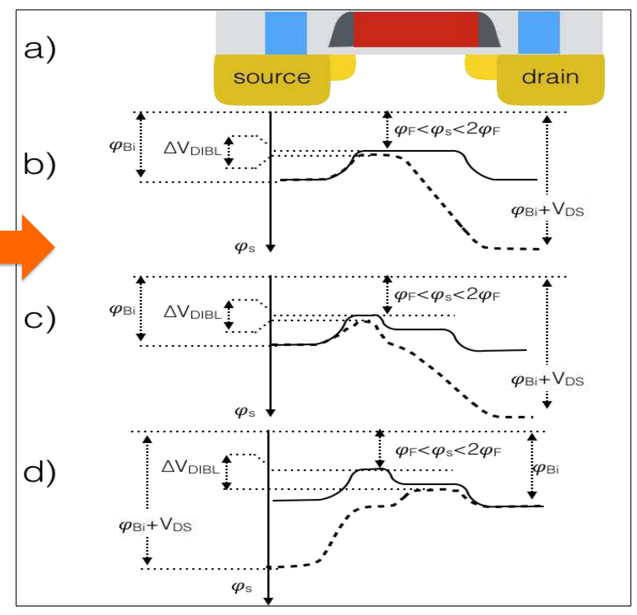

- pMOS gets asymmetric after few hours at 100°C under bias.
- This could be explained by a large amount of trapped charge in the source side of the transistor
- nMOS transistors show an asymmetric behaviour after irradiation at 25°C, due to charge trapping at the drain side

DOSE RATE DEPENDENCE

- Higher degradation at lower dose rate
  - Almost no existing literature for MOS technology

PROCESS DEPENDENCE

- Same technology from different foundries was tested
  - Qualitatively similar degradation was observed

OTHER TECHNOLOGIES

- 130nm and 28nm technologies tested
  - High degradation even at 28nm [5],[6]

BIBLIOGRAPHY

[1] Faccio, F., et al. "Radiation-Induced Short Channel (RISCE) and Narrow Channel (RINCE) Effects in 65 and 130 nm MOSFETs." *Nuclear Science, IEEE Transactions on* 62.6 (2015): 2933-2940.
[2] Schwank, James R., et al. "Radiation effects in MOS oxides." *Nuclear Science, IEEE Transactions on* 55.4 (2008): 1833-1853.
[3] Paillet, P., et al. "Comparison of charge yield in MOS devices for different radiation sources." *Nuclear Science, IEEE Transactions on* 49.6 (2002): 2656-2661.
[4] Faccio, F., et al. "Influence of LDD spacers and H+ transport on the total-ionizing-dose response of 65 nm MOSFETs irradiated to ultra-high doses" *accepted for presentation at the IEEE NSRE Conference, New Orleans, July 2017*.
[5] Zhang, C.M., et al. "GigaRad Total Ionizing Dose and Post-Irradiation Effects on 28 nm Bulk MOSFETs." *IEEE Nuclear Science Symposium*. No. EPFL-CONF-221644. IEEE, 2016.
[6] Pezzotta, A., et al. "Impact of GigaRad Ionizing Dose on 28 nm bulk MOSFETs for future HL-LHC." *Solid-State Device Research Conference (ESSDERC), 2016 46th European*. IEEE, 2016.

ACKNOWLEDGMENTS

- CERN for its financial support through the FCC R&D programme, "special technologies" Work Package.
- F.Faccio, S.Michelis and E.Lerario from EP-ESE-ME section at CERN for their constant help.
- Prof. L. Selmi (UniUD) for his support and fruitful discussions.
- S.Gerardin and S.Bonaldo (UinPD).
- Vanderbilt University (Nashville, TN)
- C. Zhang, A. Pezzotta and J. Farzan from EPFL for many useful discussion on 28nm technology.

INFO: Dott. Giulio Borghello: borghello.giulio.1@spes.uniud.it
Prof. Fabrizio Bellina: fabrizio.bellina@uniud.it

UNIVERSITÀ DEGLI STUDI DI UDINE
hic sunt futura

Corso di dottorato in Ingegneria industriale e dell'informazione

XXXI Ciclo

Viruses and Particles Detection with Nanoelectrode Array Platforms

1. Introduction

The Context

Nanoelectronics is paving the way for new, diverse, *More-than-Moore* applications. Among these, integrated nanoelectronic biosensors can bridge the gap between ICT technologies and the small building blocks of life (e.g., cells, bacteria, viruses, DNA, proteins), thus enabling seamless deployment of interconnected *Lab-on-chip* systems with huge potential for applications in environmental, biology, physiology, medicine and health [1].

The size of things

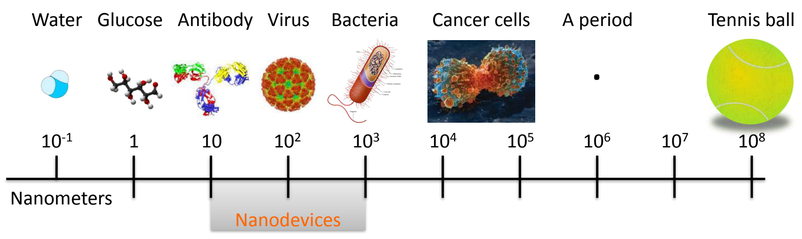

Nanotechnology enables Labs … on a chip!

High-Frequency Impedance Spectroscopy (HFIS)

Label-free impedance spectroscopy at high-frequency is a new sensing principle of special interest [2]. It allows sensing beyond the electrolyte Debye screening limit [3], thus remarkably enhancing the sensitivity at physiological salt concentration.

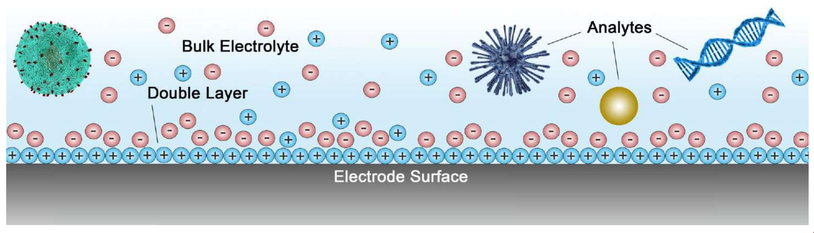

2. CMOS Biosensor Platform: Thermal model

We developed a new setup for temperature controlled sensor measures with microfluidics. The chip can be easily replaced and different fluids brought to the chamber above the chip.

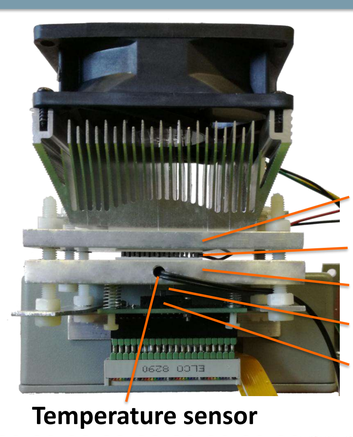

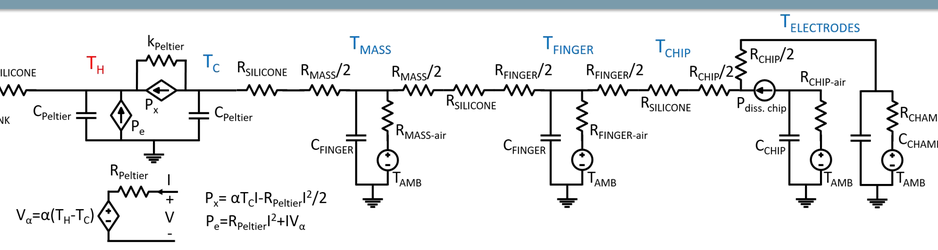

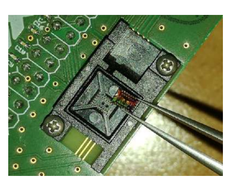

The experimental platform is thermally characterized with an equivalent Spice model.

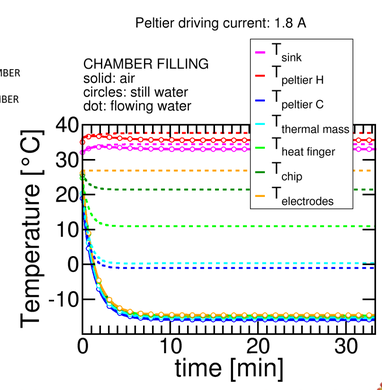

3. System response

- The signal transduction model has been substantially improved to account for the frequency and salt concentration dependence of the apparent switching capacitance and the harmonic content of the actual on-chip waveforms.
- CVFEM simulations [4,5] accounting for leakage currents and for the waveform harmonic content (Fourier analyses) reproduce the measurements with good accuracy

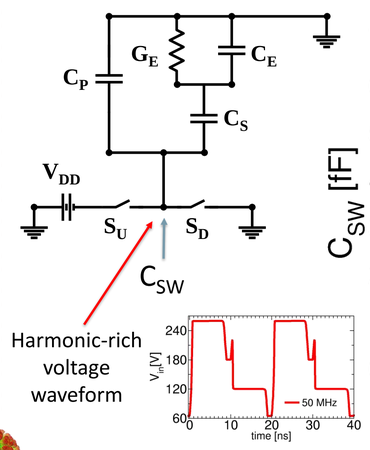

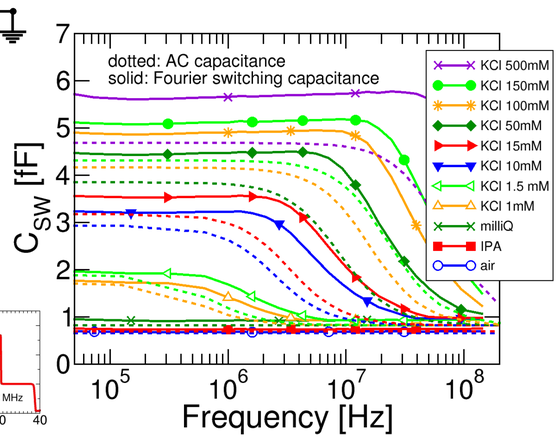

4. Detection experiment and simulations

$\Delta C = C_{with\ bead} - C_{without\ bead}$

Response to CCMV virus biomolecules

- *Cowpea Chlorotic Mottle Virus* truncated-icosahedron compact model starting from atomistic data
- Zepto-Farad resolution is required to discriminate between empty capsid and full virus (with enclosed RNA) at 50 MHz [6]

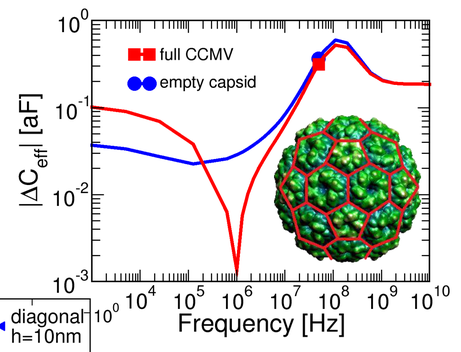

Response to dielectric microparticles

- Large dimensions: need for multi-electrode analyses
- Assessment of sensitivity to particle position [2]

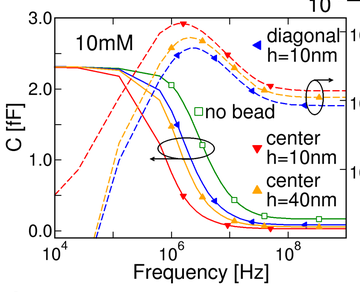

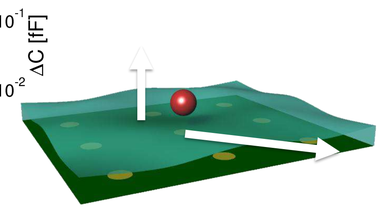

Response to oil droplets

- *ortho-dichlorobenzene* droplets in pure water
- Experimental estimation of droplet volume by means of a simulated calibration curve, image binarization and signal processing
- Monte Carlo analyses to account for noise

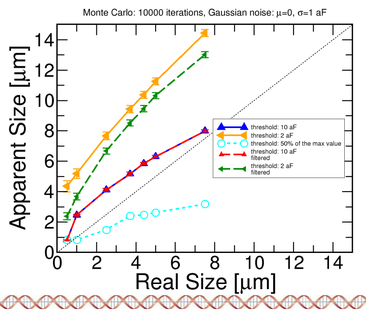

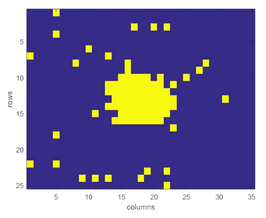

Dott. Andrea Cossettini
Prof. Luca Selmi
Info:
Tel. +39 0432 558261
cossettini.andrea@spes.uniud.it
luca.selmi@uniud.it

References

[1] M. Alam, "Principles of Electronic Nanobiosensors", *nanohub.org*
[2] S. G. Lemay *et al. Accounts of Chemical Research,* 2016.
[3] A. J. Bard, L. R. Faulkner, "Electrochemical Methods", *Wiley*, 2001.
[4] P. Scarbolo *et al.*, *https://nanohub.org/resources/biolab,* 2017.
[5] F. Pittino *et al.*, *CMAME,* 2014.
[6] A. Cossettini *et al., IEEE NANO*, 2017.

Acknowledgments
F. P. Widdershoven (*NXP Semiconductors*)
S. G. Lemay, C. Laborde, C. Renault (*University of Twente*)
P. Scarbolo, M. Sortino (*University of Udine*).

UNIVERSITÀ DEGLI STUDI DI UDINE
hic sunt futura

Corso di dottorato in Ingegneria industriale e dell'informazione

XXXI Ciclo

ELECTROMAGNETIC AND PIEZOELECTRIC SEISMIC VIBRATION ENERGY HARVESTERS

This poster contrasts the principal characteristics of two equivalent seismic harvesters using respectively electromagnetic and piezoelectric transducers. The two transducers are characterised by the same base and proof masses and by the same fundamental natural frequency.
The two systems are modelled with consistent electro-mechanical lumped parameter models, which allow the derivation of a unified formulation for the energy harvesting.
This facilitates a direct comparison of the electro-mechanical response and energy harvesting properties of the two harvesters.

Electromagnetic Seismic Harvester

The electromagnetic seismic harvester comprises a cylindrical magnetic element with an inner gap where a coil is housed. The two components are connected via soft springs and the coil is fixed to the case of the harvester

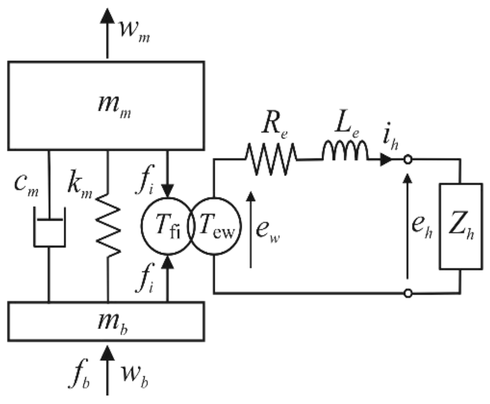

Piezoelectric Seismic Harvester

The piezoelectric seismic harvester comprises a cantilever beam with a small block mass at its tip. The beam is fixed to the harvester case and is equipped with piezoelectric patches, which are bonded to its surfaces.

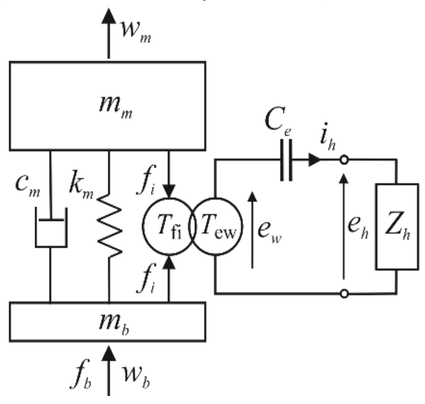

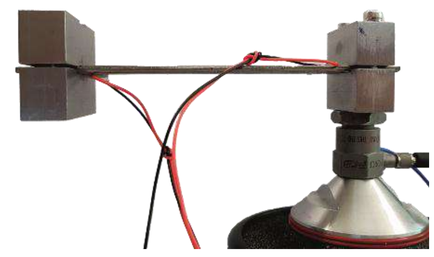

Seismic Transducers
Unified Constitutive Equations

$$f_b = Z_{mi}\dot{w}_b + T_{fi} i_h$$
$$e_h = T_{ew}\dot{w}_b + Z_{ei} i_h$$

Frequency domain – complex response:

The electro-mechanical complex response of the two transducers is expressed with two equations, which consider:

- the open circuit transducer mechanical impedance FRF
  $Z_{mi} = f_b / \dot{w}_b\big|_{i_h=0}$
- the blocked and open circuit transducer electro-mechanical transduction FRFs
  $T_{fi} = f_b / i_h\big|_{\dot{w}_b=0} \qquad T_{ew} = e_h / \dot{w}_b\big|_{i_h=0}$
- the blocked transducer electrical impedance FRF
  $Z_{ei} = e_h / i_h\big|_{\dot{w}_b=0}$

--------- → Experimental results

Electromagnetic harvester FRFs

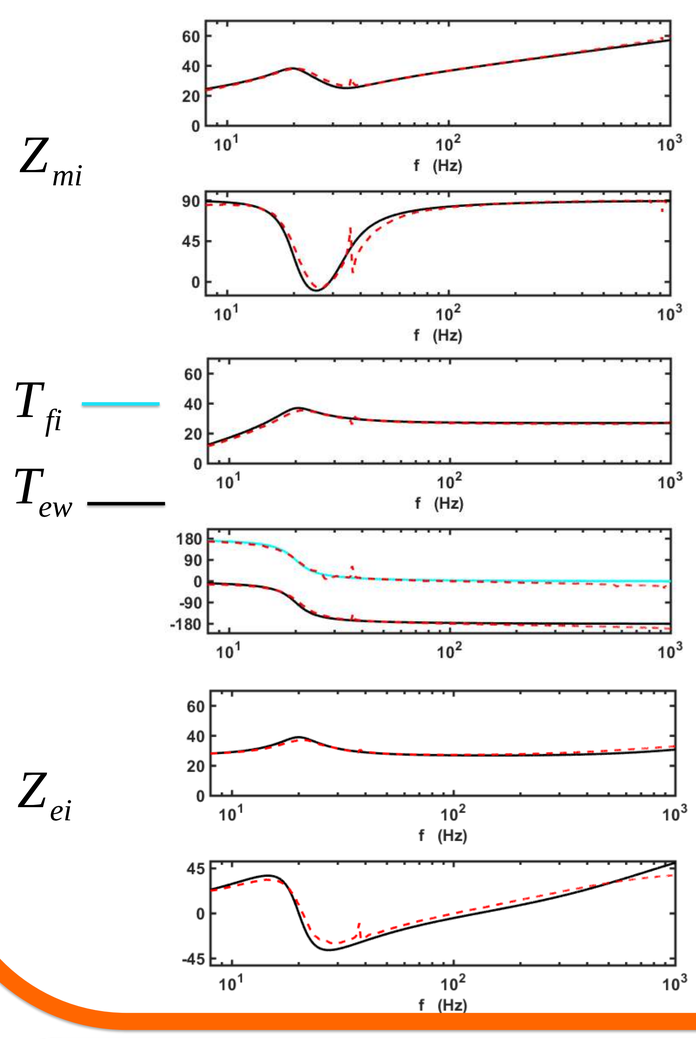

Piezoelectric harvester FRFs

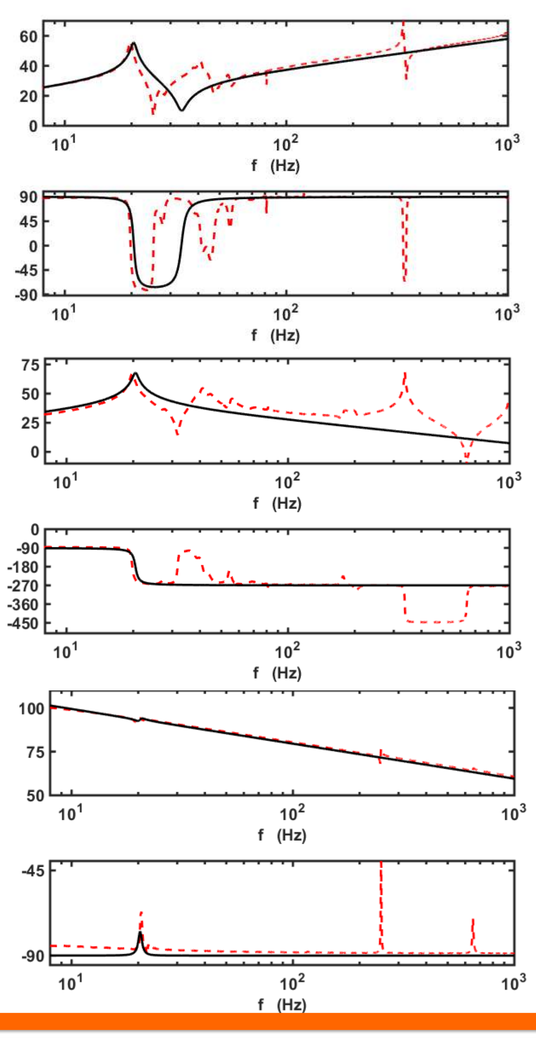

Maximisation of the harvested power

$$\overline{P}_h = \frac{1}{2}\mathrm{Re}\{Z_h\}|i_h|^2 = \frac{1}{2}\mathrm{Re}\{Z_h\}\left|\frac{T_{ew}}{Z_{ei}+Z_h}\right|^2 |\dot{w}_b|^2$$

$\overline{P}_h$ is maximised if :

- $Z_h = Z_{ei}^*$ resistive-reactive harvester load ——
- $Z_h = |Z_{ei}|$ purely resistive harvester load ——

N.B. $\omega \cong \omega_n \rightarrow \overline{P}_h \cong$ maximum
○ → Experimental results

Harvested Power (Electromagnetic)

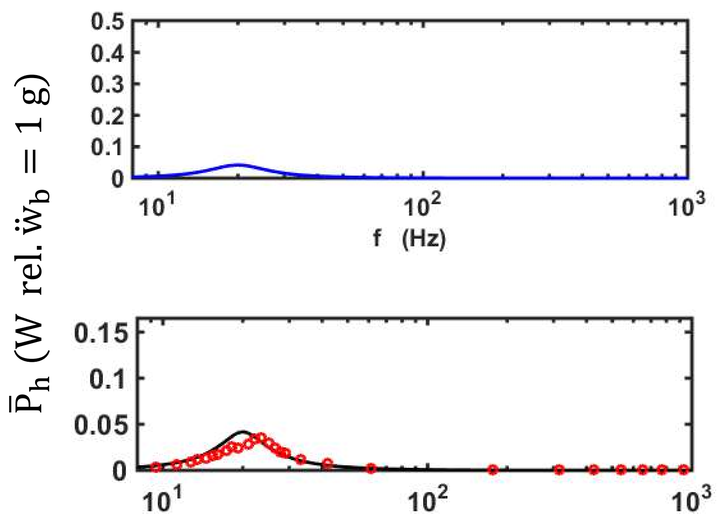

Harvested Power (Piezoelectric)

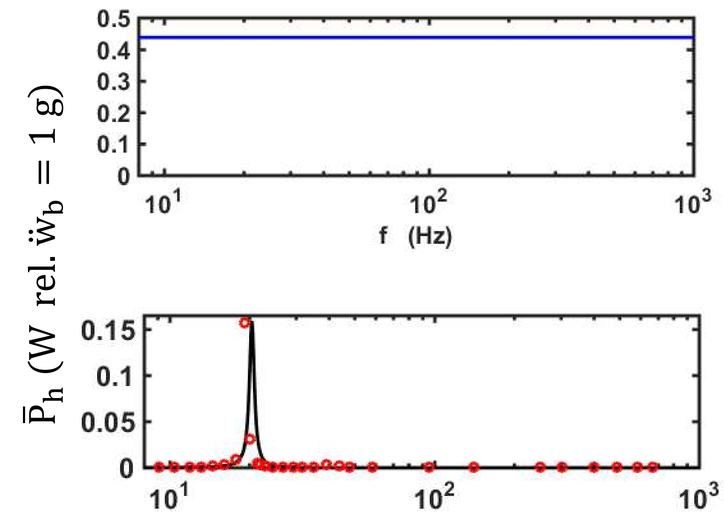

Info:
Tel. +39 0432 558035
Fax. +39 0432 507715
Indirizzo dalbo.loris@spes.uniud.it
Indirizzo paolo.gardonio@uniud.it

Dott. Loris Dal Bo
Prof. Paolo Gardonio

Riferimenti bibliografici

Comparison between electromagnetic and piezoelectric vibration energy harvesters, ISMA2016, Leuven, 19-21 September
Vibration energy harvesting with electromagnetic and piezoelectric seismic transducers: theoretical and experimental results, ECCOMAS2017, Madrid, 5-8 June
Loris Dal Bo, Paolo Gardonio, Università degli studi di Udine , Italy

UNIVERSITÀ DEGLI STUDI DI UDINE
hic sunt futura

Corso di dottorato in Ingegneria industriale e dell'informazione

XXXI Ciclo

Structural and functional blood characterization through electrical impedance sensing and optical signals analysis

From laboratory to clinic

1) Real-time thrombus formation monitoring

⟶ Consolidation of the method

TECHNICAL DETAILS

- Device (Fig. 1):
- glass slide, U-shaped gold electrodes and a SiO_2 layer
- pc chamber, artificial microchannel (width: 500 µm, height: 100 µm)
- Dynamic experiments under flow:
- substrate of thrombogenic substance
- perfusion time = 300 s, Q = 75 µl/min, $\gamma = 1500\ s^{-1}$
- Optical measurements:
- confocal laser scanning microscope
- acquisition of a 2D image sequence during the perfusion and a 3D image sequence at t = 300 s
- Electrical impedance measurements:
- high precision LCR meter (E4980A, 0.1% accuracy, Agilent), 2-wires
- frequency range of [1 kHz, 2 MHz]
- drive voltage of 100 mV

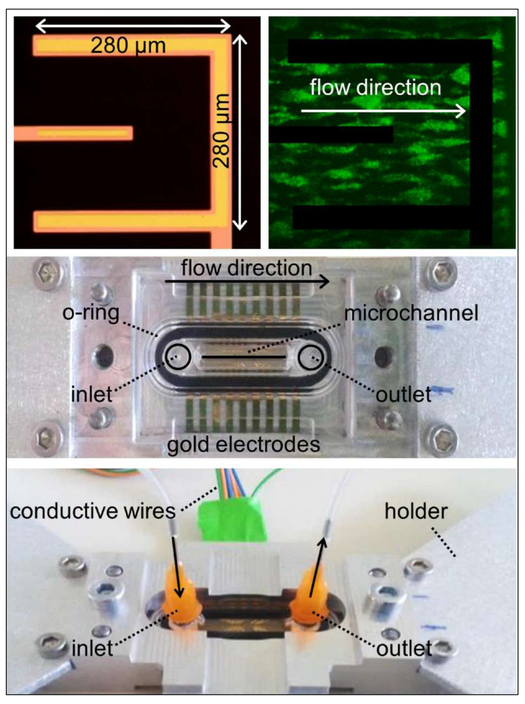

Fig. 1 Details of the device

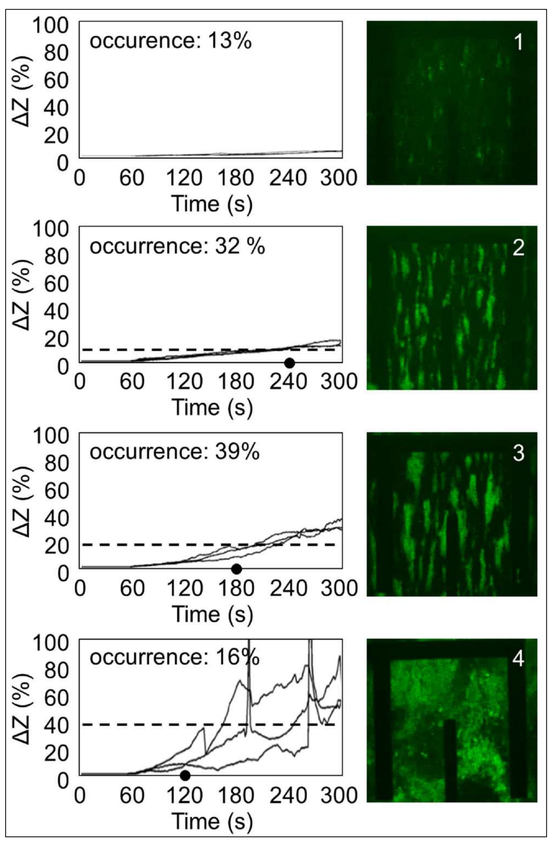

Fig. 2 Impedimetric classification of blood behavior and optical image at t = 300 s

EXPERIMENTAL RESULTS **[1-4]**

- Real-time processing (Fig. 2):
- time evolution of blood electrical properties
- classification of blood behavior
- identification of critical events
- Three-dimensional thrombus volume fast reconstruction (Fig. 3)

APPLICATION

- Point-of-Care measurements for:
- assessment, monitoring of individual thrombotic and hemorrhagic risk
- monitoring of anticoagulant and antiplatelet therapies

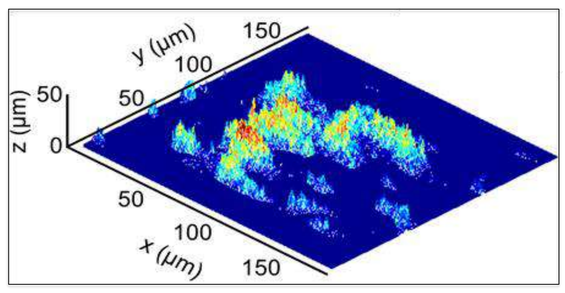

Fig. 3 Three-dimensional reconstruction of volume distribution at t = 300 s

2) Pre-analytical quality controls

⟶ Preliminary results

TECHNICAL DETAILS

- Sensor (Fig. 4):
- capacitor with parallel planar faces made of copper
- dimensions: d = 7.5 mm, l = 20 mm h = 1 mm, h' = 0.35 mm
- Samples (Fig. 5):
- whole blood (hematocrit of 38 ± 3 %)
- from the centrifugation of whole blood: blood plasma (liquid) and whole blood concentrated (red cells, white cells and platelets, hematocrit of 60 ± 3 %)
- from the centrifugation of coagulated whole blood: serum (liquid, with or without hemolysis, sometimes with fibrin white clots inside) and red clot (red cells, white cells, platelets and fibrin)
- NaCl 0.9 % (physiologic solution with high conductivity)

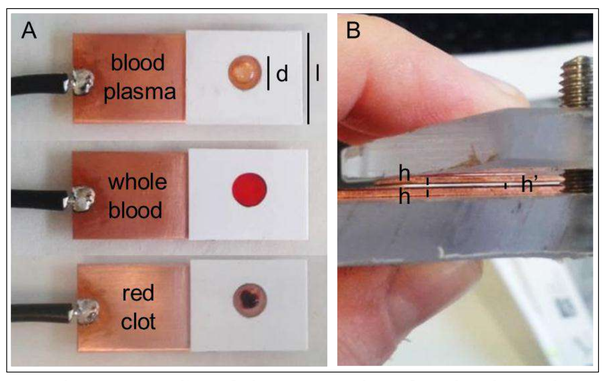

Fig. 4 Details of the capacitor for the blood impedimetric components characterization

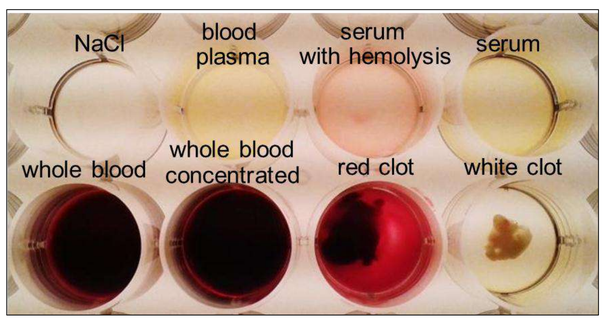

Fig. 5 Samples analyzed

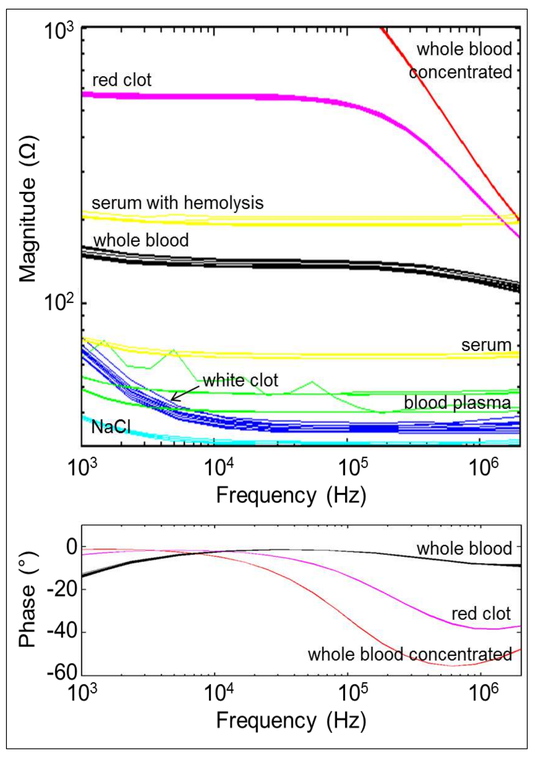

Fig. 6 Impedance signals (magnitude and phase) related to the samples analyzed

- Electrical impedance measurements:
- high precision LCR meter (E4980A, 0.1% accuracy, Agilent), 2-wires
- frequency range of [1 kHz, 2 MHz]
- drive voltage of 50 mV

EXPERIMENTAL RESULTS **[5]**

- Real-time processing (Fig. 6):
- blood components characterization
- identification of serum hemolysis
- discrimination of different amounts of cells (membrane capacitive effect)
- qualitative demonstration of the high conductivity of fibrin net

APPLICATION

- Pre-analytical quality controls in clinical laboratories:
- hemolysis quantification in serum and blood
- fast quality controls of blood before transfusion
- interferences and anomalies reduction

3) FluoLab: a new easy-to-use Graphical User Interface (GUI) for the multi-cell functional Ca^{++} signals analysis

⟶ Software development

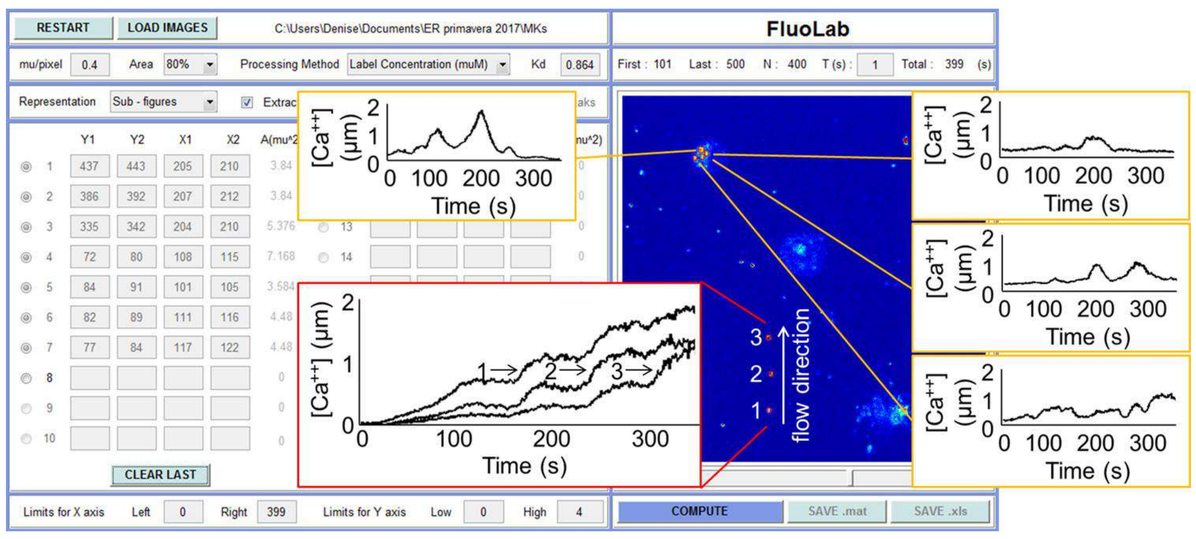

Fig. 7 FluoLab (example of extraction of Ca++ concentration)

TECHNICAL DETAILS

- Graphical User Interface (GUI) (Fig. 7):
- different cell types analysis (platelets, megakaryocytes, mesenchymal cells)
- different signal types extraction (mean representative fluorescence, dye concentration $[Ca^{++}]$, absolute or normalized signals, multi-dye analysis)
- global or regional analysis (cells, nuclei, mitochondria, granules, exosomes)

EXPERIMENTAL RESULTS **[6]**

- Fast multi-cell and multi-region Ca^{++} signals analysis:
- discovery and quantitative characterization of intra-movements and inter-communications signals
- discovery of new biological metabolic pathways
- Automatization and reduction of processing time

APPLICATION

- Bio-images analysis, metabolic multi-cell models development

Eng. Denise De Zanet [1,2]
Prof. Antonio Affanni [1]
Dr. Mario Mazzucato [2]

[1] Polytechnic Department of Engineering and Architecture, University of Udine
[2] Department of Translational Research, Stem Cells Unit, National Cancer Institute CRO – IRCCS Aviano

dezanet@cro.it +39 0434 659705
antonio.affanni@uniud.it +39 0432 558034
mmazzucato@cro.it +39

References

[1] A. Affanni, R. Specogna et al., *Combined electro-optical imaging for the time evolution of white thrombus growth in artificial capillaries*, IEEE Trans Instrum Meas, vol 62, no. 11, 2013, pp. 2954-2959

[2] A. Affanni, G. Chiorboli et al., *A Novel Inversion Technique for Imaging Thrombus Volume in MicrochannelsFusing Optical and Impedance Data*, IEEE Trans Magn, vol 50, no. 2, 2014

[3] D. De Zanet, A. Affanni, M. Mazzucato, *Misure di trombo-formazione da segnali di impedenza elettrica: identificazione di eventi critici in tempo reale*, Atti del XXXIII Congresso Nazionale dell'Associazione Gruppo Misure Elettriche ed Elettroniche – GMEE 2016, 19-21 Settembre, Benevento

[4] D. De Zanet, M. Battiston et al., *Impedance biosensor for real-time monitoring and prediction of thrombotic individual profile in flowing blood* (submitted paper)

[5] D. De Zanet, M. Battiston et al., *Blood components characterization for pre-analytical rapid quality controls through impedance measurements* (submitted extended abstract)

[6] D. De Zanet, M. Battiston et al., *FluoLab: a new easy-to-use GUI for the multi-cell functional signals analysis* (submitted extended abstract)

UNIVERSITÀ DEGLI STUDI DI UDINE
hic sunt futura

Corso di dottorato in Ingegneria industriale e dell'informazione

XXXI Ciclo

MULTI-VIEW MATCHING

PROBLEM

Given a set of object (feature) correspondences between pairs of nodes (images), the goal is to combine them in a multi-view matching, such that each object has a **unique label** in all the nodes.

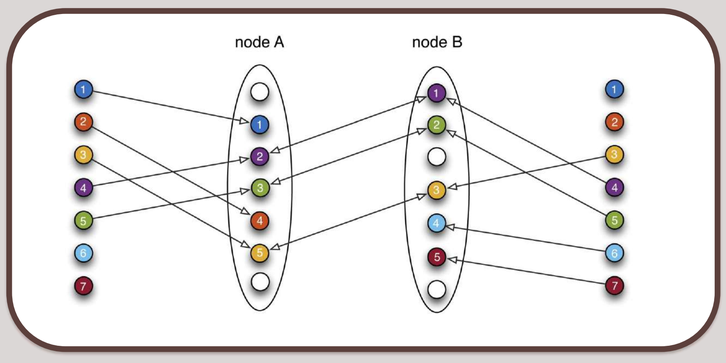

Consistency constraint

$$P_{ij} = P_i P_j^{\mathsf{T}}.$$

- P_{ij} : relative permutation of the pair (*i,j*)
- $P_i(P_j)$: absolute permutation of node *i* (*j*)

In compact form:

$$X = \begin{bmatrix} P_1 \\ P_2 \\ \dots \\ P_n \end{bmatrix} \quad Z = \begin{bmatrix} P_{11} & P_{12} & \dots & P_{1n} \\ P_{21} & P_{22} & \dots & P_{2n} \\ \dots & & & \dots \\ P_{n1} & P_{n2} & \dots & P_{nn} \end{bmatrix} \Rightarrow \quad Z = XX^{\mathsf{T}}$$

PROPOSED SOLUTION AND RESULTS

PARTIAL PERMUTATIONS SYNCHRONIZATION (*PARTIALSYNCH*)

The problem of finding the global labeling can be modeled as recovering **absolute permutations**, assuming that a set of relative permutations is known.

Optimization Problem

$$\max_{P_1,\dots,P_n \in \mathcal{S}_d} \sum_{i,j=1}^{n} \operatorname{trace}\left(P_{ij}^{\mathsf{T}} P_i P_j^{\mathsf{T}}\right) \iff \max_{X \in \mathcal{S}_d^n} \operatorname{trace}\left(X^{\mathsf{T}} Z X\right)$$

The solution [1] retrieves partial absolute permutations via:

I. Eigenvalue decomposition
II. Clustering with *k-means*
III. Projection through the Kuhn-Munkres algorithm.

Accuracy
Synthetic experiments

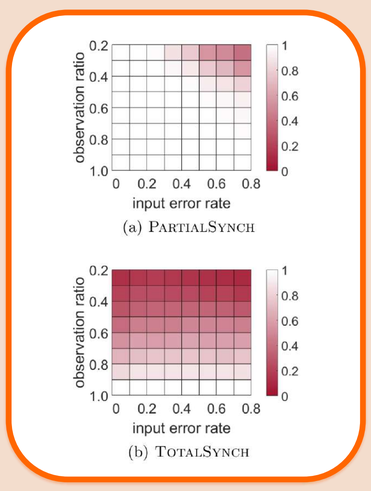

Precision
Real datasets

Data	PartialSynch [1]	TotalSynch
Fountain-P11	95.4	43.6
Herz-Jesu-P8	93.6	50.7

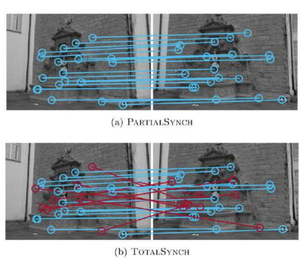
(a) PartialSynch

(b) TotalSynch

The method correctly recovers absolute permutations even when not all the objects are seen in every node and in the presence of **noise**.

FAST EIGENVALUE SOLUTION (*MATCHEIG*)

The method aims at finding **relative permutations** (independent from the size of the universe) instead of absolute permutations.

Optimization Problem

$$\max_{Z} \langle \widehat{Z}, Z \rangle = \max_{Z} \operatorname{trace}(\widehat{Z} Z^{\mathsf{T}}) \quad \text{s.t. } Z = XX^{\mathsf{T}}$$

The algorithm [2] computes the top eigenvectors of the matrix containing pairwise correspondences and projects them onto permutations through a greedy strategy to yield the output pairwise matches.

Computing time

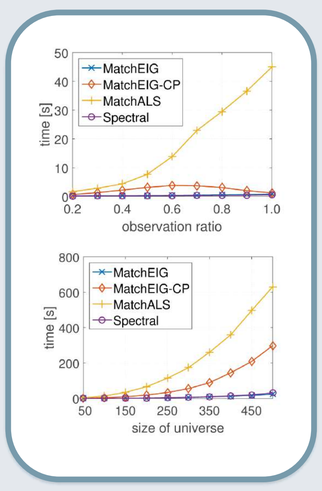

Precision
Real datasets

Dataset	n	$\bar{d}$	Input PR [%]	MatchEIG [2] PR [%]	MatchEIG [2] CM	MatchEIG [2] time [m]	MatchALS PR [%]	MatchALS CM	MatchALS time [m]
Herz-Jesu-P8	8	386	94.40	**95.08**	4545	< 1	94.87	4047	2
Entry-P10	10	432	75.11	**79.24**	5978	5	74.17	5726	4
Fountain-P11	11	374	94.35	**94.70**	6988	3	94.15	6717	3
Castle-P19	19	314	70.29	**75.21**	5109	3	66.22	7014	9
Herz-Jesu-P25	25	517	90.20	**93.45**	25120	7	89.23	32528	41
Castle-P30	30	445	72.32	**81.01**	16754	8	68.92	24844	57
Temple Ring	47	396	73.72	**88.25**	18426	6	55.91	40096	260
Dino Ring	48	340	75.37	**92.11**	23406	2	66.66	44215	94
Temple	312	689	55.50	**89.06**	379545	153	–	–	–
Dino	363	493	63.48	**95.66**	862221	88	–	–	–

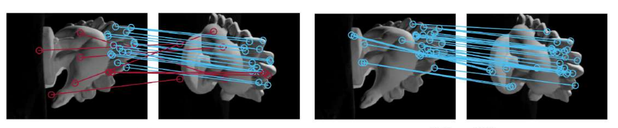
(a) Input (b) MatchEIG

Extremely simple and fast method, accuracy is comparable or superior to the state of the art, **large scale** datasets can be handled.

Dott. Eleonora Maset
Prof. Andrea Fusiello
Prof. Fabio Crosilla

Info:
maset.eleonora@spes.uniud.it
andrea.fusiello@uniud.it
fabio.crosilla@uniud.it

Acknowledgment

We wish to thank Helica s.r.l. for funding this PhD project.

References

[1] Arrigoni F., Maset E. and Fusiello A., *Synchronization in the symmetric inverse semigroup*. ICIAP 2017, submitted.

[2] Maset E., Arrigoni F. and Fusiello A., *Practical and efficient multi-view matching*. ICCV 2017, submitted.

[3] Maset E., Fusiello A., Crosilla F., Toldo R. and Zorzetto D., *Photogrammetric 3D building reconstruction from thermal images.* UAV-g 2017, submitted.

[4] Maset E., Crosilla F. and Fusiello A., *Errors-in-Variables Anisotropic Extended Orthogonal Procrustes Analysis*. IEEE Geoscience and Remote Sensing Letters, 2016.

[5] Crosilla F., Maset E. and Fusiello A., *Procrustean Photogrammetry: From Exterior Orientation to Bundle Adjustment .* New Advanced GNSS and 3D Spatial Techniques, 2016

UNIVERSITÀ DEGLI STUDI DI UDINE
hic sunt futura

Corso di dottorato in Ingegneria industriale e dell'informazione

XXXI Ciclo

LEAN HEALTHCARE:
evaluating functional and technical outcomes from both physicians' and patients' perpective

Lean Strategy and Lean Application in Healthcare
In healthcare system, Lean Strategy is to develop systematic approaches for defining value that integrate both the knowledge and clinical expertise of healthcare providers and the patients' preferences and needs. Lean applications in healthcare tend towards a tool-based approach for operational problems, with little attention paid to defining value from the patients' perspective (Radnor et Al., 2012).

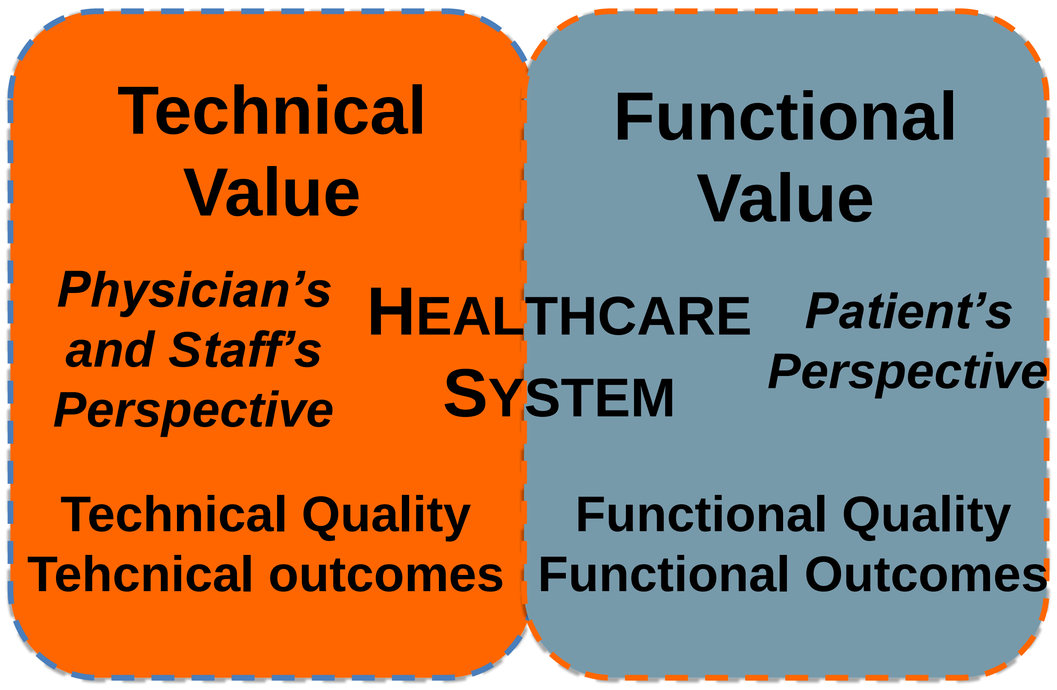

Importance of the Research
It must be noted that value is a more complex construct in healthcare than in other settings, whereas customers in other contexts may have the ability to determine the value they experience, this is far from the case in the healthcare context. Although patients can perceive the value of healing or being treated with respect, the nature of healthcare is such that good care does not always produce good health outcomes and viceversa (Poksinska et Al., 2017).
In order to have a more precise definition, value in healthcare should be co-defined by patients, who have their own preferences and experiential needs (functional quality) and by professionals, who can tell whether treatment is in line with latest evidence (technical quality). The patient sphere is not seen as an arena for value creation and is thus overlooked (Poksinska et Al., 2017). The newest suggestion in literature is to carry out service and healthcare improvements by both inside-out and outside-in perspective.

Gap
Lean interventions aim to improve quality by reducing waste and facilitate flow in care processes.
Most of the research on hospital quality is dominated by questions of **what** and does not go further to investigate the **how**, **when** and **why** (just content not context).
Success is dependent on how an organization utilizes, combines and sequences organizational resources and routines (Andersen et Al., 2017).

Research Proposal
Scientific Literature assume that too often lean is treated as a cost-cutting or efficiency approach, mitigating the opportunity to improve overall care. For being successful, lean tools must be considered as a part of a comprehensive management system.
Furthermore the perspective of the patient is not always considered in order to identify functional outcomes and value actions. For this reasons, the research is focused on:

1. Considering lean interventions by using the two dimensional framework proposed by Andersen et Al, 2017 (readiness of the system in embracing lean philosophy);
2. Identifying the functional and technical outcomes of quality from the perspective of the patient and also of the physicians and his staff;
3. Implementing lean strategy and lean tools suitable for the public healthcare system (hospital) by some kaizen projects in selected departments;
4. Analysing the results obtained by kaizen actions thanks to the two dimensional framework by Andersen et Al. (2017) and in terms of technical (physicians' perspective) and functional outcomes (patients' perspective).

Methodology
Action research in collaboration with the University Hospital of Udine.

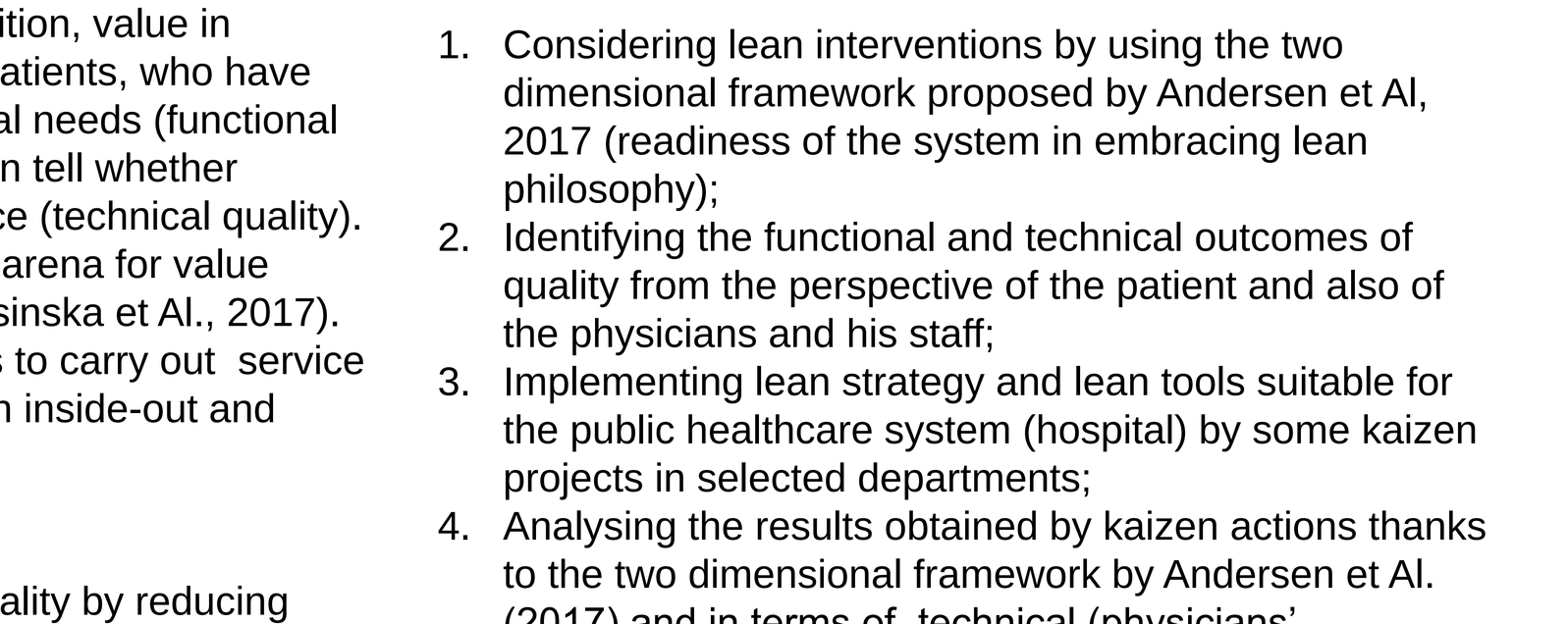

Dott.ssa Elisabetta Ocello
Prof. Alberto F. De Toni
Prof. Pietro Romano

Info:
Tel. +39 0432 558043
ocello.elisabetta@spes.uniud.it

UNIVERSITÀ DEGLI STUDI DI UDINE
hic sunt futura

Corso di dottorato in Ingegneria industriale e dell'informazione

XXXI CICLO

Development and characterization of a Soft X-Rays Imager Detector for FEL

Motivation and Goals

The growing brilliance of the 3rd generation synchrotron as well as the advent of the Free Electron Laser (FEL) source have significantly increased the demands for X-ray detectors[1][2]. **The topic of this PhD** (funded by ELETTRA, Trieste) concerns the development and characterization of a detector that is supposed to meet these new challenges[3]: **PERCIVAL** (Pixelated Energy Resolving CMOS Imager Versatile And Large) that is a soft X-ray imager under development as a collaboration project between DESY, STFC/RAL, ELETTRA, DIAMOND and PAL light sources.

The most important performances [4] of the PERCIVAL detector are:

- Energy range **250eV - 1keV** (*primary*); **100eV - 3keV** (*extended)*
- Quantum Efficiency over *primary* energy range >85%
- Pixel Size of 27 (prototypes: 25) μm
- Sensor size 2M - 1408x1484 pixels, 4x4cm^2 ; 13M - 3520x3710 pixels, 10x10cm^2
- Noise RMS: 15e$^-$
- "Full Well" > 10^7e$^-$
- Resulting Dynamic Range 10^5 photons at 250eV
- Exposure modes: - FEL, all photons in < 300 fs (150fs for FERMI)
  - synchrotron, quasi-continuous

PERCIVAL: the Sensor and the System

- 4x4cm^2 active imaging area
- Fast LVDS readout (~125 lines at ~460MHz)
- 28000 ADCs
- PGA (Programmable Gain Amplifier) stage
- 15 bit/pixel (12+1bit ovverange+2 bit gain)
- 2 FPGA-based data acquisition boards are in air
- Data streamout through nr.8 10Gbit ethernet
- Back-thinned sensor
- Back illuminated sensor

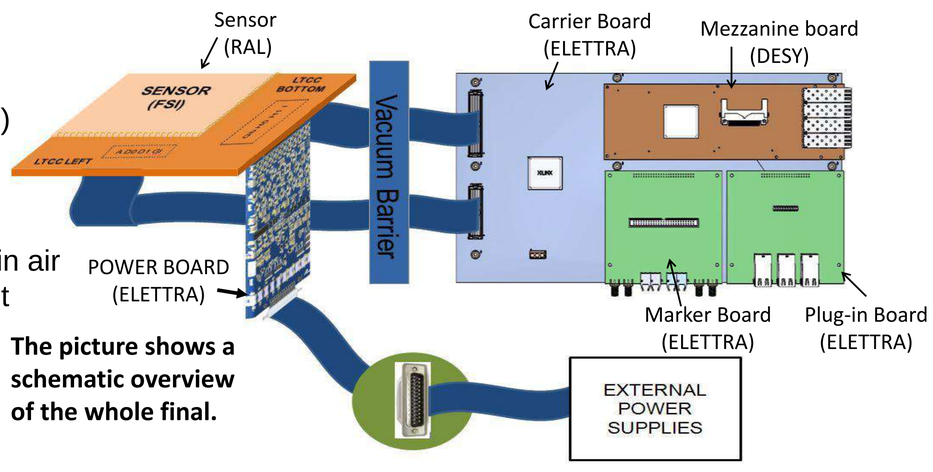

The picture shows a schematic overview of the whole final.

Example of measurement with pinhole @91.84eV

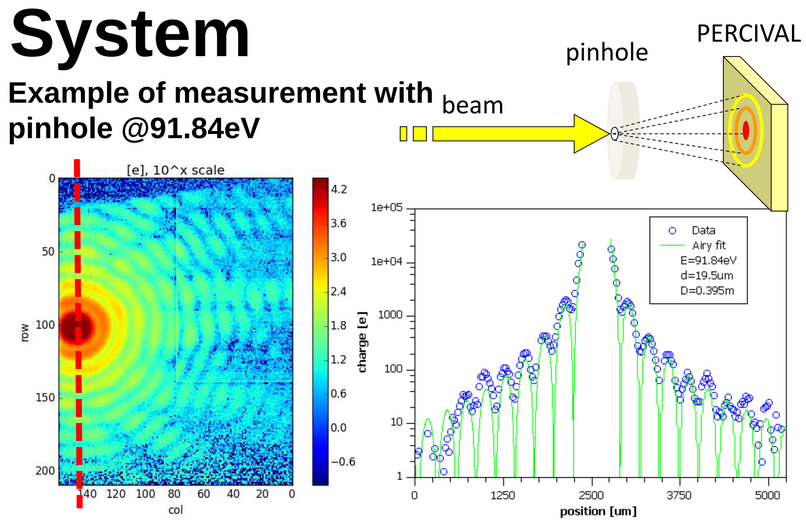

Pinhole diffraction pattern

Collected charge of the pattern on column Nr.150

Simulations and alternative strategies

To evaluate the main features of the pixel, numerical **simulations using Sentaurus TCAD tool** are been performed.
The figures show the 3D pixel model and rappresantive current waveform.

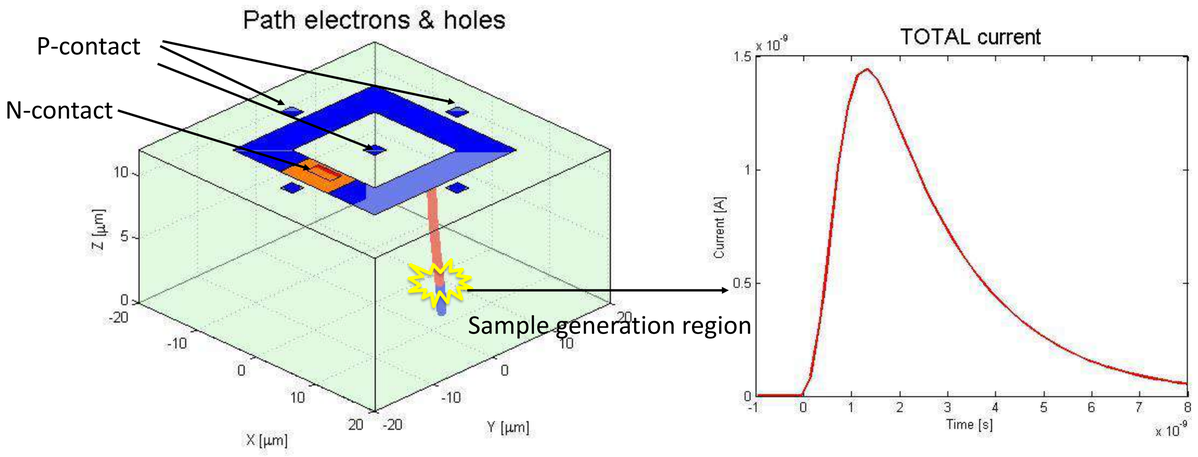

The 3D pixel model with the path of electrons (red) and holes (blue) after the generation and the associated current pulse at the terminals.

Since transient simulations are **very time comsuming** we are investigating another approach based on **Ramo's Theorem.** Example of application of a 1D P-I-N Diode.

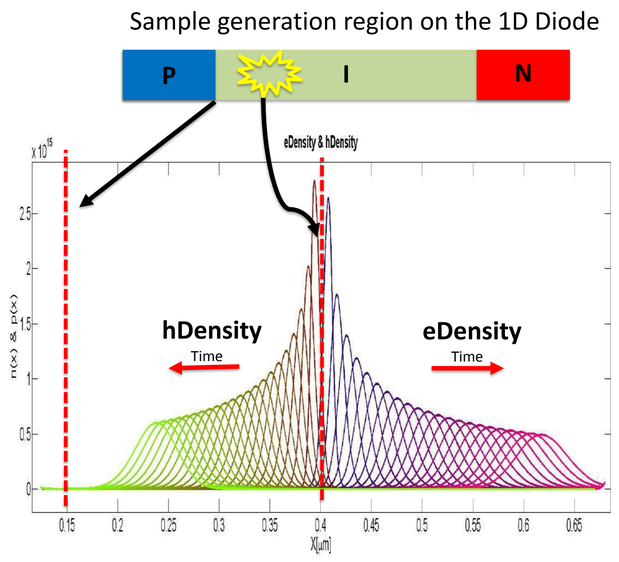

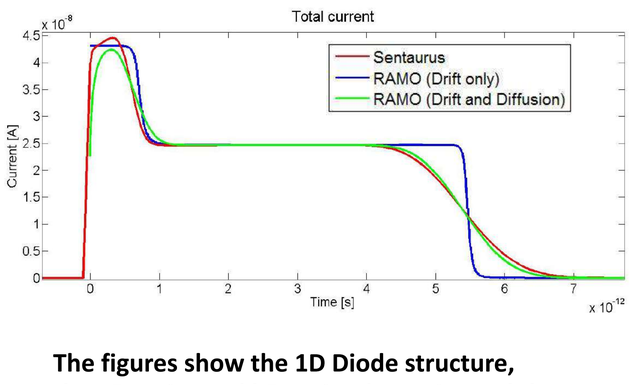

The figures show the 1D Diode structure, the eDensity and hDensity dynamics and the comparision between the corresponding current pulse from TCAD Simulation and output of the RAMO's theorem including or not the effects of charge diffusion.

The PowerBoard: Design & Measurements

Main design specs:

- Cooling constraints (componets temperature range is down to -40 °C)
- Design cooling oriented
- Supply the full sensor
- 19 different programmable current sources with μA accuracy
- 14 different programmable voltage reference sources
- 5 different voltage supplies
- Monitoring of voltage and current for each source (72 ADC channels)
- 12 layers
- ~15 W power consumption

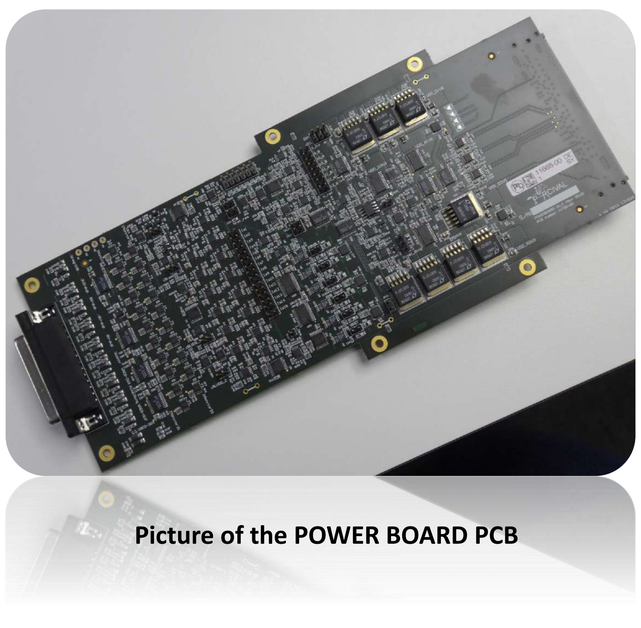

Picture of the POWER BOARD PCB

First Tests: Programmable voltage source
The figures show a scheme of the circuitry and the monitored values (ADC) of a controlled voltage source output.

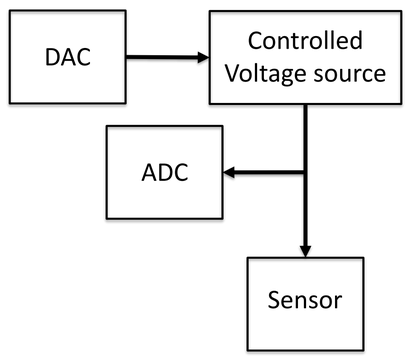

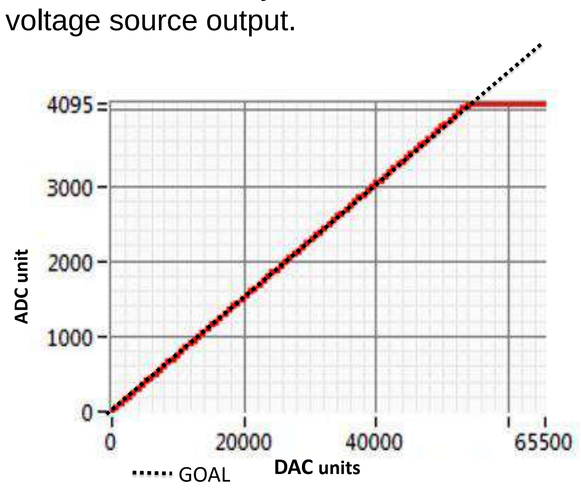

Dott. Giovanni Pinaroli
Prof. Pierpaolo Palestri
Info:
Tel. +39 040 3758310
mail: pinaroli.giovanni@spes.uniud.it
mail: giovanni.pinaroli@elettra.eu

References

[1]C.B. Wunderer et al., The PERCIVAL soft X-ray imager, J. Instrum. 10 (2015) C02008.
[2] C.B. Wunderer et al., Percival: An International Collaboration to Develop a MAPS-based Soft X-ray Imager, Synchrotron Radiat. News 27 (2014).
[3] J. Correa et al., Latest results of the PERCIVAL Soft X-Rays Imager, 17th INTERNATIONAL WORKSHOP ON RADIATION IMAGING DETECTORS (2015).
[4] M. Viti et al., Spatial resolution studies for the PERCIVAL sensor, 16th INTERNATIONAL WORKSHOP ON RADIATION IMAGING DETECTORS (2014).

Awards

- Internship at DESY, Hamburg, Germany, 2 mounth
- Internship at BESSY, Berlin, Germany, 1 mounth

UNIVERSITÀ DEGLI STUDI DI UDINE
hic sunt futura

Corso di dottorato in Ingegneria industriale e dell'informazione

XXXI CICLO

HIGH VOLTAGE DISTRIBUTION SYSTEM IN DATA-CENTER

ABSTRACT

- Today the total power consumption of data centers is becoming noticeable
- How to improve the overall efficiency?
  - Reduce conversion steps
  - Use high voltage as you can
- Energy management has become a key issue for data center → ideally no consume power when idle and gradually more power as the computation increase
- DC distribution in data center has different voltage standards
  - **12Vdc**
  - **48Vdc**
  - **380Vdc (more promising in terms of overall efficiency)**
- Output voltage 1.8V and the output current 350A with high current slew rate
- VRM designed on motherboard → high power density

VRM FROM 48V

- ZVS at primary and secondary side
- Constant ON time phase shift at primary side
- Fast phase shedding implementation
  - **High efficiency in a high range of load**

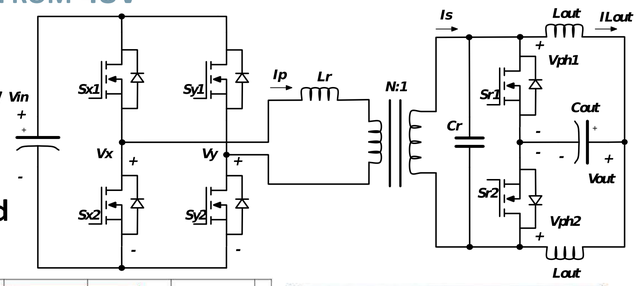

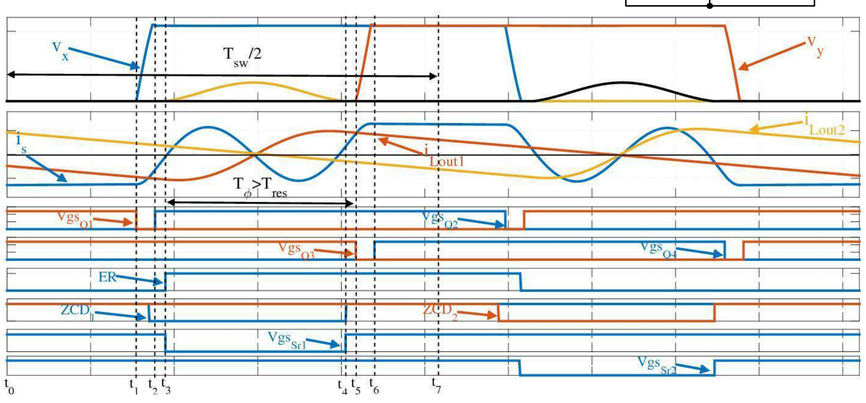

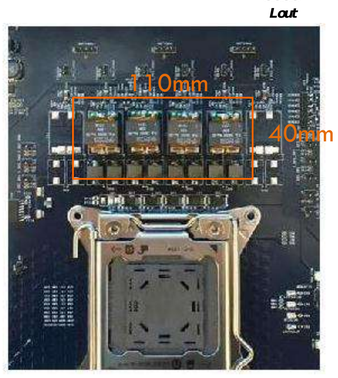

- Higher power density with integrated magnetics

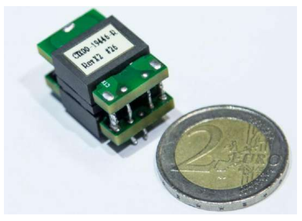

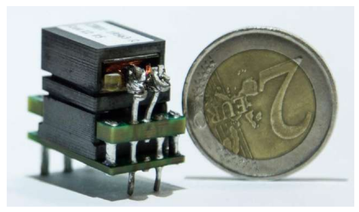

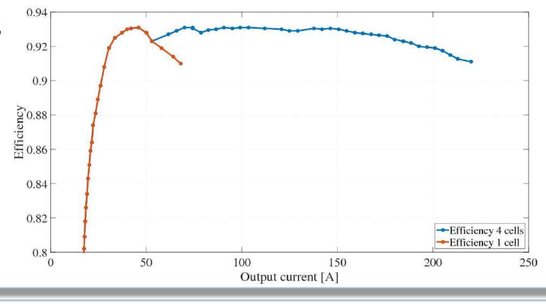

DC-DC RESONANT CONVERTER 380V TO 12V

- Solution 380V to 12V regulated
- Based on resonant topology with center taped rectifier
- N=8.5, $L_r = 48.8\mu H,\ L_{out} = 1.8uH,\ C_r = 127nF,\quad ON_{time} = 2000n\ s$
- Control system at secondary side
- Secondary side MOS related 120V
- Primary side MOS related 550V (STL33N60DM2)

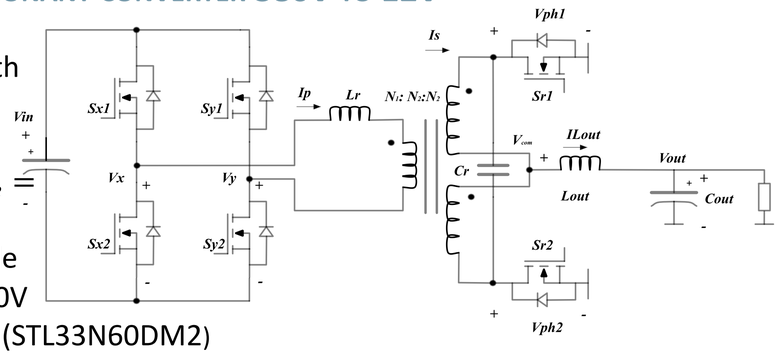

THERMAL CAMERA

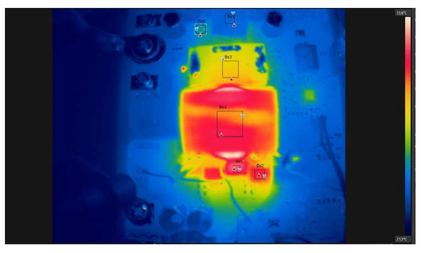

- @0A $T_{core} = 52°C$, $T_{pri,MOS} = 54°C$, $T_{sec,MOS} = 35°C$

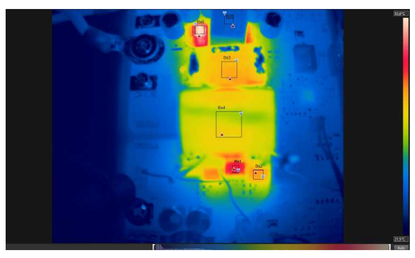

- @50A $T_{core} = 57°C$, $T_{pri,MOS} = 67°C$, $T_{sec,MOS} = 80°C$

EXPERIMENTAL RESULTS

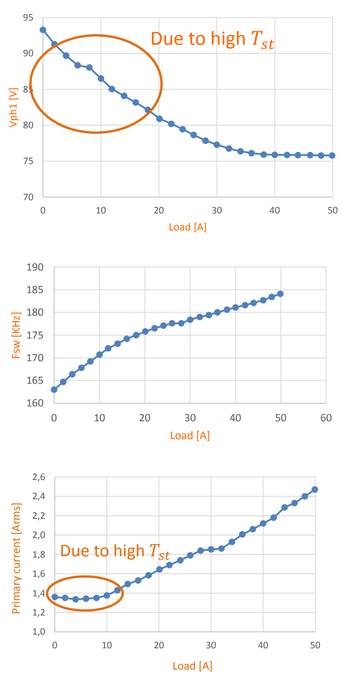

PROTOTYPE

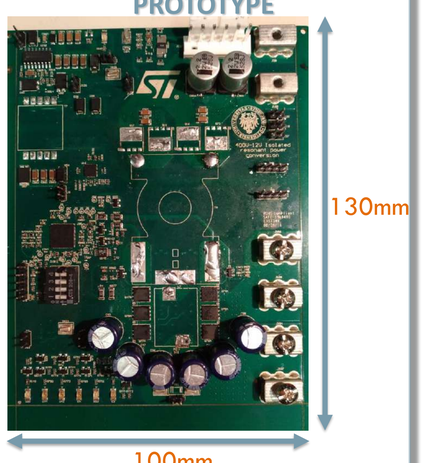

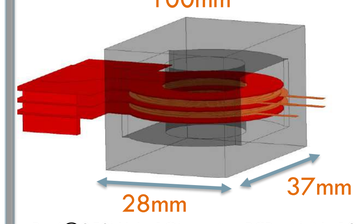

Rac(@250kHz)=1Ohm using PCB with N=10
Rac(@250kHz)=600mOhm using litz wire with N=8.5

ZVS PRIMARY AND SECONDARY SIDE

- ZVS at primary and secondary side
- Low RMS current primary side
- High V_{pk} for resonance voltage
- High circulating current due to high C_{oss}

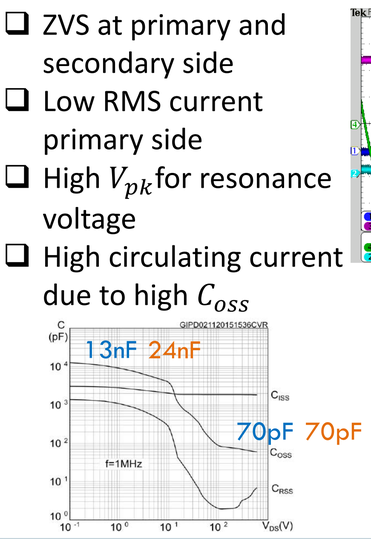

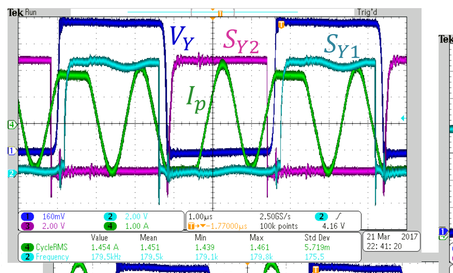

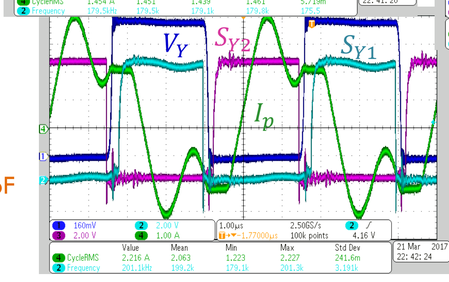

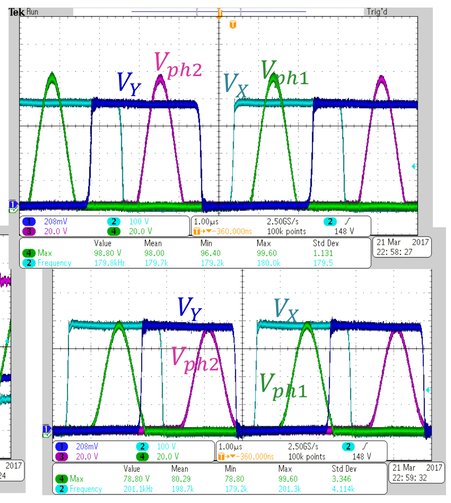

EXPERIMENTAL RESULTS

- Good dynamic performance
- High losses due to high C_{oss} MOS at primary side
- Efficiency improvement using *GaN*
- Transformer bottleneck
- Rectification problem
- Driving system primary side to be improved

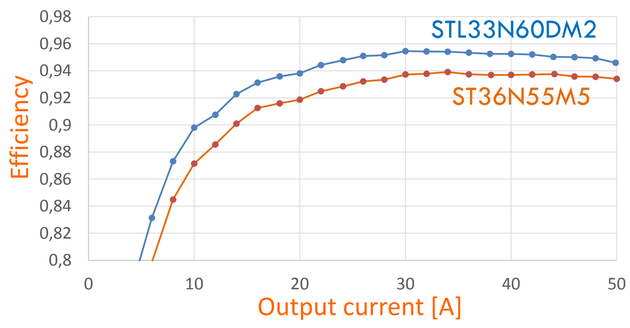

ISOLATED RESONANT MULTILEVEL MULTIPHASE TOPOLOGY FOR 380V VRM APPLICATIONS

- Buck derived topology that can performs a VRM function
- High efficiency due to ZVS primary and secondary side
- Half-bridge multilevel structure in phase-shift constant ON time
- Multilevel structure (primary MOS 250V related)
- Lower transformer turns ratio
- High power density solution closed to POL
- $I_{Lr,rms} = 400mA\ @\ I_{out} = 0A$
- $I_{Lr,rms} = 1.25A\ @\ I_{out} = 60A$

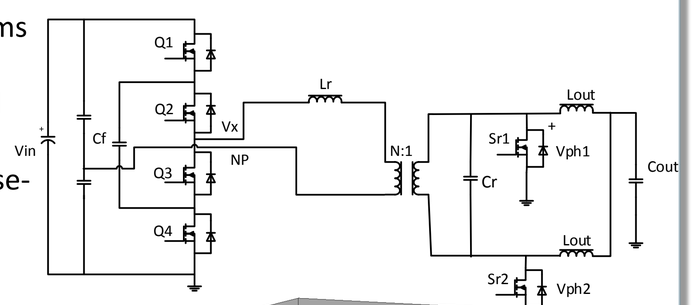

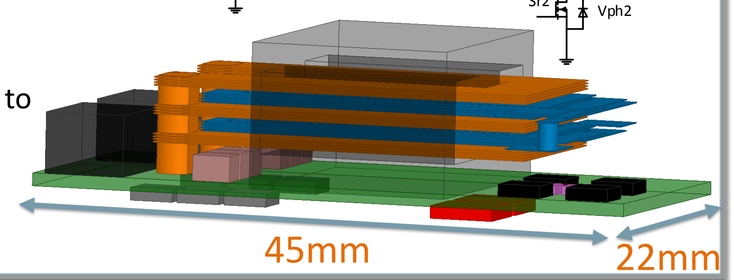

CONTROLS SYSTEM

- $I_{out} = 120A$ (2 cells implemented)
- Low frequency variation changing I_{out}

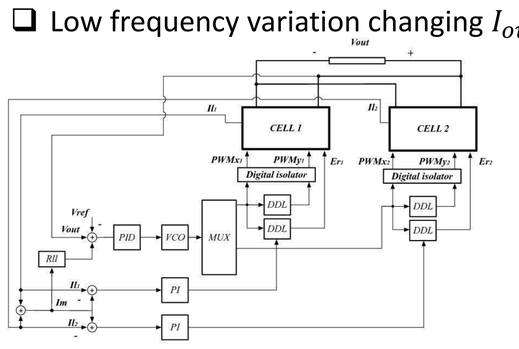

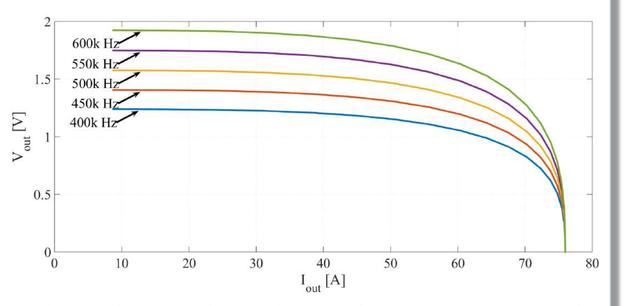

- Voltage loop is based on a frequency control
- Current sharing will be implemented

TRANSFORMER IMPLEMENTATION AND EFFICIENCY ESTIMATION

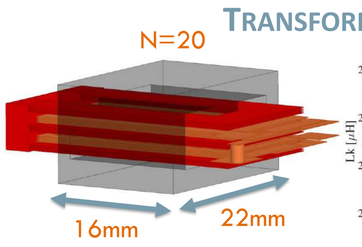

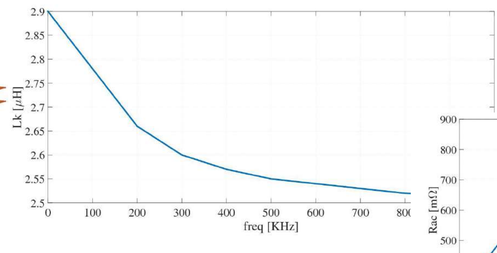

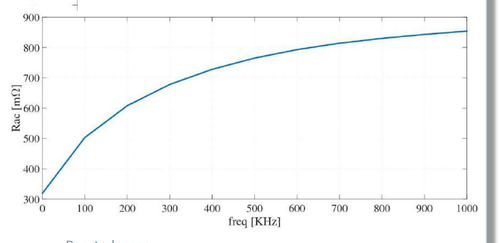

- 20 layers 70µm
- C_w<50pF

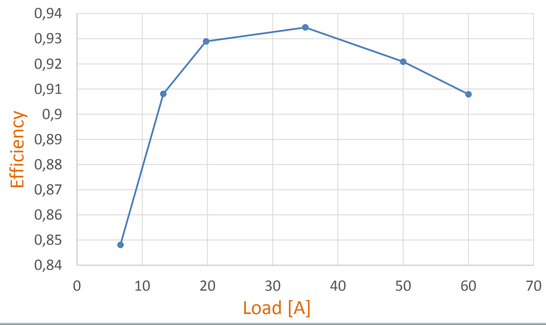

Pareto losses

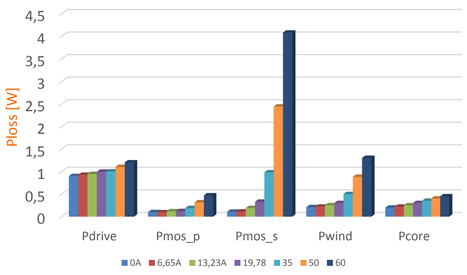

RESULTS AND ACTIVITIES

- VRM from 48V with 93.4% of efficiency
- 380V to 12V with 95.5% of efficiency
- Improve efficiency dc-dc resonant converter 380V to 12V up to 97%
- Prototype from 380V to POL will be realized based on multilevel resonant topology

Dott. Roberto Rizzolatti
Prof. Stefano Saggini
Info:
Email:
rizzolatti.roberto@spes.uniud.it
stefano.saggini@uniud.it

[1] L. A. Barroso and U. Holzle, "The Case for Energy-Proportional Computing," IEEE Journal of Computer Society, pp. 33 37, Dec 2007.
[2] M. Salato, A. Zolj, D. J. Becker, and B. J. Sonnenberg, "Power System Architectures for 380V DC Distribution in Telecom Datacenters," Int. Telecommunications Energy Conf. (INTELEC) 2012, Oct. 2012.
[3] P. Alou, J. A. Oliver, O. Garcia, R. Prieto and J. A. Cobos, "Comparison of current doubler rectifier and center tapped rectifier for low voltage applications," Twenty-First Annual IEEE Applied Power Electronics Conference and Exposition, 2006. APEC '06., Dallas, TX, 2006, pp. 7 pp.
[4] Jian Sun, K. F. Webb and V. Mehrotra, "Integrated magnetics for current-doubler rectifiers," in IEEE Transactions on Power Electronics, vol. 19, no. 3, pp. 582-590, May 2004.
[5] Paul Yeaman, and Eduardo Oliveira, "A High Efficiency High Density Voltage Regulator Design Providing VR 12.0 Compliant Power to a Microprocessor Directly from a 48V Input", Proc. IEEE Applied Power Electronics Conf. and Expo. APEC'13, pp. 410-414, 2013.
[6] Osvaldo Zambetti, Mattia Colombo, Salvatore D'angelo, Stefano Saggini, Roberto Rizzolatti,"48V to 12V Isolated Resonant Converter with Digital Controller", APEC2017
[7] Stefano Saggini, Osvaldo Zambetti, Roberto Rizzolatti, Alessandro Zafarana, Paolo Saccon, " Isolated Resonant Full-Bridge Converter with Magnetic Integratio", APEC2017
[9] Yeaman, Paul, "High Current, Low Voltage Solution For Microprocessor Applications from 48V Input." PCIM Europe, May, 2007.

UNIVERSITÀ DEGLI STUDI DI UDINE
hic sunt futura

Corso di dottorato in Ingegneria industriale e dell'informazione

XXXI CICLO

Kirchhoff's Laws and Energy Minimization in NCFETs

① Context: Era of Dark Silicon[1]

- Today's electronics has to be highly energy-efficient to meet requirements of severely energy constrained applications that developing in the Internet of Things scenario.
- **Dark Silicon**: to meet power constraints in ICs, a large fraction of the chips is underclocked and underpowered.
- To reduce power consumption, without degrading dynamic performances, new device concepts are required.
- A promising device is the **Ferroelectric Negative Capacitance Field Effect Transistors (NCFETs)** [2]

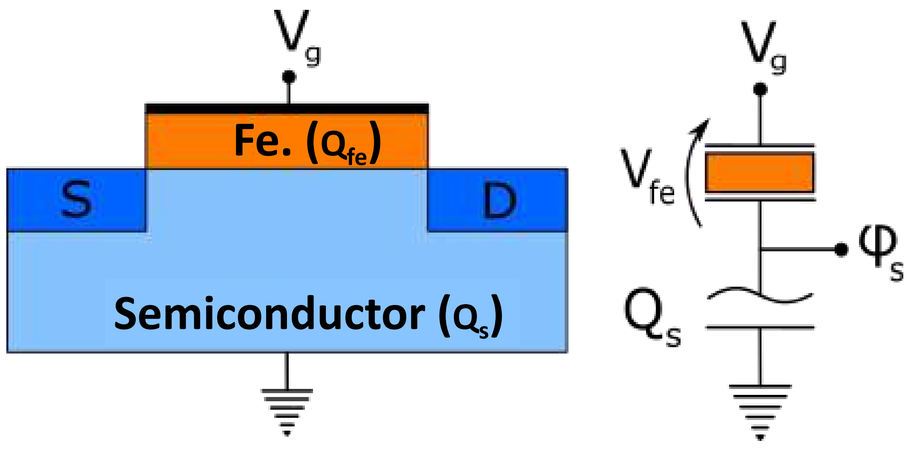

② Minimization and Kirchhoff's law in Ferroelectric NCFETs

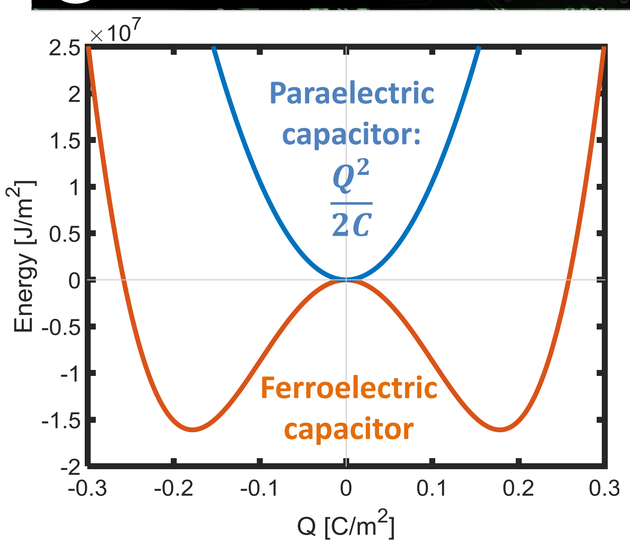

- For ferroelectric capacitors the static voltage-charge relation $V_{fe}(Q_{fe})$ is obtained by **minimizing the total Gibb's energy** (resulting in the steady-state Landau-Khalatnikov Equation -LKE-):

$$\frac{\partial U_{fe}(Q_{fe})}{\partial Q_{fe}} = 0 = \frac{\partial}{\partial Q}\left[\left(aQ_{fe}^2 + bQ_{fe}^4 + cQ_{fe}^6\right) t_{fe}\right] = V_{fe}(Q_{fe})$$

- For conventional semiconductor capacitors, instead, the voltage-charge relation $\varphi_s(Q_s)$ is obtained by solving the Poisson equation with appropriate expressions for the carrier concentrations
- In the NCFET, what approach should be used to analyse gate stacks consisting of both ferroeletric and non-ferroeletric materials ?

→ **Minimization of the NCFET energy** *VS* **enforcement of Kirchhoff's laws** (almost universally employed[3-4])

③ Theoretical framework

- 1st approach: Kirchhoff's voltage law for the series of capacitors
  a) equate the shared charge: $Q_{fe} = Q_s = Q$;
  b) Kirchhoff's voltage law: $V_{fe}(Q) + \varphi_s(Q) = V_g$ (1) ➡ solve for Q

  BUT: Does Q from Eq.1 minimize the total energy of the system ? [5]

- 2nd approach: obtain Q by minimizing the overall Gibb's energy

$$\underbrace{\frac{\partial}{\partial Q}\left[\left(aQ^2 + bQ^4 + cQ^6\right) t_{fe}\right]}_{\text{LKE}} + U_s(Q) - QV_g = 0 \quad (2)$$ ➡ solve for Q

  where QV_g is the energy of the stimulus and $U_s(Q)$ the energy of the semiconductor.

  BUT: Does *Q* from Eq.2 to satisfy Kirchhoff's voltage law?

- The energy delivered to the semiconductor (or any capacitor) is:

$$U_s(Q) = \int_0^{+\infty} (Power)dt = \int_0^{+\infty} (\varphi_s(t) \cdot dQ/dt)\, dt = \int_0^{Q} \varphi_s(q)\, dq$$

$$\Rightarrow \boldsymbol{\partial U_s/\partial Q = \varphi_s(Q)}$$

MAKES

Eq.2 equivalent to **Eq.1**

⇒ **APPROACH 2** equivalent to **APPROACH 1**

④ Numerical validation

- Results of *ad-hoc* NCFET Schrödinger-Poisson numerical simulator [6]:

1st approach (Poisson)

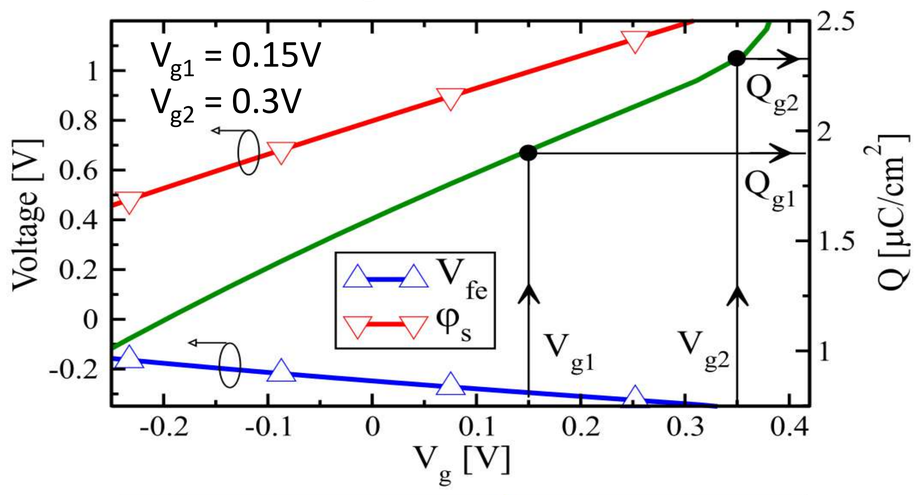

2nd approach (Energies)

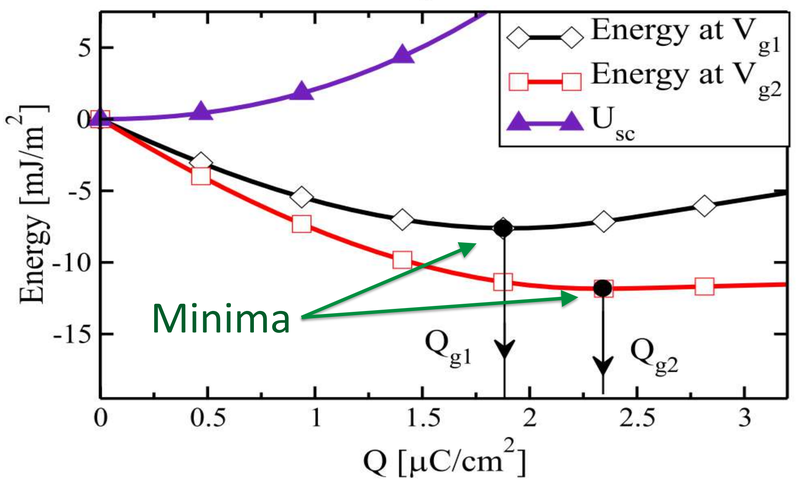

→ At a chosen V_g, the corresponding charge Q_g computed from the Poisson simulator identifies univocally the total energy minimum [7].

Dott. Tommaso Rollo
Prof. David Esseni

Info:
Tel. +39 0432 558261
rollo.tommaso@spes.uniud.it
david.esseni@uniud.it

References:
[1] M. B. Taylor, DAC, 2012.
[2] S. Salahuddin et al., Nano Letters, 2008.
[3] S. Khandelwal et al., IEEE EDL 2017.
[4] Saedi et al., IEEE TED, 2016.
[5] K. Majumdar et al., IEEE TED, 2016
[6] T. Rollo et al., ESSDERC, 2016.
[7] T. Rollo et al., IEEE EDL, 2017.

UNIVERSITÀ DEGLI STUDI DI UDINE
hic sunt futura

Corso di dottorato in Ingegneria industriale e dell'informazione

XXXI Ciclo

DYNAMIC MODELING AND SIMULATION OF FLEXIBLE MULTIBODY SYSTEMS

Why modeling flexible multibody systems?

- Nowadays, in industrial robotics the demand for better performances and higher speed operations is increasing.
- Due to the dynamic effects of structural flexibility that arises in lightweight systems, design and control become more difficult and challenging.
- For these reasons, accurate dynamic models of flexible multibody mechanisms and manipulators are needed.

Equivalent Rigid-Link System (ERLS) formulation

- In the last years a formulation based on an ERLS has been developed and applied for several purposes [1].
- This approach is suitable in the case of large displacements and small elastic deformations.
- It enables the kinematic equations of the ERLS to be decoupled from the compatibility equations of the displacement at the joints.
- The absolute position vector $\mathbf{p}_i$ of a generic point inside the *i*-th finite element is given by: $\mathbf{p}_i = \mathbf{e}_i + \mathbf{u}_i$ where $\mathbf{u}_i$ is the nodal displacement vector and $\mathbf{e}_i$ the nodal position vector of a point of the *i*-th element of the ERLS (Fig.1).

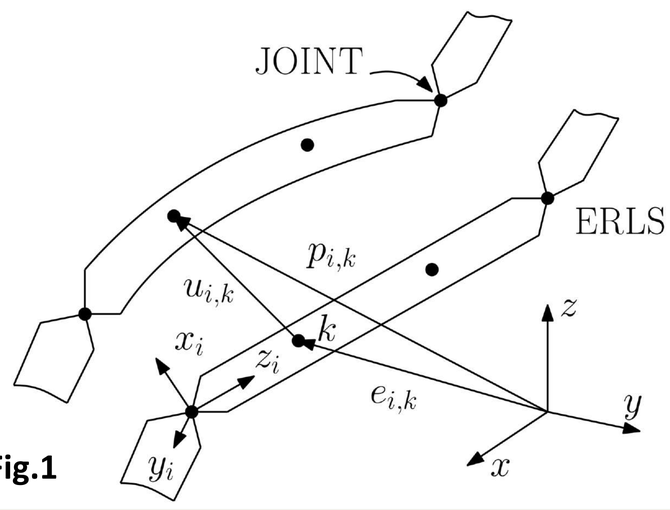

Fig.1

Comparison between Finite Element Method (FEM) and Component Mode Synthesis (CMS) approaches

- The ERLS approach, firsly exploited through a FEM approach [2], has been recently extended through a modal formulation, i.e. CMS technique [3], so as to obtain a more flexible solution based on a reduced-order system of equations.
- The two formulations have been compared by means of numerical simulations on a L-shape mechanism (Fig.2).
- The results have been evaluated in terms of dynamic behaviour and computational time (more than 80% of reduction with 14 considered vibration modes).

Comparison of Model Order Reduction Techniques

- The ERLS approach has been implemented in combination with different reduction techniques (i.e. Craig-Bampton, Interior Mode Ranking, Guyan, Least Square Model Reduction and Mode Displacement Method) [4].
- These techniques have been applied to a L-shaped system under different input conditions (gravity and step torque).
- The accuracy of the models has been numerically evaluated through a comparison in frequency domain (Fig.3), computational time and by means of modal vector correlation methods, i.e. MAC, NCO, CO (Fig.4).

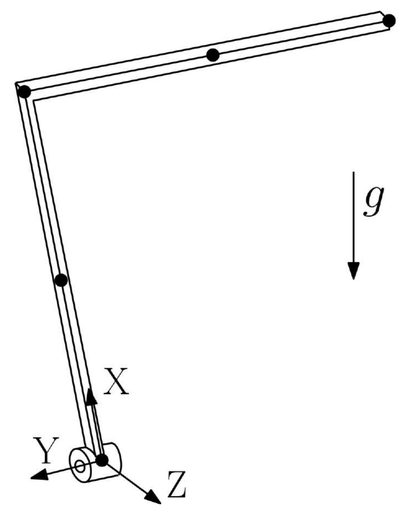

Fig.2

Future developments

- Comparison of Model Order Reduction Techniques on a two (or more) degrees-of-freedom mechanism.
- Experimental tests.
- Development of real-time control systems for flexible-link robots.

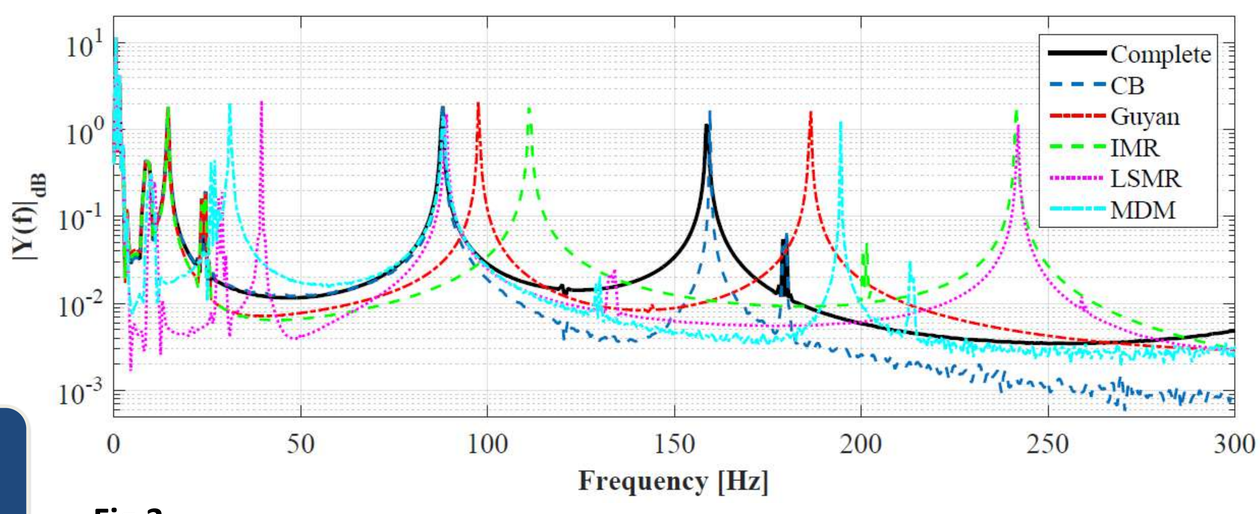

Fig.3

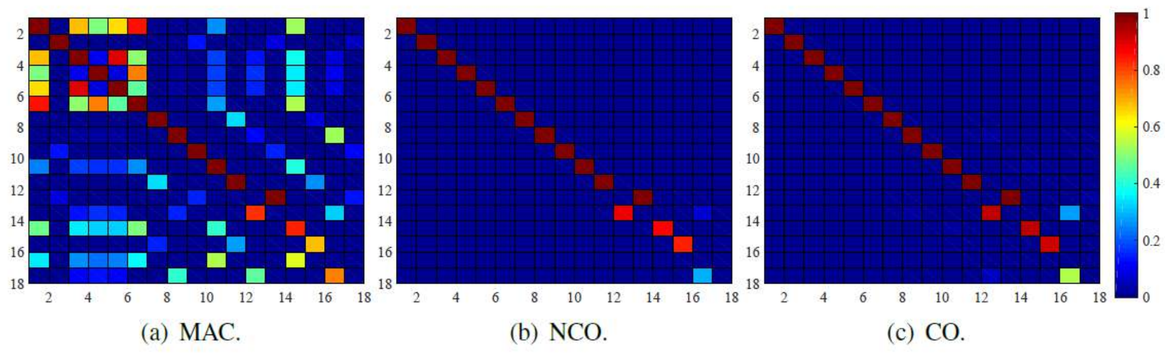

Fig.4

References

1. Boscariol P. , Gallina P. , Gasparetto A., Giovagnoni M. , Scalera L. , and Vidoni R. ***Evolution of a dynamic model for flexible multibody systems.*** Advances in Italian Mechanism Science, Springer, 2017.
2. Vidoni R., Gasparetto A. and Giovagnoni M. ***A method for modeling three-dimensional flexible mechanisms based on an equivalent rigid link system***. Journal of Vibration and Control, 2014.
3. Vidoni R., Gallina P., Boscariol P., Gasparetto A. and Giovagnoni M. ***Modeling the vibration of spatial flexible mechanisms through an equivalent rigid-link system/component mode synthesis approach***. Journal of Vibration and Control, 2015.
4. Vidoni R., Scalera L., Gasparetto A., Giovagnoni M. ***Comparison of Model Order Reduction Techniques for Flexible Multibody Dynamics using an Equivalent Rigid-Link System Approach***. Proceedings of the 8th ECCOMAS Thematic conference on Multibody Dynamics, Prague 2017.

Dott. Lorenzo Scalera
Prof. Alessandro Gasparetto

Info:
alessandro.gasparetto@uniud.it
scalera.lorenzo@spes.uniud.it

UNIVERSITÀ DEGLI STUDI DI UDINE
hic sunt futura

Corso di dottorato in Ingegneria industriale e dell'informazione

XXXI Ciclo

Optimization of Selective Laser Melting process parameter

Introduction

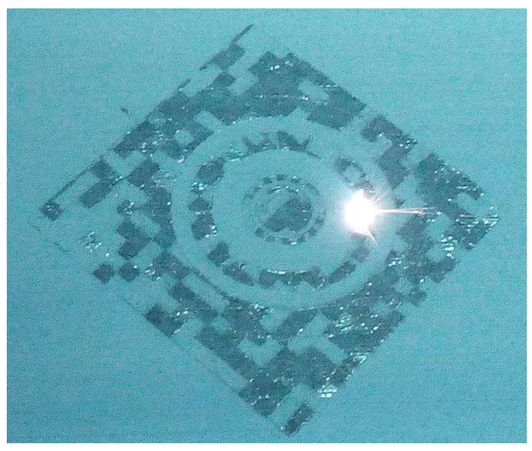

Selective Laser Melting:
High-performing Additive Manufacturing technology for metallic materials (e.g. **aluminium alloys, high-alloy steels such as stainless steels, titanium and nickel-based alloys** and many others).

Features:

- Innovative design solutions thanks to the feasibility of complex geometries
- Excellent physical and mechanical properties of both bulk and surface
- High dimensional accuracy and surface quality

Application

- Aeronautical, aerospace and automotive

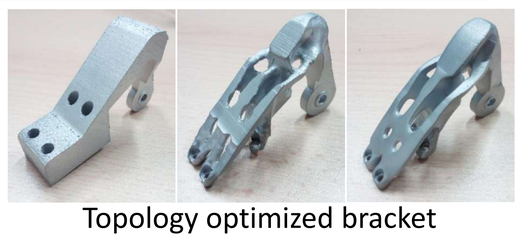

Topology optimized bracket

- Biomedical and dental

bone structure obtained through CT

- Industrial components

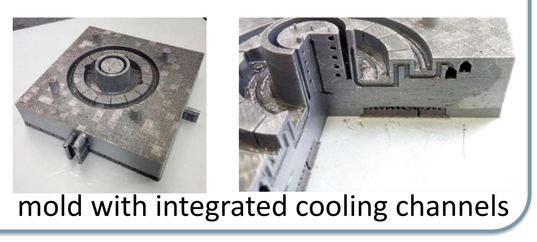

mold with integrated cooling channels

Process Parameters

description	Too low	Too high
Spot size: diameter of the laser beam.	Low build rate	poor level of detail
Trace distance: distance between the axes of two successive molten track	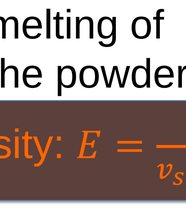	
Layer thickness: thickness of each metal powder layer	Low build rate	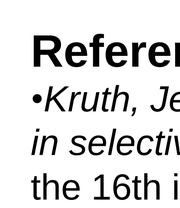
Scan speed: speed of the laser spot displacement	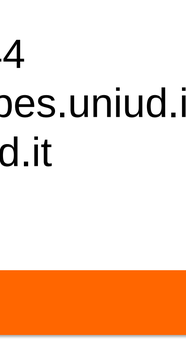	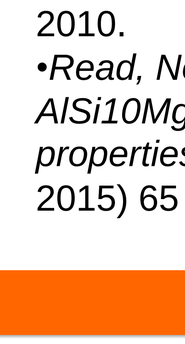
Laser power: power of the laser beam	Sintering effect due to non complete melting of the powder	accuracy problems due to poor control of the molten pool

Energy density: $E = \frac{P_L}{v_s \cdot L_t \cdot D_t}$

Methodology

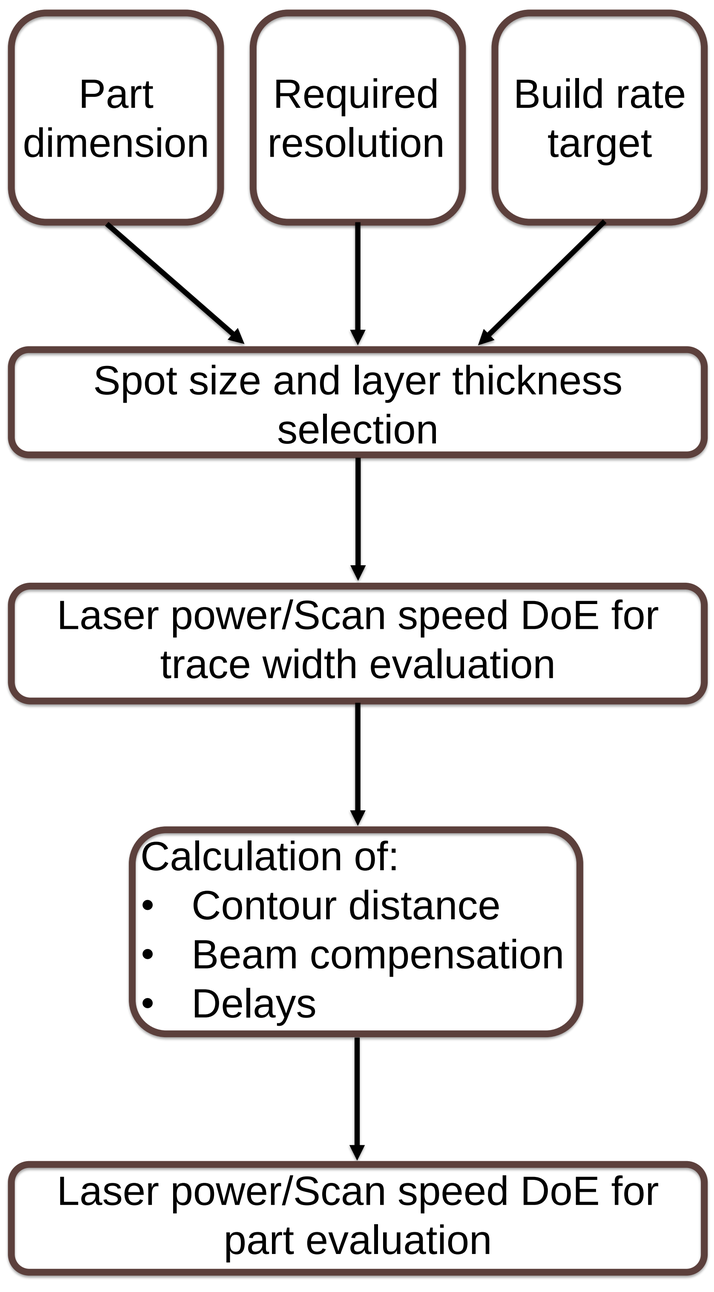

Indicators and Designed Specimens

- Resolution and dimensional accuracy

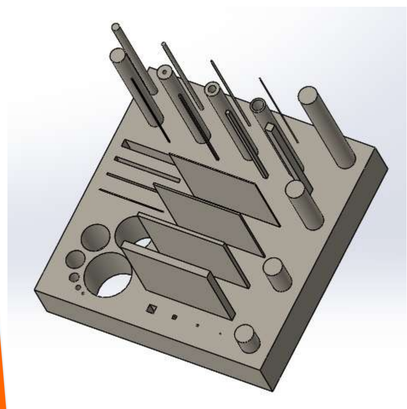

- aesthetic/surface quality:

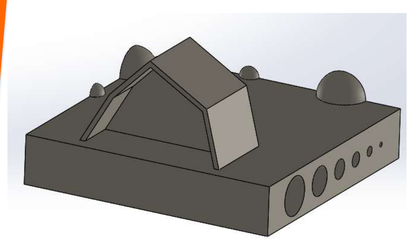

- mechanical properties:

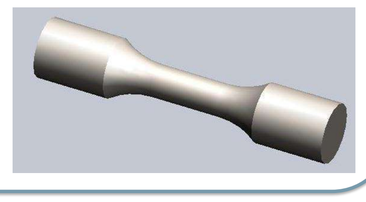

Dott. Emanuele Vaglio
Prof. Marco Sortino

Info:
Tel. +39 0432 558044
vaglio.emanuele@spes.uniud.it
marco.sortino@uniud.it

References
•*Kruth, Jean-Pierre, et al. "Part and material properties in selective laser melting of metals."* Proceedings of the 16th international symposium on electromachining. 2010.
•*Read, Noriko, et al. "Selective laser melting of AlSi10Mg alloy: Process optimisation and mechanical properties development."* Materials & Design (1980-2015) 65 (2015): 417-424.

Acknowledgements
I would like to gratefully acknowledge the Advanced Mechatronics Laboratory LAMA FVG of the University of Udine, the University of Trieste and the International School for Advanced Studies of Trieste (SISSA).

UNIVERSITÀ DEGLI STUDI DI UDINE
hic sunt futura

Corso di dottorato in Ingegneria industriale e dell'informazione

XXXI Ciclo

MULTIVARIABLE MODELLING OF THE DYNAMIC RESPONSE OF PROFESSIONAL WASHING MACHINES

Introduction

Energy saving and performance, are the main drivers of companies producing domestic and professional appliances.
All components of a washing machine should therefore be optimized to reach higher extraction speeds and reduced vibration levels. This is central to improve machine efficiency and to satisfy costumers' requirements.

Research plan

- Develop a 1D lumped parameter model of a washing machine
- Model time-spatial unbalance properties for different working cycles
- Simulate and validate the model
- Extend the model to multiple degrees of freedom
- Develop a multivariable analysis
- Optimize the main components of the machine in order to reduce vibration and to increase dewatering

Machine Model – 1 Dimensional

The vertical oscillations of the clothes washer were modelled with the following second order differential equation:

$$M_{tot}(t)\,\ddot{y}(t) + c\,sign(\dot{y}(t)) + ky(t) = F(t)$$

where the unbalance effect produced by the washing load was modelled with a vertical force:

$$F(t) = m_u(t)\,r(t)\,\omega(t)^2\cos(\omega(t)\,t + \varphi)$$

Simulation

Initial simulations have been carried out considering the angular rotation of the clothes washer undergoes a ramp followed by a constant speed time history.

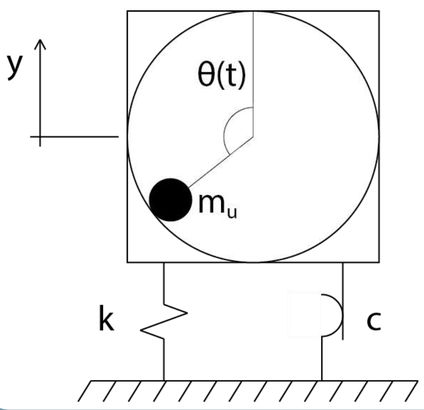

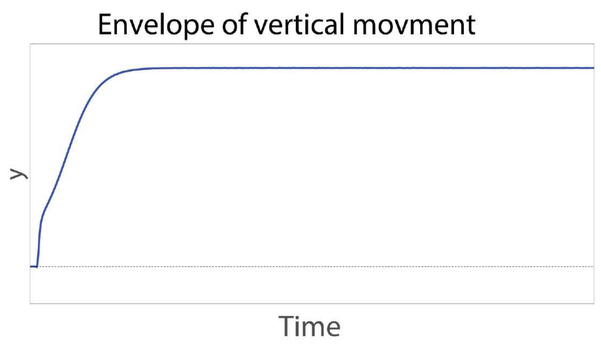

Retention Model – 1 Dimensional

During the extraction phase, the increased rotation speed of the clothes washer intensifies the “retention force” which controls the dewatering and thus influences the working time and unbalance conditions. For a pours media the radial flow is regulate by the Non-Darcy’s law while the retention R describes the amount of water in the textile.

$$-\frac{\partial p}{\partial r} = \frac{\mu}{k} v_r + \beta \rho\, v_r^2$$

$$R\% = 100\,\frac{m_{tot} - m_{dry}}{m_{dry}}$$

Simulation

Water retention for a cloth during the extraction phase.

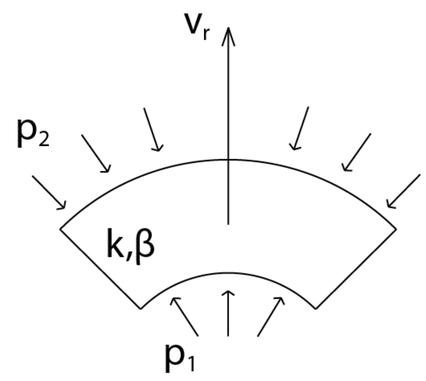

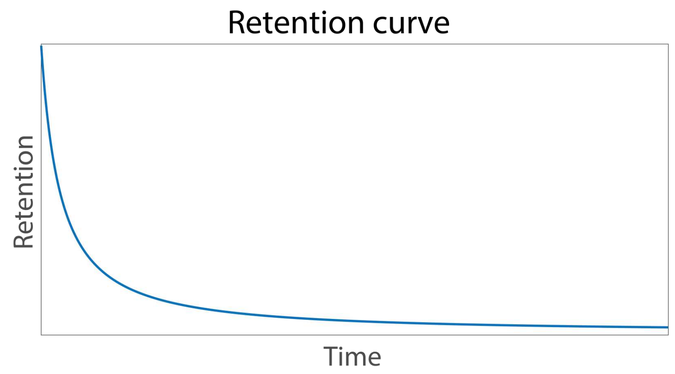

Future work

- To design and build a test rig for the characterisation of different textiles in terms of permeability
- To validate the SDOF and MDOF models
- To optimize the washing cycles in such a way as to minimise the unbalance effects and thus a) reduce vibrations
  b) reduce cycle time
  i.e. reduce washing costs

Dott. Nicola Battistella
Prof. Paolo Gardonio
Ext. Supervisor Mattias Johansson (Electrolux)

Info:
Tel. +46 372 662 48
nicola.battistella@spes.uniud.it
paolo.gardonio@uniud.it

Acknowledgement
The authors gratefully acknowledge the Electrolux Professional Laundry Research Hub

UNIVERSITÀ DEGLI STUDI DI UDINE
hic sunt futura

Corso di dottorato in Ingegneria industriale e dell’informazione

XXXII Ciclo

The European Monitor of Reshoring & The Drivers of Reshoring Strategy

Li Wan
Emal: wan.li@spes.uniud.it

Prof. Guido Nassimbeni
Email: guido.nassimbeni@uniud.it

What is European Monitor of Reshoring (EMR)?

The European Monitor of Reshoring is an online database. It collects information on reshoring cases from several sources (e.g., media, specialized press, scientific literature). It is organized through a secured access and updated regularly.

Collaboration between Eurofound and four Universities

UNIVERSITÀ DEGLI STUDI DI UDINE
hic sunt futura

UNIVERSITÀ degli STUDI di CATANIA

UNIVERSITÀ DEGLI STUDI DE L'AQUILA

ALMA MATER STUDIORUM UNIVERSITÀ DI BOLOGNA

Project period: 2016-2018

The EMR Results

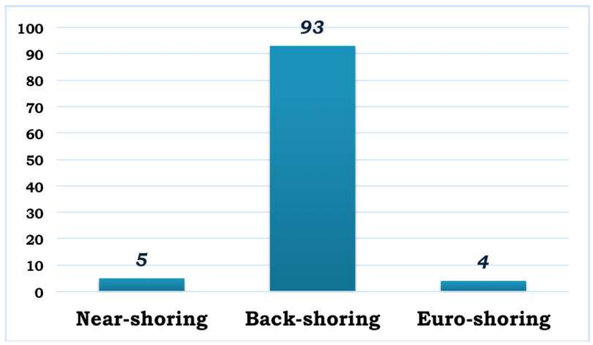

Near-shoring: EU Companies move manufacturing activities from offshored country to **near country** within EU.

Back-shoring: EU Companies move manufacturing activities from offshored country back to **home country**.

- **Euro-shoring:** EU Companies move manufacturing activities from **offshored country(within the EU)** back to home country.

Reshoring – "the relocation of value creation tasks from offshore locations to geographically closer locations such as domestic or nearshore countries" (Fratocchi et al., 2015).

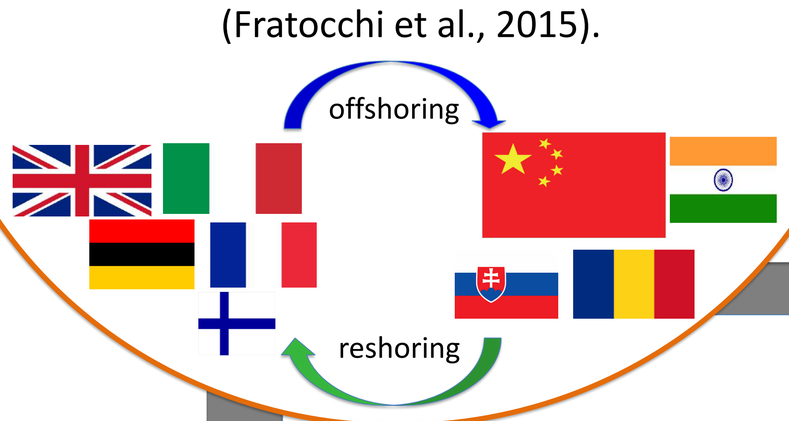

The EMR Results: Reshoring country

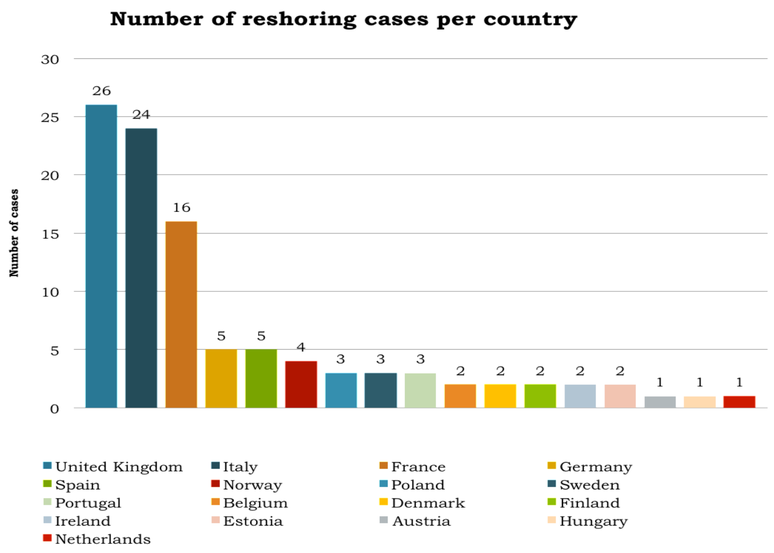

Top 3: United Kingdom Italy Germany

The EMR Results: Offshoring country

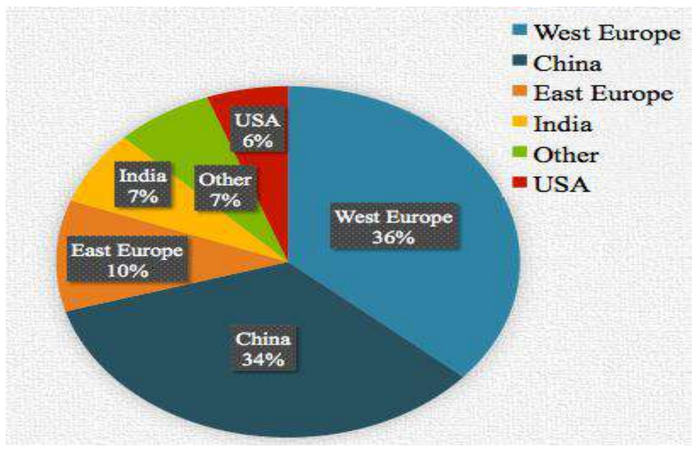

High proportion of reshoring from WE, motivated by:

- exploitation of untapped capacity at home
- reorganisation of production sites

Reshoring Strategies

Location decision

&

Entry mode decision

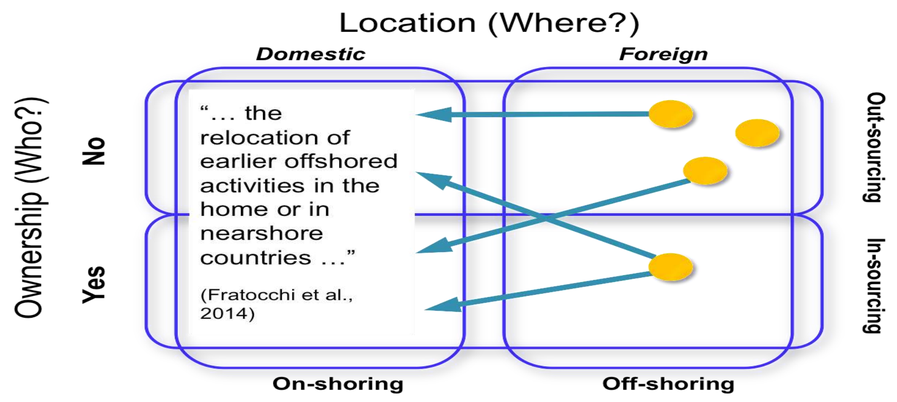

Drivers of Reshoring Strategy

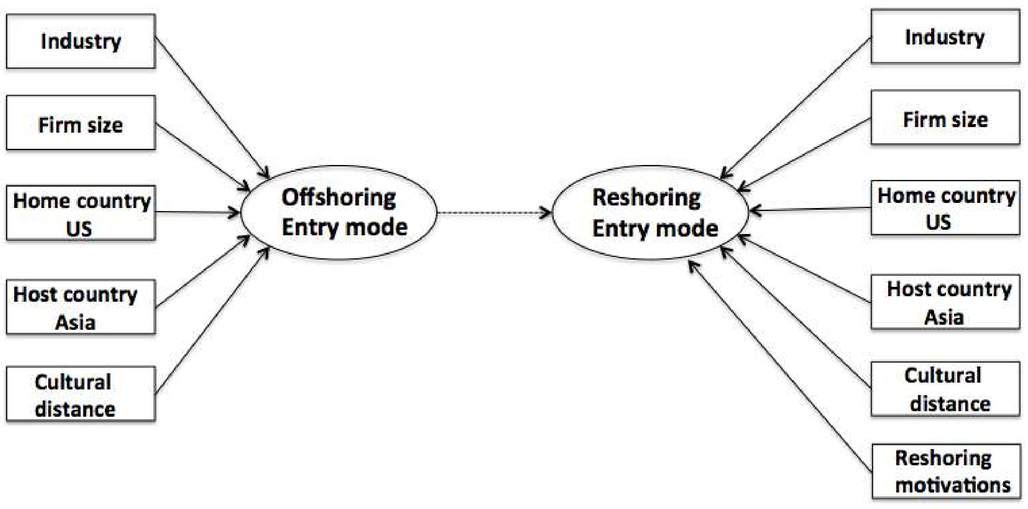

- Entry modes: **outsourcing** vs. **insourcing**
- Effect of **offshoring entry mode** choice on **reshoring entry mode** choice

Key Findings

- Reshoring strategy is fundamentally a decision concerning location and entry mode
- Offshoring entry mode choice significantly affect reshoring entry mode choice

Insourcing → Insourcing	Outsourcing → Outsourcing
Offshoring Outsourcing	**Reshoring Outsourcing**
+ Clothing + Automotive + SMEs	+ Clothing – Government incentives

UNIVERSITÀ DEGLI STUDI DI UDINE
hic sunt futura

Corso di dottorato in Ingegneria industriale e dell'informazione

XXXII Ciclo

Managing the evolutionary path in Sales and Operations Planning

1. Introduction and research objectives

Sales and Operations Planning (S&OP) is a key process that improves integration and communication between business functions and aligns the plans of a company into one integrated set of plans. My research focuses on the so-called S&OP "maturity models", which describe the successive stages in the advancement of S&OP process according to a precise set of dimensions. The weakness of these models is that they are specifically thought to plan the transitions towards advanced stages, but do not provide guidance on how to execute them. Therefore, the aim of my research is to address this gap by investigating how the dimensions evolve and interact during the transition from one maturity stage to the following one.

2. Methodology

Starting from a literature review on S&OP maturity models, I identified the S&OP dimensions and stages usually acknowledged in the literature and developed the maturity model presented in Table 1.
The model was then used to analyse three cases of transitions in three different companies that recently invested to develop their S&OP process: a transition from stage 1 to 2 in Company A, from 2 to 3 in Company B and from 3 to 4 in Company C.

3. Results

The three transitions are summarized in Figure 1: the rectangles represent the main steps the companies passed through and the letters are related to the dimensions that were most involved during the execution of each step. The comparison between the three transitions shows that there is not a unique temporal sequence that must always be used to develop the process dimensions and that the degree of "seriality" of this sequence depends on the maturity stage of S&OP process. Indeed, while in the less evolved transition the dimensions were developed in a "serial" way (i.e., one dimension after the other), in the other two cases, and especially in the most advanced one, some dimensions were so interdependent that should be addressed simultaneously, making the transition more difficult to realise. Finally, the study reveals that the importance of "people and organization" dimension increases with the S&OP maturity stage, becoming the main object of investment in the most evolved transitions.

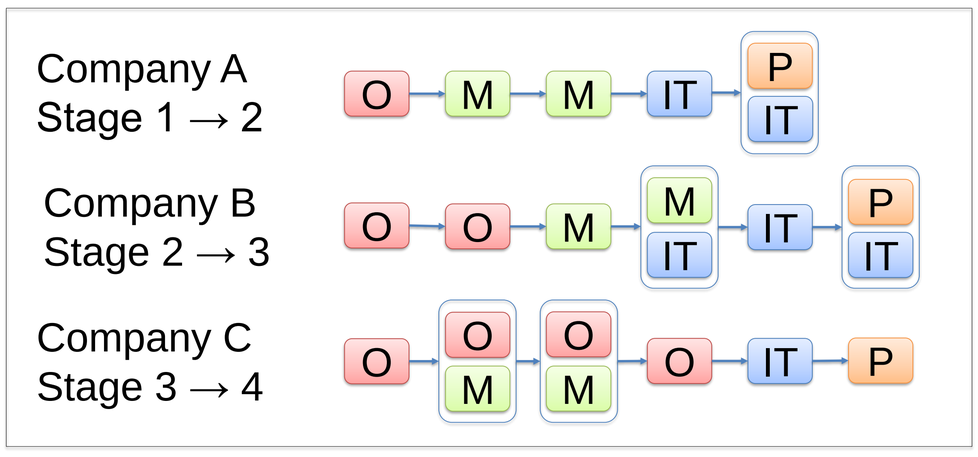

Figure 1: Summary of the transitions. Note: O = "people and organisation", M = "process and methodologies", IT = "information technology", P = "performance measurement".

4. Theoretical and managerial implications

As regards the theoretical aspect, the study innovatively contributes to existing literature on S&OP maturity models by proposing a model that is focused more on real execution rather than on process planning.
As regards managerial implications, it is possible to derive the following guidelines: (1) the need to invest in all S&OP dimensions to reach the subsequent maturity stage, (2) the advice not to underestimate "People and organization" dimension, (3) the possibility to prevent possible failures by considering how the dimensions can interact over time.

Table 1: S&OP maturity model

S&OP dimensions	Stage 1 No S&OP process	Stage 2 Reactive	Stage 3 Standard	Stage 4 Advanced	Stage 5 Proactive
People and organisation	Silo culture domination	Some collaboration between functions	Excellent commitment and formal S&OP team	Collaboration with main customers/suppliers	Involvement of the entire network
Process and methodologies	No formal S&OP process	Emerging but still inconsistent process	Formalised and structured process	Process balanced with the external partners	Event-driven meetings
Information technology	Personal spreadsheets	Functional IT solutions	Integrated planning software	Technology to access external partner data	Technology that links all the supply network
Performance measurement	Basic measurements	Functionally specific metrics	Integrated internal supply chain metrics	External supply chain metrics	Measures of impact on the ecosystem

Dott.ssa Margherita Molinaro
Prof. Pietro Romano

Info:
Tel. +39 0432 558043
molinaro.margherita.1@spes.uniud.it

UNIVERSITÀ DEGLI STUDI DI UDINE
hic sunt futura

Corso di dottorato in Ingegneria industriale e dell'informazione

XXXII Ciclo

Statistical fluctuation Effects on Nano Electronic Bio-Sensors

Motivation: The development of new nanoelectronic biosensors is attracting increasing attention, especially for screening, safety and diagnostics. CMOS nanoelectronics is an ideal technology platform to fabricate sensors with high sensitivity and low cost, thus potentially enabling personalized medicine and early diagnostics, and paving the way to dramatic improvements in our ability to fight diseases and quality of life.

Challenge: The goal of our PhD is to do mathematical modelling and simulation for nano-electronic bio-sensors based on CMOS technology.

Objective for the first year:

Development of models to investigate statistical fluctuations in nano-electrode array biosensors.

Case study: High-frequency impedance spectroscopy CMOS platform based on nanoelectrode array

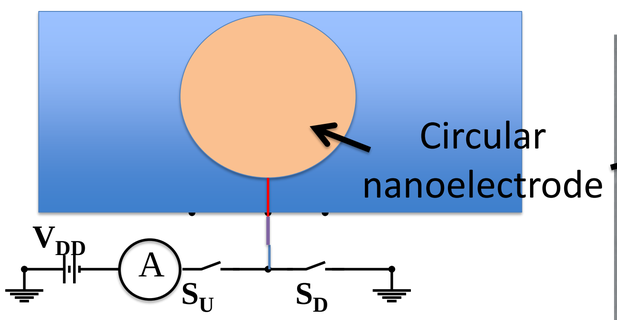

Schematic of the electrode capacitance
C_{SW} measurement circuit

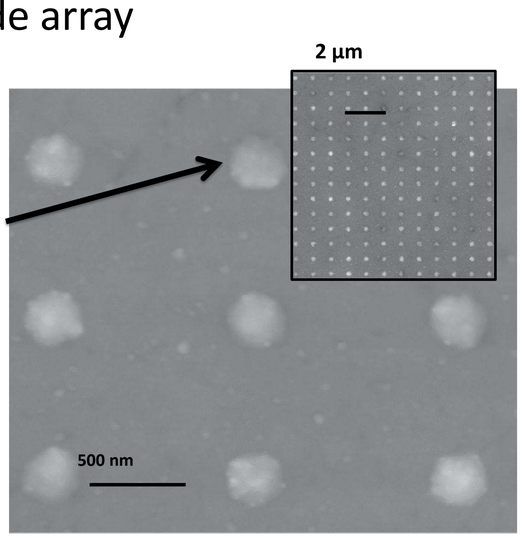

AFM images of the nanoelectrode array

Sources of Statistical Fluctuations:

Statistical fluctuations affect many aspects of a CMOS nanoelectronic biosensor. Each is described by a proper random process and PDF.

- Electrode geometry
- Surface roughness
- Material properties
- Characteristics of read-out transistors
- Dirt and dust
- Biological noise

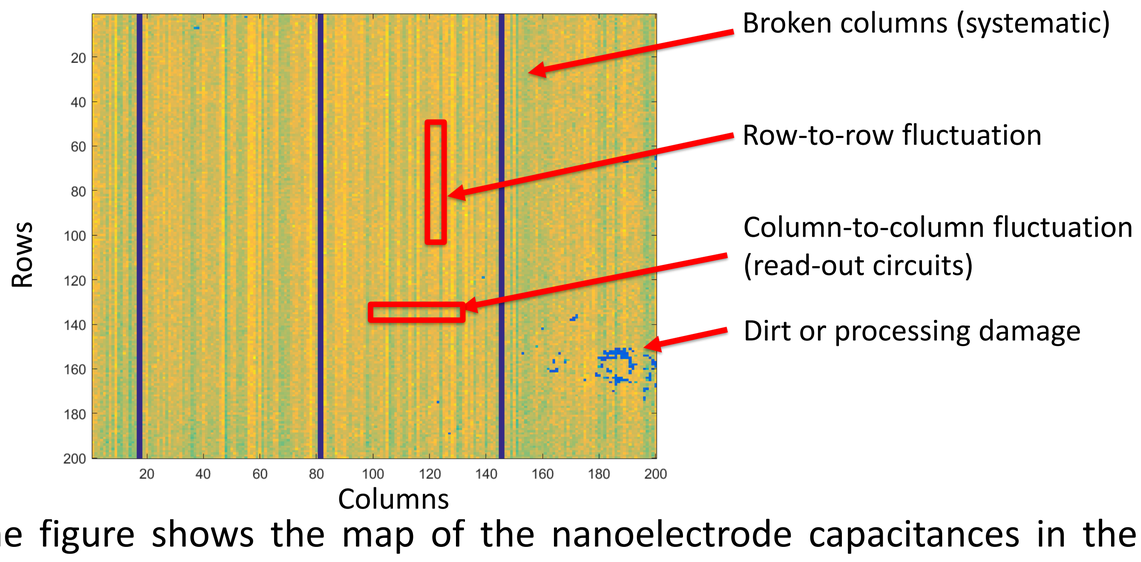

The figure shows the map of the nanoelectrode capacitances in the array during measures in air. We clearly see many source of systematic and random (local and global) variation among electrodes.

Simulation platforms to investigate fluctuation:

We started the analysis using the following simulation platforms: ENBIOS (in house tool) and COMSOL Multiphysics solvers of the dc and ac Poisson-Nernst-Planck equations; NETGEN mesh generator and MATLAB data analysis toolboxes.

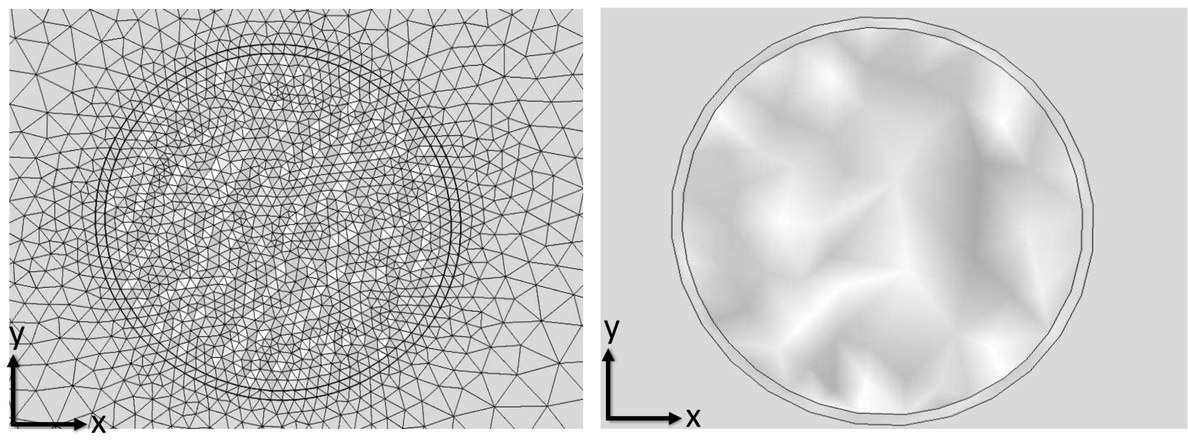

The figure shows the grid and height map for one rough electrode.

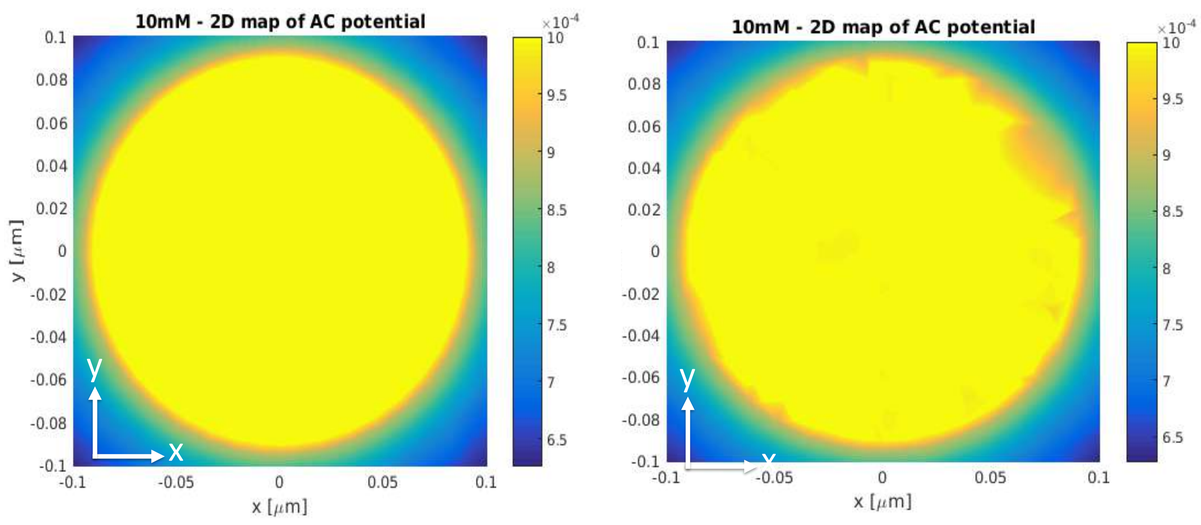

Figure shows the 2D map of the ac potential at the surface of a smooth (left) and roughened (right) electrode. 1 nm r.m.s. roughness

Results:

We compare the electrode capacitance spectra with (dashed) and w/out (solid) surface roughness. Roughness increases the effective electrode area, hence the capacitance. The effect is more pronounced at large ionic strength (thin electrical double layer).

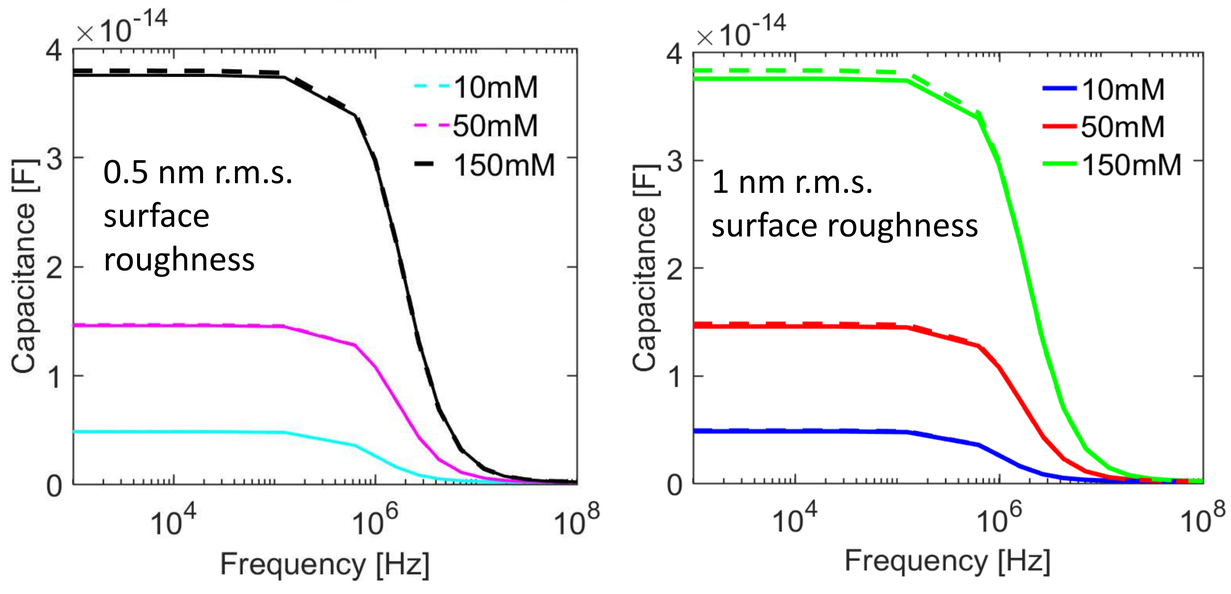

The figure show the switching capacitance for flat (solid) and rough (dashed) electrode surfaces. Capacitance is proportional to the electrode area and field intensity, hence larger for rough surfaces and thinner electrical double layer, that is, higher salt concentrations.

Future activities

We plan to extend the analysis to other sources of random fluctuation and to develop statistical compact models to understand signal-to-noise ratio and limits of detection.

Dott. Muhammad Naseer
Co-tutors:
Prof. Luca Selmi (Univ. Udine)
Prof. Clemens Heitzinger (TUWien)

Info:
naseer.muhammad@spes.uniud.it

References

[1] M. Alam, “Principles of Electronic Nanobiosensors” nanohub.org online course.
[2] F. Pittino et al., Comput. Methods in Appl. Mech. Eng., 2014
[3] Prospects of nanoelectronic biosensing with high-frequency impedance spectroscopy, F. Pittino PhD thesis, 2015.
[4] C. Boucher, Sampling Random Numbers from Probability Distribution Functions

Acknowledgement
I would like to acknowledge Andrea Cossettini for his useful help to understand ENBIOS.

UNIVERSITÀ DEGLI STUDI DI UDINE
hic sunt futura

Corso di dottorato in Ingegneria industriale e dell’informazione

XXXII ciclo

FPGAs for real time particle trajectory reconstruction in the ATLAS experiment at the LHC

1. Introduction

The ATLAS experiment is planning an important upgrade, involving the replacement of the present Inner Detector (tracker), and of a large part of the electronics for the trigger and data acquisition, in view of the increase of the LHC accelerator luminosity foreseen for the Phase-II operations. The project presented here is focused on a contribution to the development of a communication and data process software design for this new Inner Tracker (ITK) using FPGAs.

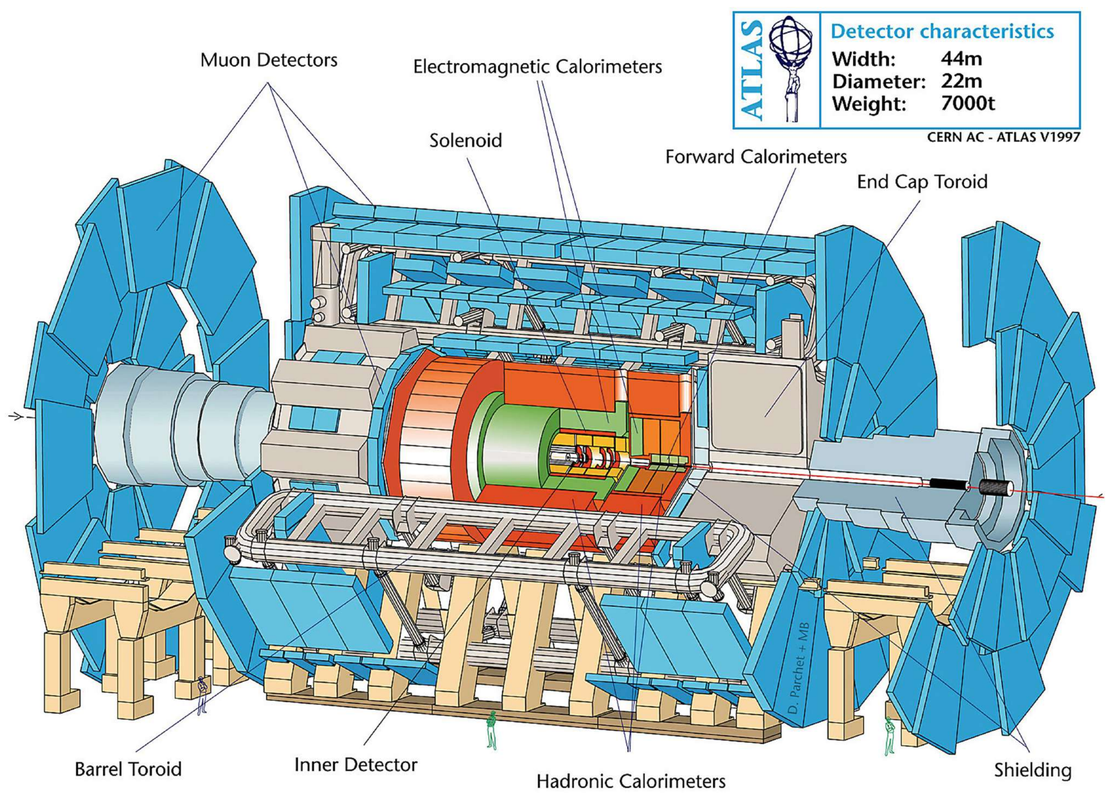

ATLAS layout before the upgrade

2. The LHC accelerator and the ATLAS experiment

The Large Hadron Collider (LHC), at the CERN laboratory (Geneva, CH), is a research project which uses state-of-the art instruments and technologies to explore the outer reaches of our understanding of the Universe.
In order to explore the fundamental nature of matter and the forces that shape our Universe, high energy particles collisions are performed in controlled conditions. Protons are accelerated in the LHC, an underground accelerator ring 27 km long. The particle beams, travelling almost to the speed of light, are steered to collide, at a center of mass energy of about 14 TeV, in the middle of the ATLAS detector, which makes a sort of picture of what happens in these collisions: according to the Einstein equation $E=mc^2$, the colliding proton energies gives rise to (hundreds of) new particles, most of them already known, but some which can constitute a new discovery. It is the world's largest general-purpose particle detector, measuring 46 meters long, 25 metres high and 25 meters wide; it weighs 7000 tons and consists of 100 million sensors.
Studying the particles produced in these collisions, through their interaction with the material which composes the various layers of the ATLAS detector, we can reconstruct their energy, charge and mass, unveiling the fundamental laws of nature.

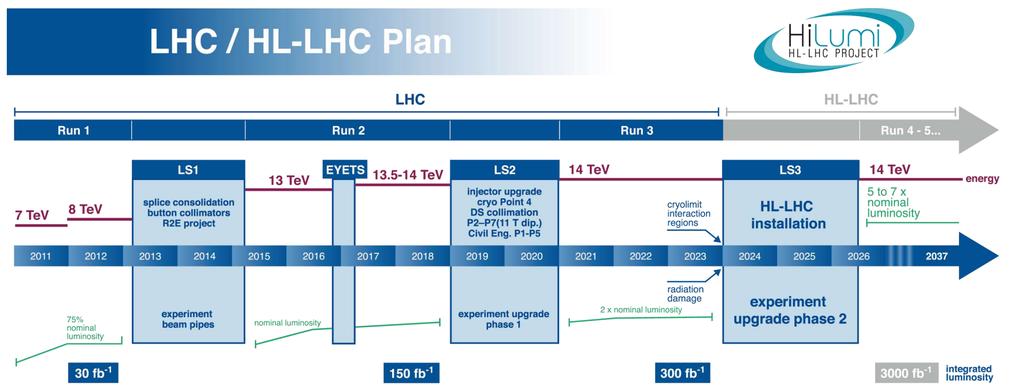

Timescale of the LHC Phase II project

3. Tracking challenges at HL-LHC

The Tracker is the inner part of the ATLAS experiment, and the closest to the proton collision point. The Tracker measures the direction, momentum, and charge of electrically-charged particles. The high luminosity upgrade of the LHC (HL-LHC) in 2026 will provide new challenges to the tracking detector. The so-called luminosity is an accelerator parameter related to the number of proton collisions per unit of time. The delivered instantaneous luminosity under HL-LHC conditions is expected to be in the range $5 \cdot 10^{34}$ to $7.5 \cdot 10^{34}$ $cm^{-2}s^{-1}$. This leads to a very high number of additional proton-proton interactions, in addition to the one we want to study, called pile-up. To cope with this, an accurate reconstruction and selection of tracks and an efficient rejection of pile-up jets is crucial. In ATLAS the current tracker system will be replaced by a new one, called ITK, consisting of a five barrel layer Silicon Pixel surrounded by a four barrel layer Silicon Strip detector.

FPGA dev kit KCU105 from Xilinx

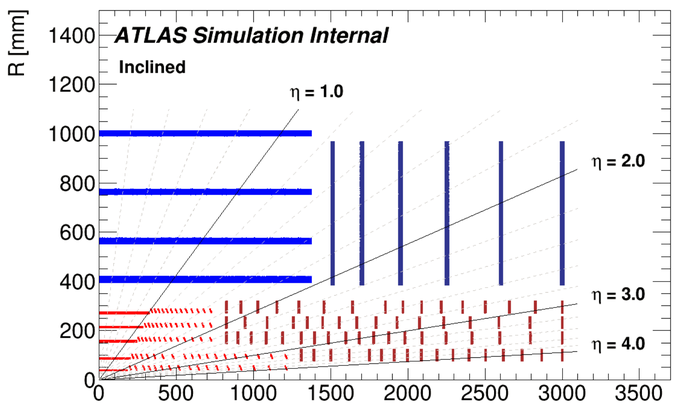

One configuration for the ITk layout (pixel tracker is in red)

4. ITK and FPGAs

The thesis work will be centered on the development of a part of the Read-out system of the Pixel part of the ITK sub-detector. This read-out will make use of FPGAs.
A Field Programmable Gate Array (FPGA) is an integrated circuit designed to be configurated after manufacturing by a design first a than a synthesis process to implement complex digital circuits.
The advantages of using an FPGA are: fast time-to-market, low cost to create prototypes, re-programmability, re-usability. The ITk front-end chip will be designed to provide a maximum data rate of 5 Gbit/s and will have over 1000 data links. Due the highly parallel structure in the readout system and the flexibility of easy reconfiguration FPGA-based solutions for the digital data acquisition system (DAQ) are currently under evaluation. Several laboratories are developing prototype readout systems to be used to test the ITk prototype front-ends, including Udine.
.

Dott. Filippo Pascolo
Prof. Marina Cobal

Info:
Tel. +39 0432 55-8206
Tel. +39 0432 55-8235
filippo.pascolo@uniud.it
marina.cobal@cern.ch

References
CERN-LHCC-2015-020
PLOT-UPGRADE-2014-003
ATL-ITK-SLIDE-2016-673
LHCC-G-166
Images from CERN
https://twiki.cern.ch/twiki/bin/view/Atlas/ITK

Acknowledgements
I would like to express my sincere acknowledgement to the components of the Multidisciplinary Laboratory of ICTP http://mlab.ictp.it/ and the ITk group of INFN Bologna

UNIVERSITÀ DEGLI STUDI DI UDINE
hic sunt futura

Corso di dottorato in Ingegneria industriale e dell'informazione

XXXII Ciclo

Iterative solution of eddy current problems on polyhedral meshes

INTRODUCTION

This work concerns the computation of the current induced in conductors surrounded by magnetic fields at industrial frequency.

Advantages of the integral formulation in [1]:

- **only conducting domain discretization** is needed;
- domain discretization realized with **arbitrary polyhedra**.

Disadvantages:

- the system to be solved is:

$$(\mathbf{K}_R + i\,\mathbf{K}_M)\mathbf{T} = \mathbf{b}_s, \qquad (1)$$

where K_R is a sparse matrix while $\boldsymbol{K_M}$ **is fully populated**.

ITERATIVE FORMULATION

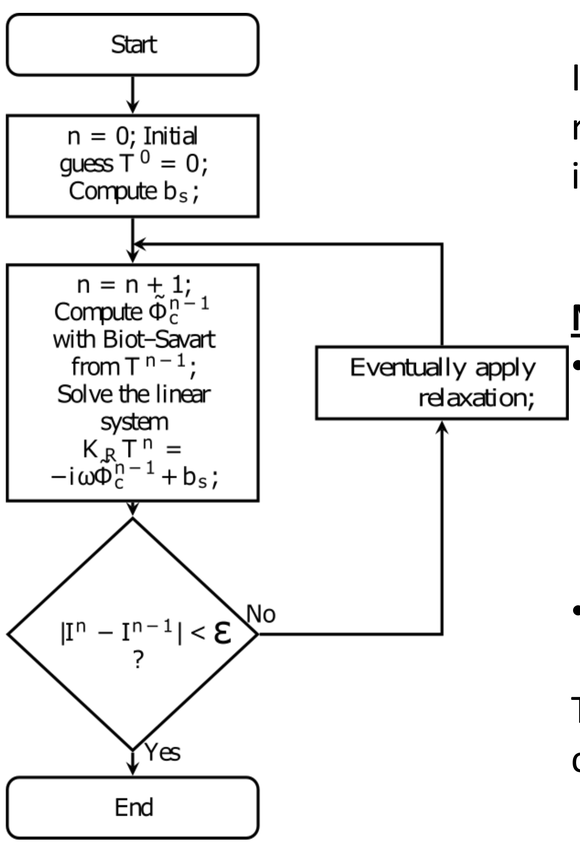

Inspired by [2], the problem is reformulated as the fixed point iteration

$$\mathbf{T}^n = -i\,\mathbf{K}_R^{-1}\,\mathbf{K}_M\,\mathbf{T}^{n-1} + \mathbf{K}_R^{-1}\,\mathbf{b}_s \quad (2)$$

Novelties with respect to (2):

- **avoiding the computation of $\boldsymbol{K_M}$** by directly computing the right-hand side of the equation at each fixed point step, using the Biot-Savart law;
- treating **not simply connected conductors**.

The problem equation to be solved consequently becomes:

$$\mathbf{K}_R\mathbf{T}^n = -i\omega\tilde{\mathbf{\Phi}}_c^{n-1} + \mathbf{b}_s \quad (3)$$

TEST PROBLEM GEOMETRY

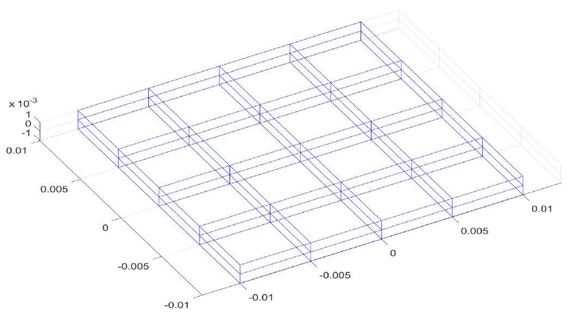

Fig.1 *Plate discretization (32 volumes)*

Initial tests were performed on a square plate: original dimensions are $20x20x2$ [mm].

Three different meshes with, respectively, 32, 256 and 2048 elements were used.

CONVERGENCE (1)

number of iterations with $\boldsymbol{\alpha}$ variation

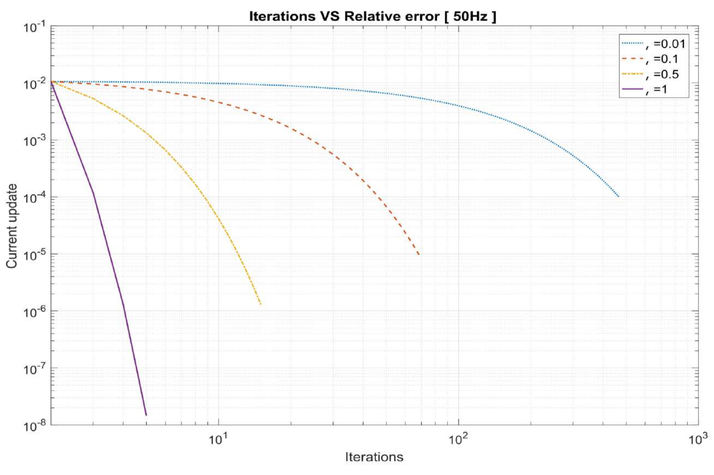

CONVERGENCE (2)

frequency and $\boldsymbol{\alpha}$ variation with increasing mesh density ($\boldsymbol{\varepsilon}=10^{-8}$)

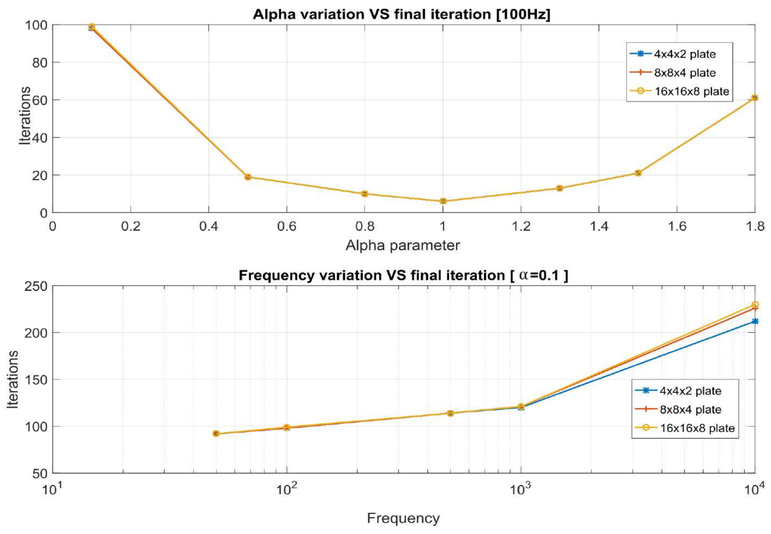

Fig.2 *Final iterations with varying alpha parameter and frequency*

Plate size increase behaviour

Mesh size	1:1	10:1	50:1
α_{min} value	1	0.5	0.01
Iterations	5	30	964

NUMERICAL RESULTS

a) Simply connected domain: sphere in a uniform magnetic field

Sphere mesh

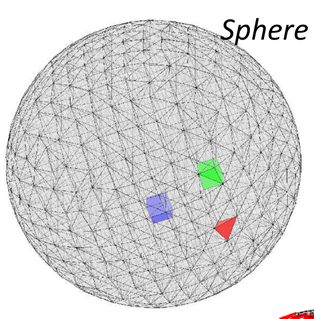

Imaginary current solution

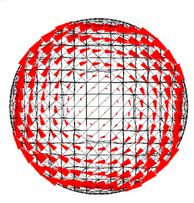

$\boldsymbol{\varepsilon}=10^{-6}$
$\boldsymbol{\alpha}$=0.5
Total iterations: 38

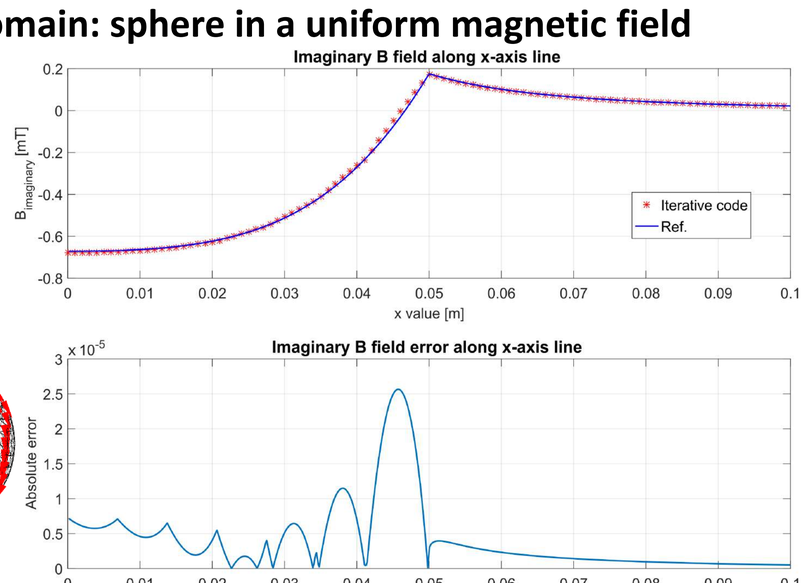

Fig.3 *B field comparison with the exact analytical solution and absolute error*

b) Not simply connected domain: slab with holes

Mesh solicitation with vertical field
B=1 T, $\boldsymbol{\rho}=10^{-5}\,\boldsymbol{\Omega}$·m, f=50 Hz

$\boldsymbol{\varepsilon}=10^{-6}$, *Iterations= 3*

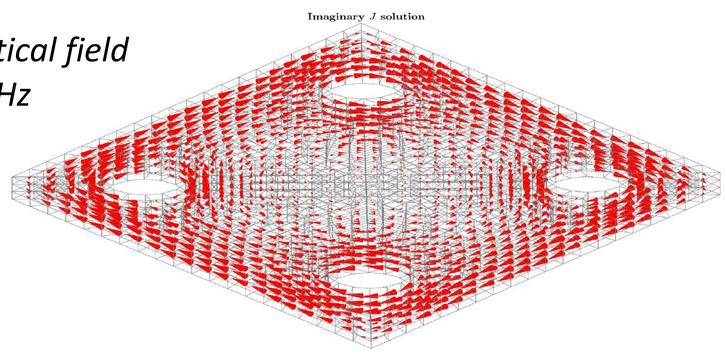

CONCLUSION

The convergence of the method has been shown to be dependent by overall mesh size and skin depth as also reported in [3]. Consequently, the method is particularly effective to treat problems with small domains and relatively high frequencies or large domains with high resistivity. Possible applications might thus be in biomedical engineering or in geophysical inversion methodologies where these parameters ranges are verified.

Dott. Mauro Passarotto
Prof. Ruben Specogna

Info:
Tel. +39 0432 558025
Indirizzo mail
passarotto.mauro@spes.uniud.it

Riferimenti bibliografici

[1] P. Bettini, M. Passarotto, R. Specogna, *A volume integral formulation for solving eddy current problems on polyhedral meshes*, IEEE Trans. Magn., DOI: 10.1109/TMAG.2017.2663112, 2017.

[2] T. Takagi, T. Sugiura, K. Miyata, S. Norimatsu, K. Okamura, K. Miya, *Iterative solution technique for 3-D eddy current analysis using T-method*, IEEE Trans. Magn., vol. 24, no. 6, pp. 2682-2684, 1988.

[3] I. D. Mayergoyz, G. Bedrosian, *Iterative solution of 3-D eddy current problems,* IEEE Trans. Magn., vol. 29, no. 6, pp. 2335-2340, 1993

Riconoscimenti

Progetto “HEaD HIGHER EDUCATION AND DEVELOPMENT OPERAZIONE 1 – UNIUD” - Decreto n. 2242 dell’11 aprile 2016 la Regione Autonoma Friuli Venezia Giulia – Fondo Sociale Europeo – Investimenti in favore della crescita e dell’occupazione

UNIVERSITÀ DEGLI STUDI DI UDINE
hic sunt futura

Corso di dottorato in Ingegneria industriale e dell’informazione

XXXII Ciclo

Positioning using LTE signals

MOTIVATIONS AND APPLICATIONS

The Global Navigation Satellite System (**GNSS**), which provides autonomous geo-spatial positioning with global coverage, is the most used and famous positioning system. The main problem of GNSS is the large position estimation error in no line of sight (**NLOS**) conditions, such as in indoor and urban canyon locations. It is therefore necessary to have good position estimates in environments where the GNSS fails. One method to attain this goal is to exploit the 4G LTE cellular system.

LONG TERM EVOLUTION (LTE)

LTE is a standard used for high speed wireless communication based on OFDM modulation.

The standard is developed by the 3rd Generation Partnership Project (**3GPP**) [1]. In the LTE standard a Reference Signal can be used for time measurements.

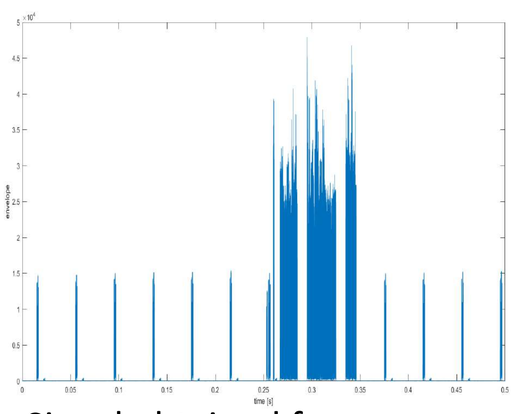

Signal obtained from an acquisition.

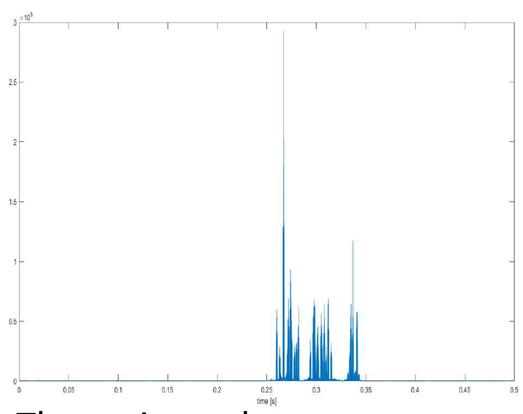

The main peak represents the time when the reference signal arrives at the receiver.

POSITIONING

The most common positioning setting consists of some anchors with a known position and a blind node in an unknown position. The positioning process consists of two main steps [2]:

1. Measurement phase
2. Localization phase

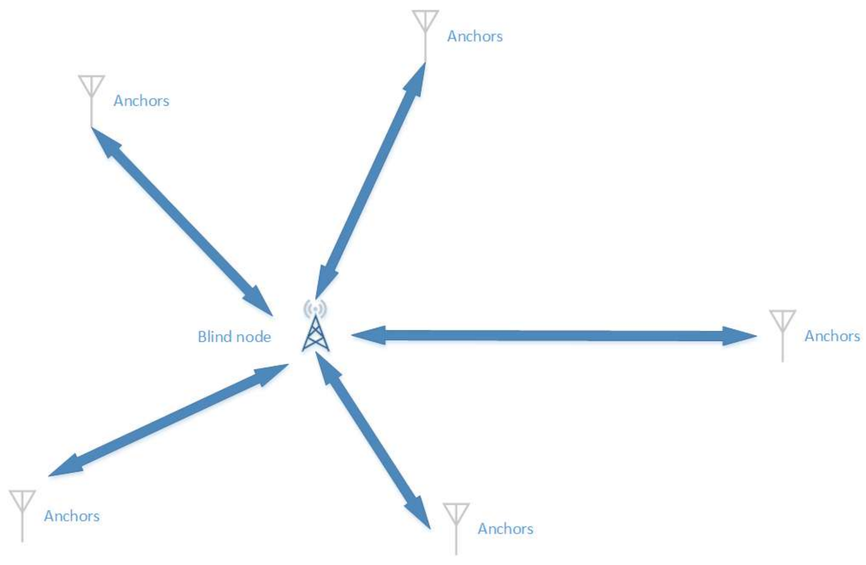

MEASUREMENT

A positioning system exploits the parameters of a received signal which are later used in the location phase to estimate a position.

The most common measured parameters are:

- Time of arrival (TOA)
- Time difference of arrival (TDOA)
- Received signal strength (RSS)
- Direction of arrival (DOA)

POSITIONING TECHNIQUES

In the localization phase, an algorithm is used to estimate the position. The choice of the algorithm depends on the type of measurement made in the previous phase.

The most common algorithms are [2]:

TRILATERATION

Exploits distance estimates between the blind node and the multiple anchors in a known position. These distances are usually estimated using TOA or RSS measurements.

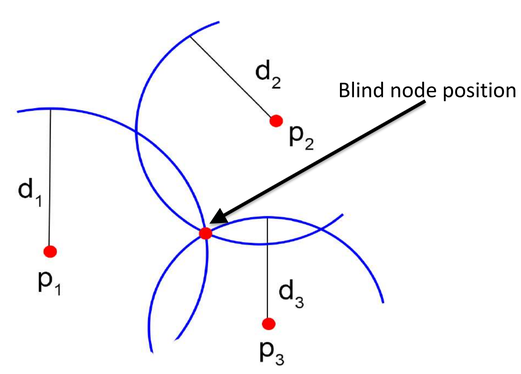

HYPERBOLIC POSITIONING

Hyperbolic positioning techniques are used when differential measurements are available, like in the case of TDOA.

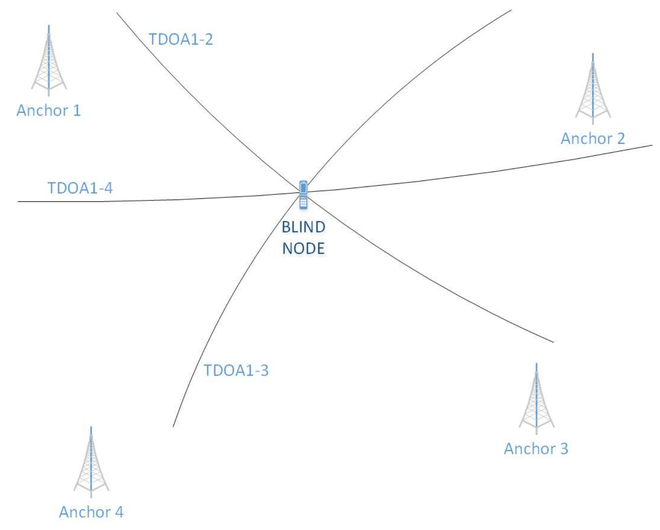

PROJECT

The project investigates the use of asynchronous positioning techniques, similarly to those in [3], which exploit the LTE signal in an opportunistic way, i.e., using transmitted/received LTE signals and the communication protocol characteristics.

Dott. Alessandro Pin
Prof. Roberto Rinaldo (Uniud)
Prof. Andrea Tonello (AAU)
Info:
Tel. +39 0432 558046
pin.alessandro.1@spes.uniud.it

References

[1] 3GGP http://www.3gpp.org

[2] J. Figueiras and S. Frattasu, Mobile Positioning and Tracking. From Conventional to Cooperative Techniques.

[3] N. Facchi et al., Computer Networks, Vol. 88, 2015, pp.202-217

Acknowledgements

Drs. Chris Marshall, Marco Driusso and Andrea Dalla Torre from u-blox for their assistance and interesting discussions.
My tutors Prof. Rinaldo, and Prof. Tonello from Alpen-Adria-Universität, Klagenfurt, for their assistance in these first months of my PhD journey.

UNIVERSITÀ DEGLI STUDI DI UDINE
hic sunt futura

Corso di dottorato in Ingegneria industriale e dell'informazione

XXXII Ciclo

Processing of bio-signals for biomedical applications and psyco-physical state analysis

OBJECTIVE

The objective of the research is to apply signal processing techniques to bio-physical signals in order to possibly identify stress and wellness conditions. One foreseen application is the automatic stress assessment of car drivers.

Skin Potential Response (SPR) is caused by the Electro Dermal Activity (EDA) of the human body and represents the differential voltage on the skin between a place where there are sweat glands and a place where sweat glands are not present [1].

SPR is strictly related to the sympathetic nervous system activity, and through its measurement we are able to obtain information about the emotional state of a subject under test.

In SPR measurements there are several components not related to the sympathetic system, in particular Motion Artifacts (MA). MA originates from stretch deformation and movements due to everyday activities [1].

In order to have usable data, MA has to be removed from the measurements.

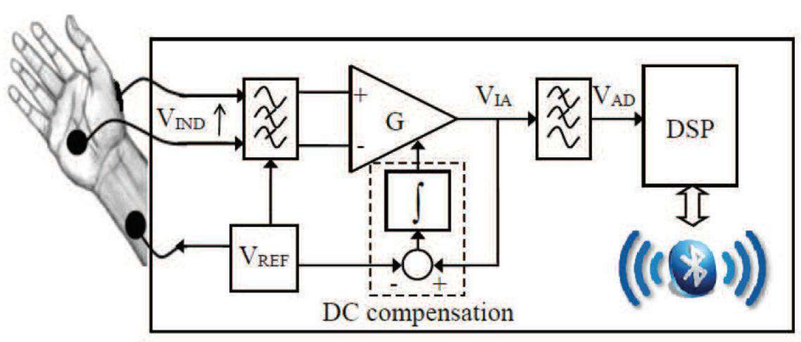

Fig. 1 Measurement System [1].

ANALYSIS OF A DRIVER'S STRESS SIGNAL

The aim of our work is to obtain the Stress Signal (SS) from SPR measurements of a driver during a car race. SPR is measured by a sensor connected on the driver's left hand (Fig. 1).

Measured SPR is affected both by emotional state and physical movements performed for driving. In addition to SPR measurements, Steering Wheel (SW) angle is recorded (Fig. 2).

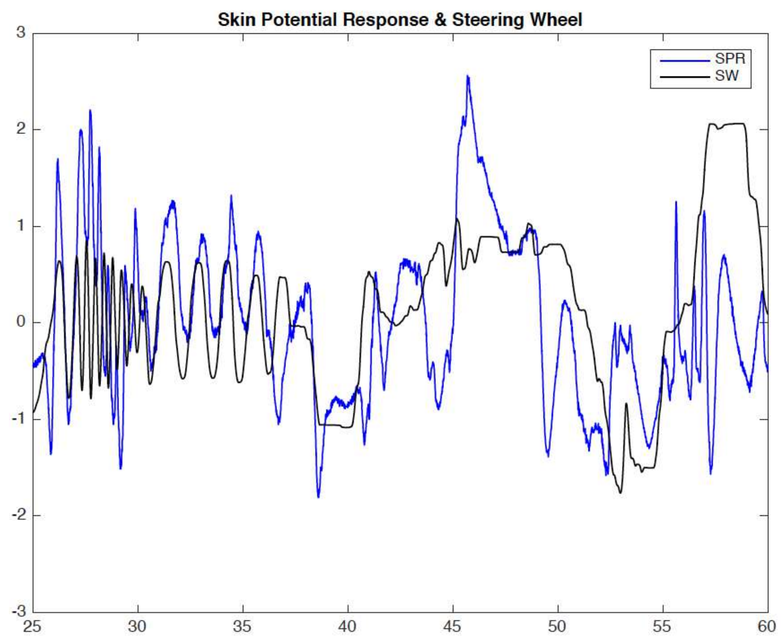

Fig. 2 Skin Potential Response (blue line) & Steering Wheel (black line).

ADAPTIVE FILTERS

For splitting the SPR components, Least Mean Square (LMS) algorithms are implemented using digital adaptive filters [2].

Correlation between SW and MA are used in order to identify the Motion Artifact and to obtain the Stress Signal.

Taken SW as filter input and SPR as reference signal we obtain MA.

Fig. 3 shows estimated Motion Artifact (MA) using Normalized Least Mean Square adaptive filter [2].

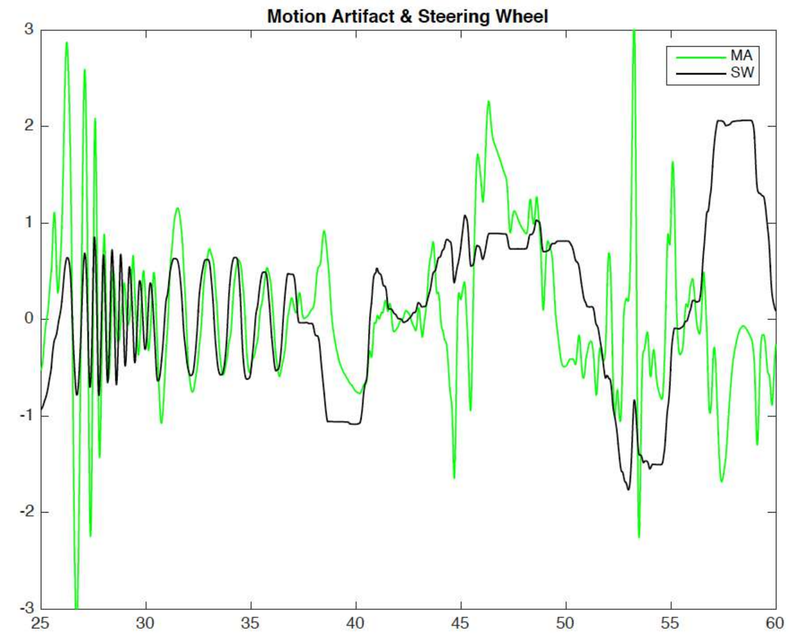

Fig. 3 Motion Artifact (green line) & Steering Wheel (black line) obtained using NLMS adaptive filter [2].

Residual error represents driver's inner Stress (S) signal.

In Fig. 4 Stress signal power is shown.

The instants during which the driver has been mostly stressed can be recognized by signal peaks.

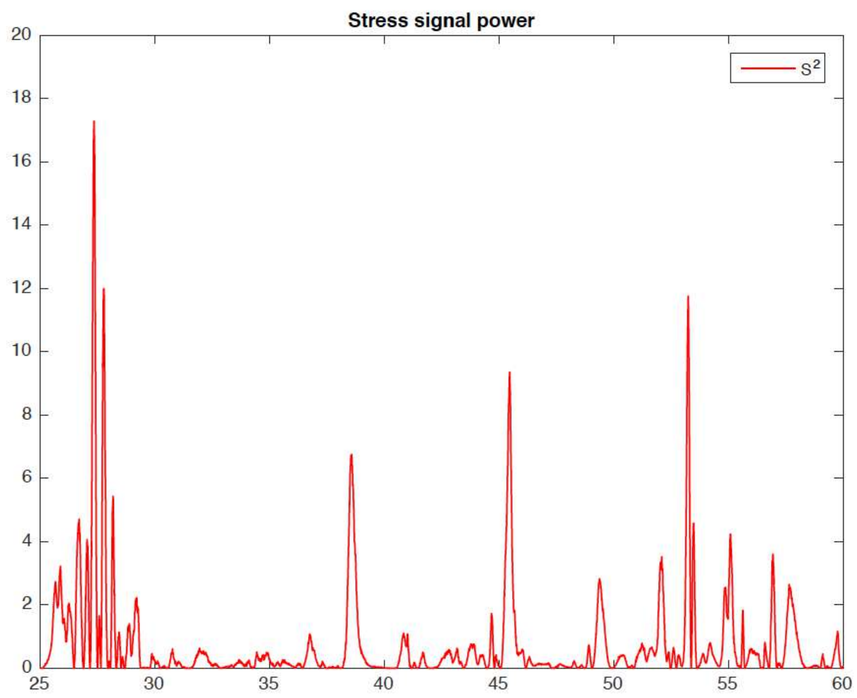

Fig. 4 Stress (S) signal power (red line) using NLMS adaptive filter [2].

Dott. Alessandro Piras
Prof. Roberto Rinaldo (Uniud)
Info:
Tel. +39
piras.alessandro@spes.uniud.it

References

[1] A. Affanni, G. Chiorboli, D. Minen "Motion artifact removal in stress sensors used in "Driver In Motion" simulators".

[2] S. Haykin, B. Widrow, "LEAST-MEAN-SQUARE ADAPTIVE FILTERS".

Acknowledgements

My thanks go to Prof. Roberto Rinaldo and Prof. Antonio Affanni, University of Udine, for their assistance and support during the research activity.

UNIVERSITÀ DEGLI STUDI DI UDINE
hic sunt futura

Corso di dottorato in Ingegneria industriale e dell'informazione

XXXII Ciclo

OPTIMIZATION OF COMPONENTS DESIGNED FOR AM, SIMULATION AND MONITORING OF SLM PROCESS

Fields of research

Additive manufacturing and specifically metal selective laser melting (SLM) processes are rapidly being industrialized. In order for this technology to see more widespread use as a production modality, especially in heavily regulated industries such as aerospace and medical device manufacturing, there is a need for improvements in some strategical areas.

- **Development and validation of methods for fast predictions of residual stress and distortion of AM parts**
- **Optimization and design of innovative mechanical components exploiting advantages of SLM manufacturing process**
- **Development of optimal heat treatments to improve mechanical properties and reduce distortions of parts**
- **Development of specific process parameters tailored on parts geometry and material**
- **Development of robust process monitoring and control capabilities to reduce process variation and ensure quality**

Process simulation

Distortion of parts during the printing and manufacturing process is a major impediment to companies not realizing the full benefits of the additive manufacturing process. An enormous amount of unproductive time and cost spent on trial and error.

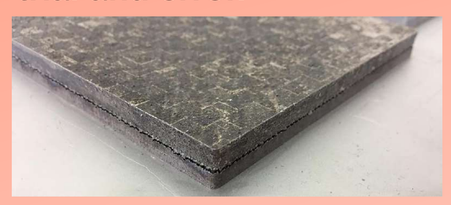

Unwanted separation of the part from the support structure. Crack propagates due to thermal stresses induced during SLM process.

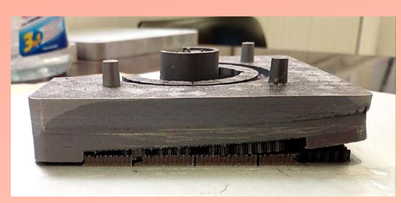

Detachment of the part from the build platform during early stages of the printing job. Thermal stresses tend to build up layer by layer, when supports fail the result are huge deformations.

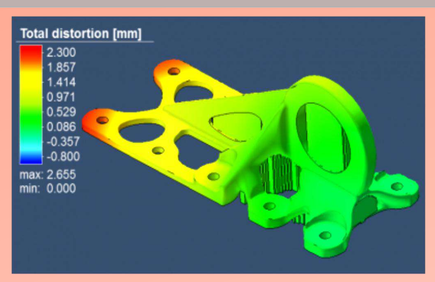

Total distortion - 3D printing process simulated with MSC Simufact Additive

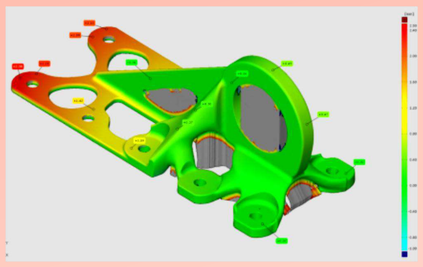

Total distortion - optical measurement

Development and validation of new approaches that allow replacing the time consuming thermo-mechanical simulation of the process by a static mechanical one will enable a practical usage of FEM based method for AM process simulation.

The code should help the designer to fulfill these tasks:

- **Calculate the deformation of the final part and reduce/avoid distortion**
- **Minimize residual stress**
- **Optimize the build-up orientation**
- **Optimize the support structure**
- **Evaluate stresses and deformations after heat treatment, base plate and support removal**

Design, optimization and in-process monitoring

Designers use strategies and optimization methods to tackle practical design problems with traditional manufacturing processes in mind. These approaches have significant manufacturing constraints and a compromise has to be made between optimality and ease of manufacture. With Additive manufacturing (AM) the part is built up layer-by-layer. Parts of significantly greater complexity can be produced without a significant effect on the cost of the process, providing the designer with significantly greater design freedom and enabling the built part to be closer to the optimum design. Optimization and monitoring of process help to improve performance and reduce costs.

Topology Optimization: structural optimization method that calculates the optimal material distribution inside a design domain by varying the pseudo-density of its elements. For instance, it could be used to reduce weight and to keep under control frequency response.

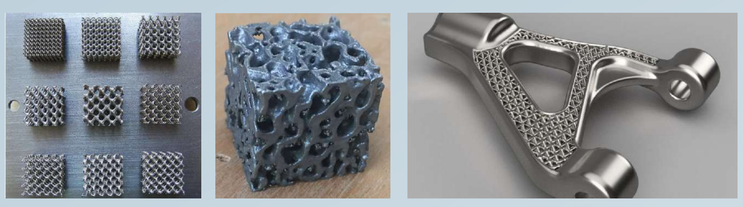

Lattice and bionic structures: designing parts incorporating these structures enables engineers to manufacture lightweight parts and also improve system performances, for example heat dissipation and frequency response (vibrations).

High efficiency compact heat sinks and heat exchangers: with 3D printing it is possible to build parts with highly complex internal geometries such as compact heat sinks and heat exchangers that maximize surface area and flow.

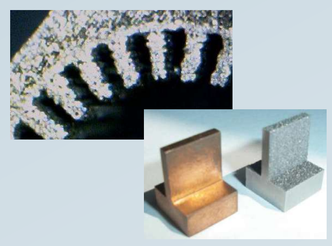

Integrated cooling channels: conformal cooling channels are internal geometries often difficult to machine with traditional manufacturing processes. Additive manufacturing allows components to be designed for maximum performance and intent, rather than the traditional mindset of manufacturability.

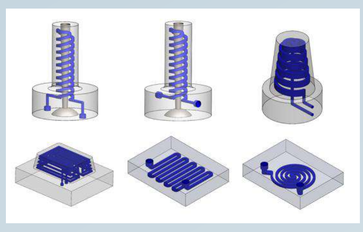

✗

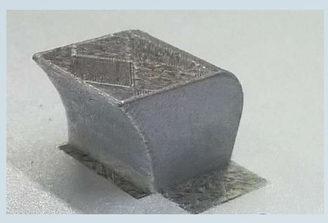

✓

Optimization of process parameters and heat treatments: optimization of SLM process parameters is necessary in order to improve the quality of parts. Optimization of heat treatments may improve the microstructure, hardness and tensile properties.

Optical in-process monitoring of SLM process: ensuring repeatability and consistency is essential for the advancement of AM technology. The final part quality is heavily influenced by various factors (eg. material, exposure parameters, power, scan speed, exposure strategies). Several strategies and systems could be implemented to enable quality assurance during the process, for example camera based powder bed monitoring and diode, pyrometer or camera-based in process monitoring.

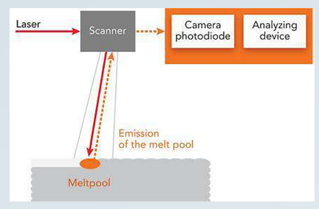

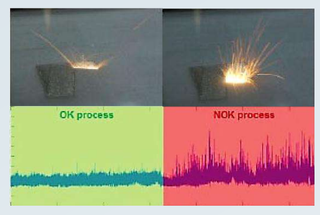

Dott. Federico Scalzo

Prof. Marco Sortino

Info:
Tel. +39 0432 558044
scalzo.federico@spes.uniud.it
marco.sortino@uniud.it

References

• N. Keller, V. Ploshikhin, *New method for fast predictions of residual stress and distortion of am parts",* Solid Freefrom Fabrication, 2014, pp. 1229-1237
• A. Mertens, O. Dedry, D. Reuter, O. Rigo, J. Lecomte-Beckers, *Thermal treatments of AlSi10mg processed by laser beam melting*, Proceedings of the 26th International Solid Freeform Fabrication Symposium, 2015, pp. 1007-1016
• L. Ventola, E. Chiavazzo, F. Calignano, D. Manfredi, P. Asinari, *Heat transfer enhancement by finned heat sinks with micro-structured roughness*, Journal of Physics: Conference Series, 2014
• T.Grünberger, R. Domröse, *Optical In-Process Monitoring of Direct Metal Laser Sintering (DMLS)*, Laser Technik Journal, Volume 11, Issue 2, 2014 , pp. 40-42
• S. Berumen, F. Bechmann, S. Lindner, Jean-Pierre Kruth, T. Craeghs, *Quality control of laser- and powder bed-based Additive Manufacturing (AM) technologies*, Physics Procedia, Volume 5, 2010, pp. 617-622
• T. G. Spears, S. A. Gold, *In-process sensing in selective laser melting (SLM) additive manufacturing*, Integrating Materials and Manufacturing Innovation, 2016, pp. 1-25

Acknowledgements
I would like to thank the Advanced Mechatronics Laboratory LAMA FVG for making available machines and advanced tools to support my research, ALMATEC and MSC Software for their collaboration.

UNIVERSITÀ DEGLI STUDI DI UDINE
hic sunt futura

Corso di dottorato in Ingegneria industriale e dell'informazione

XXXII Ciclo

A new model for the simulation of a cable-in-conduit cabling procedure

Introduction

A new model able to give a verisimilar geometry of the so called *Cable-In-Conduit-Conductors* (CICC) is being developed for the THELMA code, a coupled thermal-electromagnetic numerical model for the description of superconducting cables and magnets.

- CICCs are composed by a very large number of superconducting strands twisted together in multiple cabling stages and then inserted in a metal jacket;
- For cooling, supercritical He flows through the interstices between the strands and the central channel if any;
- Copper strands can be included in the cable to provide a low resistivity current path in the case of transition of the superconductor to the normal state.

Manufacture of CICCs: cabling higher stage
(courtesy of L. Muzzi, ENEA)

ITER CS cable
(courtesy of C. Sanabria, NHMFL)

The cabling sequence

The model approach is based on a virtual cabling sequence followed by a cable compaction procedure down to the final rectangular or circular cross-section:

- The cable is initially made of a bundle of straight individual wires or smaller bundles, suitably arranged in the space;
- The strands are then rotated at one end of the cable, to simulate the action of the cabling rotating drum.

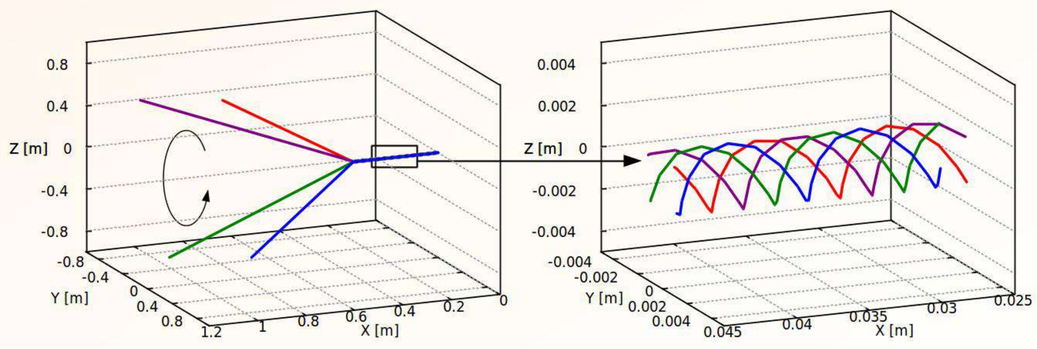

During cabling the strands are subjected to a tensile force.

The interference removal process

An iterative approach is adopted for the interference removal. At the generic iteration, wherever a geometrical interference C_{ij} between the *i-th* and *j-th* strands takes place as a consequence of rotation and final compaction, an interstrand resulting elastic force $F_i(x)$ acting on the *i-th* strand cross section (*yz*-plan) is considered at the generic curvilinear coordinate *x*. This force is computed starting from the local interference C_{ij} on the basis of the strand transverse stiffness K_i and K_j, and therefore the interference is iteratively removed through the (current) resulting displacements ΔS_i. A simplified formulation for *N*-strands case follow below:

$$\mathbf{F}_i(x) = \sum_{j=1}^{N} \frac{\mathbf{C}_{i,j}(x)}{\frac{1}{K_i} + \frac{1}{K_J}} \qquad \Delta\mathbf{S}_i(x) = \frac{\mathbf{F}_i(x)}{K_{i_T}(x)} \qquad K_{i_T}(x) = \sum_{j=1}^{N} \frac{\delta_{i,j}}{\frac{1}{K_i} + \frac{1}{K_J}}$$

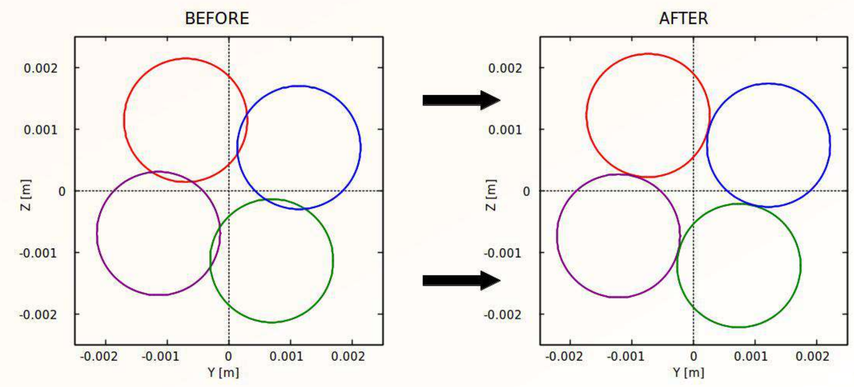

Application: superconducting fusion magnets

Some scientific applications require very intense magnetic fields (up to more than 10 T). Because of the high currents required, normal conductors would involve excessive losses. Therefore, superconducting cables are needed.

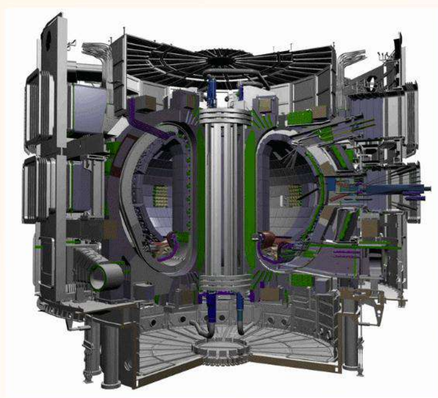

Tokamak: the magnetic confinement fusion reactor
(courtesy of ITER organization)

Thanks to their robust design and cooling capabilities, CICCs are widely used in fusion magnets like those of ITER.
NbTi and Nb_3Sn are still the most important superconducting materials for this kind of application.

dott. Francesco Stacchi
Prof. Fabrizio Bellina

Info:
Tel. +39 0432 558025
stacchi.francesco@spes.uniud.it

Bibliography

- F. Bellina, D. P. Boso, B. A. Schrefler, and G. Zavarise, "*Modelling a multistrand SC cable with an electrical DC lumped network*", IEEE Trans. Appl. Supercond., vol. 12, pp. 1408–1412, March 2002.
- M. N. Wilson, "*Superconducting Magnets*", 1983.
- G. Manfreda, "*Numerical analysis of coupled thermal-electromagnetic problems in superconducting cables*", PhD thesis, University of Udine, 2014.

UNIVERSITÀ DEGLI STUDI DI UDINE
hic sunt futura

Corso di dottorato in Ingegneria industriale e dell'informazione

XXXII Ciclo

PARALLEL RESONANT HIGH-POWER-DENSITY CONVERTERS FOR DATA CENTER AND MOBILE APPLICATIONS

ABSTRACT

- High efficiency power conversion has become an important issue in modern CPU power supply
- Energy conversion chain in data centers requires optimization for each stage
- The last converter is built close to the CPU to comply with strict performance requirements in terms of current capability and transient response
- This conversion is usually achieved through classical multi-phase buck converter which power-density is hardly improvable

- In this study two novel converter topologies are presented for the 12 V → 1,8 V conversion which are based on the sigma-converter architecture
- The first proposed topology is based on a LLC converter while the second one is based on a switched-capacitor architecture

FULL/HALF-BRIDGE SIGMA CONVERTER FOR 12 V → [0.5, 2] V CONVERSION

$$\frac{P_{LLC}}{P_{BUCK}} = \frac{V_{IN,LLC}}{V_{IN,BUCK}}$$

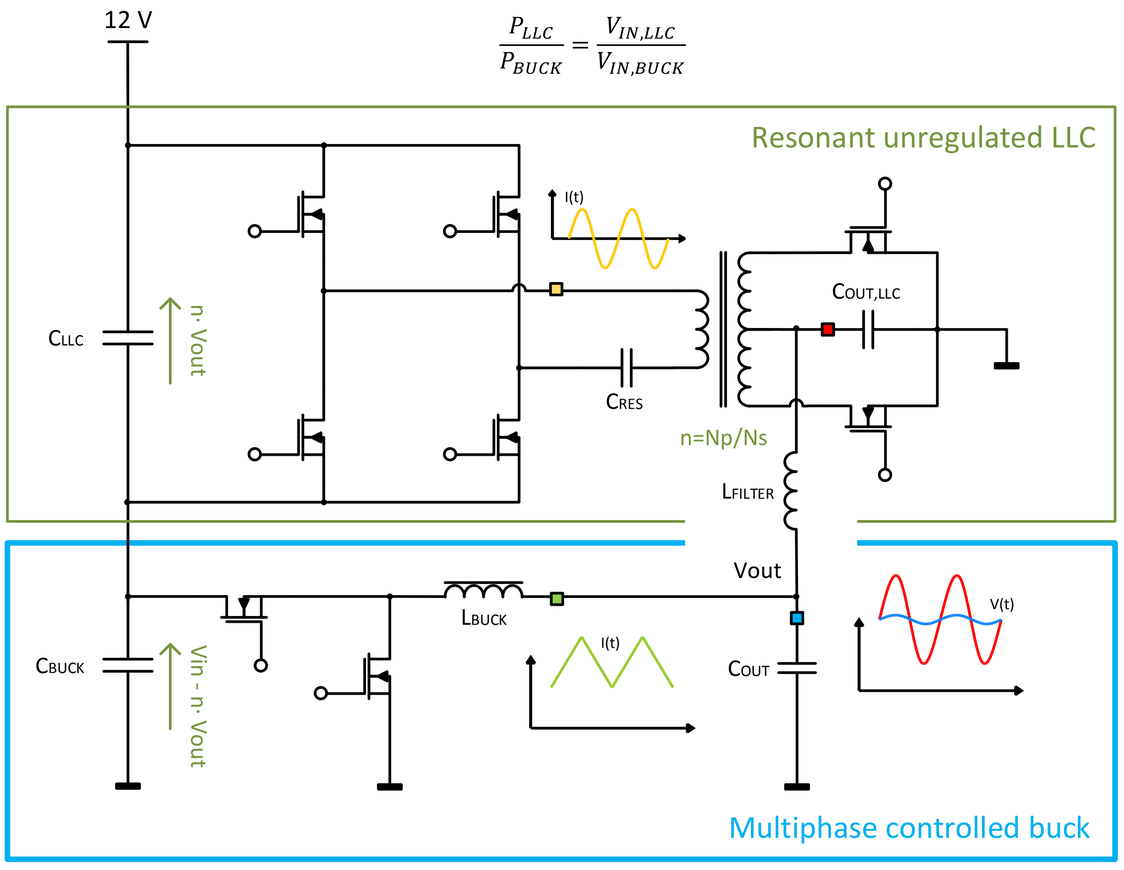

- A **high-efficiency LLC** unregulated converter is **in series** (input) with a multiphase regulated buck
- **Outputs are in parallel** and LLC voltage is filtered through PCB inductance (*Lfilter*)
- Input currents are equal → **power delivery ratio depends on input voltage ratio**
- **Power is mainly delivered through the high-efficiency resonant LLC** converter which achieves ZVS, ZCD for every switch

- LLC steady-state input voltage is fixed and **depends on transformation ratio *n***
- **LLC can operate in half-bridge or full-bridge mode** adapting to output voltage
- **The buck converter finely regulates output voltage and assures strong transient responses**

- **Total efficiency is the power-weighted mean of the two converters' efficiencies**
  → as the output power delivery is dominated by the LLC, this topology yields optimal efficiency while load transients are handled by a very small buck converter with reduced input voltage

LLC CENTER-TAPPED 5:1:1 PLANAR TRANSFORMER DESIGN

14/3.5/5 core size

8 layers, interleaved
Copper thickness: 100 µm
Dielectric thickness: 30 µm

EI 3F45 core, 50 µm gap on every leg, reduced fringing effects

$R_{AC,pri}$ (1 MHz) = 41.1 mΩ
Lm = 4.7 uH

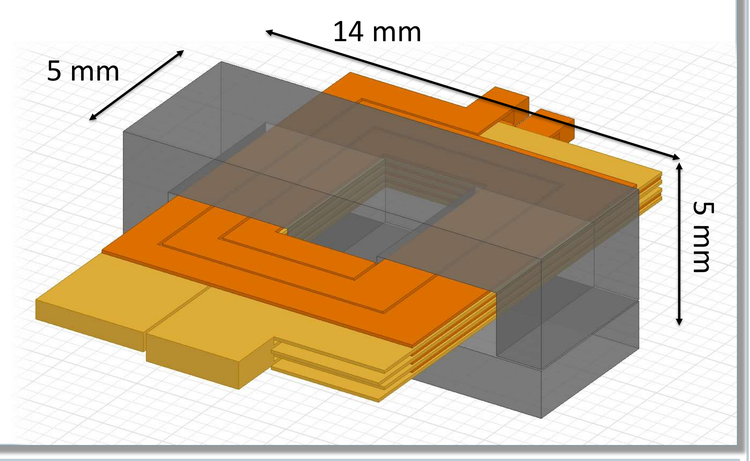

Full load simulation (400 A)
Output power waveforms

Single LLC
Single phase Buck
$f_{SW} = 1$ MHz

- Low buck input voltage
- Smaller buck inductor size with same current ripple

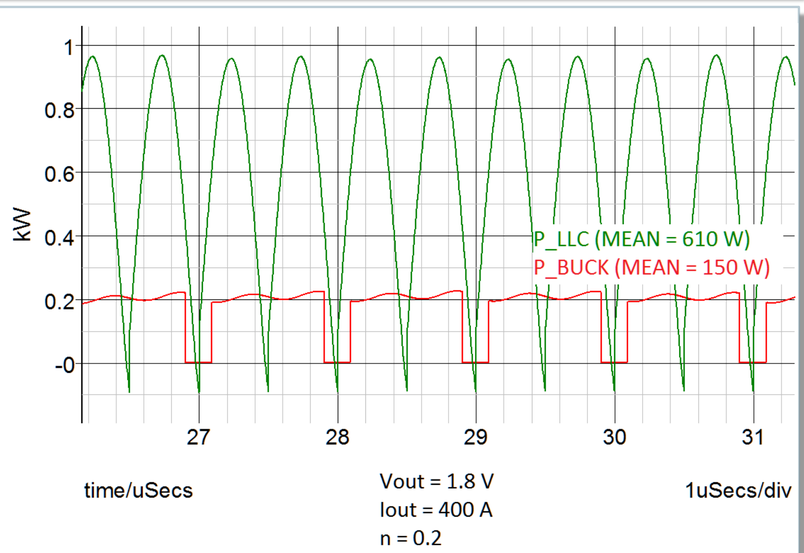

Dott. Mario Ursino
Prof. Stefano Saggini

Info:
ursino.mario@spes.uniud.it
stefano.saggini@uniud.it

PhD Expo 2017
DPIA Udine

PROPOSED LAYOUT COMPARED TO PREVIOUS STATE-OF-THE-ART MULTIPHASE BUCK

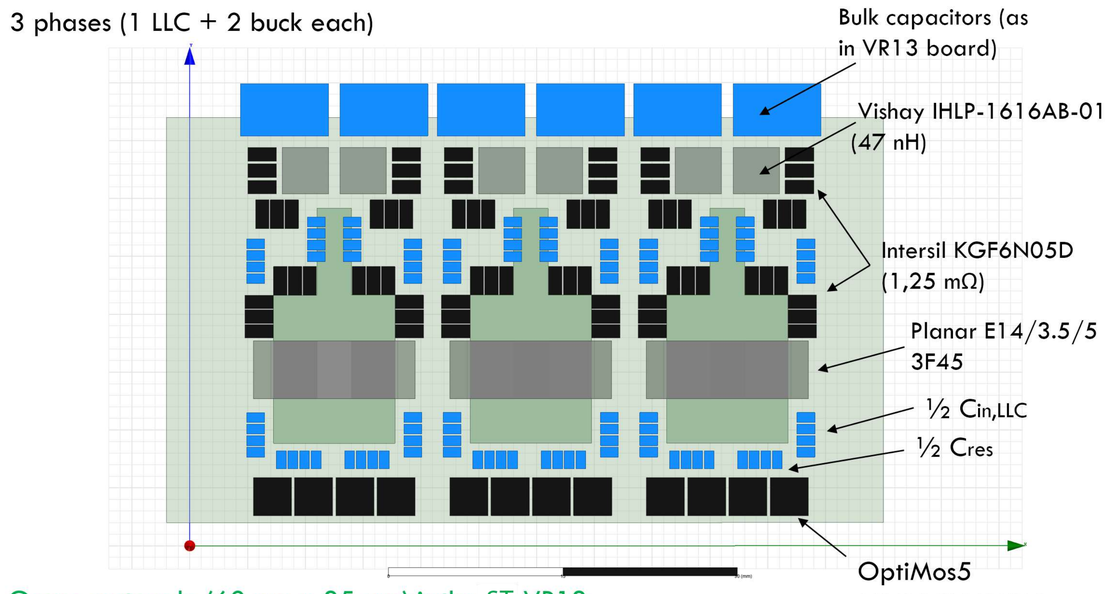

Green rectangle (62 mm x 35 mm) is the ST VR13 board occupation area

SIGMA-ARCHITECTURE KEY POINTS

- Low profile
- High power density
- Scalable topology
- Current sharing achieved through buck-DC regulation
- Low voltage MOSFETs

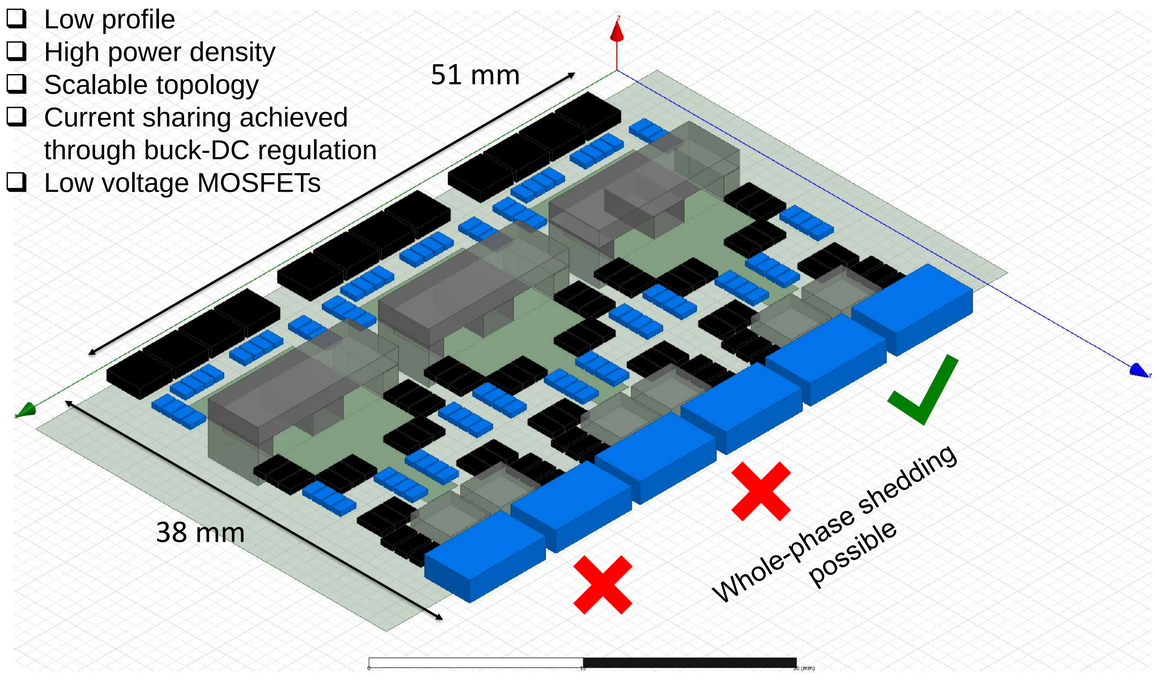

NOVEL SWITCHED-CAP-BASED CONVERTER FOR ULTRA-HIGH POWER DENSITY CONVERSION

- Two interleaved switched-capacitor converters supply fixed **portions of V_{IN} alternatively** to the following conversion stages
- **Power is mainly delivered to the output** through two high efficiency, **fully-resonant voltage dividers**
- A dual-phase, **low input voltage buck** converter handles **load transients** and **fine voltage regulation** (as in the sigma-converter case)
  → small power inductors, low voltage MOSFETs
- All switches achieve **ZVS and ZCD** (except for the low-power bucks' primary switches)
  → almost negligible switching losses
- **Total efficiency is again the power-weighted mean of the two converters' efficiencies**
- **Voltage dividers have a predicted efficiency of 98-99%** [4]
- Mobile application is being researched

References
[1] High-Efficiency High-Power-Density 48/1V Sigma Converter Voltage Regulator Module, Mohamed Ahmed, Chao Fei, Fred C. Lee and Qiang Li Center for Power Electronics Systems (CPES), Apec2017
[2] A High Efficiency LLC Resonant Converter with Wide Ranged Output Voltage Using Adaptive Turn Ratio Scheme for a Li-Ion Battery Charger, Hyeong-Gu Han, Yeong-Jun Choi, See-Yong Choi, and Rae-Yong Kim, Vehicle Power and Propulsion Conference (VPPC), 2016 IEEE
[3] Switched Capacitor DC-DC Converter: Superior where the Buck Converter has Dominated, Vincent Wai-Shan Ng Seth R. Sanders, Electrical Engineering and Computer Sciences University of California at Berkeley, August 17, 2011
[4] Dr. Shuai Jiang and Xin Li, Google, "Google 48V Power Architecture", APEC2017

UNIVERSITÀ DEGLI STUDI DI UDINE
hic sunt futura

Corso di dottorato in Ingegneria industriale e dell'informazione

XXXII Ciclo